Regulation of EZH2 in Triple-Negative Breast Cancer

by

Talha Anwar

A dissertation submitted in partial fulfillment
of the requirements for the degree of
Doctor of Philosophy
(Molecular and Cellular Pathology)
in the University of Michigan
2018

Doctoral Committee:

Professor Celina G. Kleer, chair
Professor Gregory R. Dressler
Professor Sofia D. Merajver
Assistant Professor Andrew G. Muntean
Associate Professor Zaneta Nikolovska-Coleska

Talha E. Anwar

tanwar@umich.edu

ORCID iD: 0000-0003-3974-1247

Dedication

To Amee and Abu

Acknowledgements

This dissertation would not be possible without many wonderful people in my life - I'm deeply thankful to you all for helping me get this far.

Endless thanks go to my mentor and friend Dr. Celina Kleer. I've learned so much from you about juggling science, writing, clinical service, and managing other parts of a busy life - all while being an incredibly kind, caring person. I couldn't be more thankful for the culture of support and creativity you've cultivated for our lab and for the independence to explore my ideas over the past four years.

I am deeply indebted to my incredibly selfless dissertation committee: Drs. Greg Dressler, Sofia Merajver, Andy Muntean, and Zaneta Nikolovska-Coleska. I've reached out to each of you many times over the past few years. Thank you for your insight, expertise, and support, which has really improved the quality of our work and my training.

Deepest thanks to members of the Kleer lab, past and present: Heather, Emily, Wei, Kathy, Maria, Caroline, Boris, Sabra, Mai, and Suny – you've made it a pleasure to come in every day, and I couldn't have asked for better labmates.

I've been fortunate to be part of two wonderful programs. Thank you to Ron, Ellen, Justine, Laurie, and Hilkka of the MSTP and to Zaneta and Laura of MCP for running these programs perfectly and for always looking out for me. Along those lines, this work was truly a collaborative effort, and I credit the fantastic collaborative and friendly environment of the MCP program for ideas and data for from this project. Special thanks

go to fellow MCP students Jim Ropa and Sierrah Grigsby, who contributed directly to some of the work presented in this dissertation,

Finally, thank you to my wonderful friends and family – you've made the most challenging times of the past few years bearable. Special thanks to my mom and dad who have sacrificed so much for their kids and are still supportive of my perpetual studenthood.

Table of Contents

List of tables

List of figures

List of abbreviations

AB – alveolar bud
AEBP – adipocyte enhancer binding protein
AR – androgen receptor
BL – bioluminescence
BLI – biolayer interferometry
DAVID - Database for Annotation, Visualization and Integrated Discovery
Dox - doxycycline
EED – embryonic ectoderm development
EMT – epithelial to mesenchymal transition
ER – estrogen receptor
EZH2 – enhancer of zeste homologue 2
GFP – green fluorescent protein
H3 - histone H3
H3K27me3 – histone H3 trimethylated at lysine 27
HDAC – histone deacetylase
HER2 – human epidermal growth factor receptor 2
HMT – histone methyltransferase
MET – mesenchymal to epithelial transition
MMTV – mouse mammary tumor virus
p38 MAPK – p38 mitogen activated kinase
PHF1 - PHD finger protein 1
PLA – proximity ligation assay
PcG – Polycomb group
PR – progesterone receptor
PRC2 – Polycomb repressive complex 2
PRE – Polycomb response element
RbAp48 - Retinoblastoma Associated Protein 48
SAINT - Significance Analysis of INTeractome
shRNA – short hairpin RNA
STAT3 – signal transducer and activator of transcription 3
SUZ12 – suppressor of zeste 12
T367A – threonine mutated to alanine at position 367
TrxG – trithorax group
TEB – terminal end bud
TNBC – triple-negative breast cancer
WT – wild type

Abstract

Overexpression of the Polycomb group protein EZH2 in estrogen receptor negative (ER-) breast cancer promotes metastasis. EZH2 has been mainly studied as a transcriptional repressor and an enzymatic component of the Polycomb Repressive Complex 2 (PRC2) that trimethylates histone H3 at lysine 27 (H3K27me3). However, how EZH2 drives metastasis, despite the low levels of H3K27me3 observed in ER- breast cancer, and the function of extranuclear EZH2 are unknown. Here, we report that phosphorylation of EZH2 at T367 plays a critical role in breast cancer invasion and metastasis. In human invasive carcinomas and distant metastasis, cytoplasmic EZH2 phosphorylated at T367 is significantly associated with ER- disease and low H3K27me3 levels. We uncover a previously unrecognized PRC2-independent mechanism by which p38-mediated EZH2 phosphorylation at T367 promotes EZH2 cytoplasmic localization and potentiates EZH2 binding to vinculin and other cytoskeletal regulators of cell migration and invasion. Ectopic expression of a phospho-deficient mutant of EZH2, where T367 has been replaced with Ala, is sufficient to inhibit EZH2 cytoplasmic expression, to disrupt binding to cytoskeletal regulators, and to reduce EZH2-mediated adhesion, migration, invasion, and the development of spontaneous metastasis. These results point to a novel non-canonical mechanism for EZH2 pro-metastatic function and suggest a new therapeutic approach for metastatic breast cancer.

Chapter 1 Introduction

1-1 Breast cancer

1-1.1 Epidemiology of breast cancer

Breast cancer is the most common and second deadliest cancer in women in the United States. Although improvements in screening, early detection, and treatment have contributed in dropping the death rate of breast cancer nearly 40% over the past 30 years (1), breast cancer remains a significant clinical challenge. The probability a woman will develop an invasive breast cancer over her life is 12.4% in the United States. In 2018, there will be an estimated 266,120 new cases of breast cancer diagnosed and an estimated 40,920 deaths from breast cancer (1). Globally, breast cancer is both the most common and deadliest cancer in women, with 2.4 million incident cases and 733,300 deaths in 2015 (2). In general, outcomes for breast cancer are good compared to other cancers with a 90% five-year survival rate (3). Prognosis drops off significantly, however, with higher stage disease; indeed, five-year survival for patients with distant metastases at the time of diagnosis has a 6% 5-year survival compared to patients with regional or localized cancer (31% and 62%, respectively) (3).

Outcomes of breast cancer also vary significantly by race and ethnicity (4). These differences comprise both biological factors (e.g., inherent differences in tumor grade, receptor status, or other features) and non-biological factors (e.g., social, economic, demographic, or cultural factors that might contribute to a woman's access to care (4, 5).

Incidence of breast cancer for non-Hispanic black women from 2010-2014 was 2% lower than non-Hispanic white women, but death rates were 42% higher in non-Hispanic black women (6). These differences are reflected in five-year survival rates as well: for all women diagnosed with breast cancer in the United States it is 91% but for black women it is 81%. Additionally, for women with stage I breast cancer, the actuarial risk of death at seven years is significantly higher for black women than non-Hispanic white women, and black women are significantly more likely to die with smaller tumor size after adjusting for income and estrogen receptor status (4).

1-1.2 Breast cancer progression and metastasis

Breast cancer is an umbrella term that refers to many different neoplasms with distinct histological patterns, molecular expression profiles, risk factors, and clinical courses. The overwhelming majority (>95%) of cancers of the breast are adenocarcinomas and arise from the ducts (invasive ductal carcinomas, 80%) or lobules (invasive lobular carcinomas 5-15%) (7, 8). Less common are other tumor types such as lymphomas, sarcomas, and phyllodes tumors (9). In a simplified model proposed almost 50 years ago (10), breast cancer follows a linear pattern of progression (**Fig. 1.1)**. Briefly, a normal terminal ductal lobular unit (TDLU) undergoes stepwise accumulation of genetic and epigenetic aberrations that lead to hyperplasia, atypical hyperplasia, ductal carcinoma, and invasive carcinoma in situ. Carcinoma in situ can then develop into an invasive carcinoma that metastasizes to distant organs. Progression at any of these stages is non-obligatory and time in each stage may last decades (10, 11). It is important to note that there is still debate as to whether the sequential breast cancer progression

model is broadly applicable; some, for example, have posited a parallel model in which breast tumor initiating cells disseminate early, which might suggest that invasion is not a prerequisite for metastasis *per se* (12).

As one of the hallmarks of cancer (13), metastasis is responsible for the overwhelming majority (90%) of cancer-associated deaths (14). A simplified model of breast cancer tissue invasion and metastasis is a sequential, three-step process (**Fig 1.2**). In the first step of this process, tumor cells invade locally into surrounding tissues. After local invasion, tumor cells intravasate into the circulatory system, through either vessels or by way of the lymphatic system. In the vasculature, they undergo arrest and avoid immunosurveillance. The third step is extravasation and colonization of distant organs, where tumor cells may proliferate to form micrometastases, and later into frank, clinically detectable lesions (15). The metastatic process is highly inefficient, with an estimated 99.98% (16)of all tumor cells failing to reach this step.

How can breast cells of epithelial origin, confined initially by basement membrane and then surrounding stromal architecture, undergo changes necessary to initiate this process? One of the prevailing views is that tumor cells are plastic and can co-opt a set of developmental programs known as the epithelial-to-mesenchymal transition (EMT). The EMT is characterized by the acquisition of a morphological and molecular phenotype marked by dysfunctional cell-cell adhesion, loss of apical-basal polarity, increased resistance to apoptosis, and gain of motility (17, 18). Both EMT and its reverse process, the mesenchymal-to-epithelial transition (MET), are fundamental in normal development and formation of the body plan. Loss of cell-cell adhesion is regulated by transcriptional repression and relocalization of cadherins, occludins, claudins, and desmoplakin (19),

and activation of mesenchymal markers including N-cadherin, vimentin, smooth muscle actin, and fibronectin (20). Cells also produce matrix metalloproteinases (MMPs) and the urokinase plasminogen activator (uPA) that degrade extracellular matrix (ECM) to allow local invasion into stroma (21). This cellular plasticity is governed by a set of transcription factors from three families: Snail, Twist, and Zeb (20, 22-25). Lineage tracing experiments have supported a role for EMT in mammary tumors driven by MYC (26). However, it is worth noting that whether EMT occurs in different cancers and its contribution metastasis remains a topic of intense debate (22, 27-31) and in the future may require a more nuanced appreciation of markers of EMT transcription factors, of mesenchymal cells, and of temporal regulation of this process (32). The underlying premise that breast tumor cells can exhibit plasticity, however, is well-supported.

Once tumor cells have penetrated the stroma and entered the vasculature, they undergo cell cycle arrest and must avoid anoikis (a form of apoptosis due to loss of extracellular matrix detachment), immunosurveillance, and shear stress from blood flow (33). Similar genes that facilitate the process of intravasation process may promote extravasation: MMPs, Epiregulin, COX2, and Fascin promote both angiogenesis and vascular remodeling and facilitate the intravasation/extravasation processes (34-36). Some organ-specific physical barriers, such as the blood-brain barrier, necessitate the activation of additional genes to facilitate their entry (34). The propensity of certain breast tumor subtypes to form metastases in certain organs may be explained by their likelihood of activating transcription of these additional genes.

1-1.3 Classification of breast cancers

Although breast carcinomas arise from breast epithelial cells, they can display significant histological and molecular heterogeneity. Seminal studies from nearly twenty years ago profiling the gene expression pattern of breast tumors have shaped how breast cancers are classified (37, 38) and how they are managed clinically. In general, breast cancer molecular subtyping has been based on expression of estrogen receptor (ER), progesterone receptor (PR), and whether the HER2 (ERBB2) gene is amplified. Guidelines for clinical diagnosis of receptor positivity is $\geq$1% tumor cells are immunoreactive by immunohistochemistry (39). This dissertation will focus on triple-negative breast cancers (TNBCs), which lack ER, PR, and HER2 amplification; however, there are many additional methods of clustering breast cancers based on gene expression patterns.

Indeed, over the past fifteen years, advances in molecular gene expression profiling have led to different molecular sub-classification systems with distinct clinical outcomes. Initial studies used a 456 cDNA set (427 genes) to classify breast cancers into five intrinsic subtypes based on gene expression patterns, each with distinct clinical outcomes and histologic staining patterns (37). Luminal A (23.7% of all tumors) and luminal B (52.8% of all tumors) express hormone receptors and have good and intermediate-poor outcomes, respectively. By immunohistochemistry, luminal A tumors are HER2- and Ki67- (a marker of cellular proliferation), while luminal B tumors can be HER2+/- and are Ki67+. A third group, HER2+ overexpressing tumors (11.2% of all tumors) are hormone receptor negative but show amplification of the HER2 gene and tend to have poorer outcomes. Normal-like tumors (7.8%) are hormone receptor positive,

HER2-, Ki67-, and have intermediate outcomes. Finally, basal-like tumors (12.3%) are hormone receptor and HER2- negative and express a basal marker (40, 41). Others have modified or expanded upon these initial group's gene signatures. A six-group gene signature based on 706 cDNA probes classifies breast carcinomas into 3 luminal-like, 1 HER2-like, and 2 basal-like breast cancers, for example. The PAM50 classification system, is a 50-gene classifier (+5 control genes) that identifies luminal A, luminal B, HER2-enriched, and basal-like tumors by surveying genes associated with hormone receptor, proliferation, and myoepithelial/basal features (40, 42).

1-1.4 Triple negative breast cancer

Triple-negative cancers, which lack ER, PR, and HER2 amplification account for about 10-20% of all breast cancers (43). In general, prognosis for patients with TNBC is poor compared to other subtypes: fifty percent of patients with early stage TNBC will experience recurrence, and 37% of patients will die the first five years after surgery (44). A study of 15,204 who presented to national comprehensive cancer networks found that women who presented with TNBC had significantly worse survival, even after adjusting for age, race, TNM, and whether they received chemotherapy (45). Metastatic dissemination is more common in patients with TNBC, particularly to the lungs and brain. Unlike tumors that express hormone receptor or HER2, there are no specific targeted therapies for TNBC (e.g., tamoxifen, trastuzumab, or labitinib). Demographically, TNBC patients tend to be younger (46), have higher staged disease at the time of diagnosis, and are disproportionately of African/African-American descent (45, 47) . Histologically, the majority of TNBCs show an invasive ductal carcinoma not otherwise specified (IDC-

NOS) pattern, i.e., they have no differentiating histologic patterns. However, rarer histologic subtypes of breast cancer such as metaplastic carcinoma (<1% of all breast cancers) and medullary breast cancers (<5% of all breast cancers) are overwhelmingly triple-negative (48). Additionally, TNBCs tend to show more frequent copy number variations, particularly in PTEN, EGFR, VEGFA, suggesting a greater frequency of genomic instability in these cancers (48).

Based on the intrinsic model of classification discussed above, basal tumors account for 60-90% of all TNBCs. Although the terms are used interchangeably, not all triple-negative tumors (based on clinical assays of <1% expression of these markers) are basal tumors (determined by cDNA array). More recent systems of classification have divided TNBC into six groups: basal-like 1, basal-like 2, immunomodulatory, mesenchymal, mesenchymal stem-like, and luminal androgen receptor subtype (49). This profiling is useful for preclinical modeling in that cognate cell lines have been identified for each of these categories. The system also underscores the great degree of molecular heterogeneity TNBCs.

Treatment for TNBCs have remained largely the same in recent years (44). Systemic management for both early and late stage TNBCs is sequential, single-agent cytotoxic chemotherapy. Adjuvant treatment is typically an anthracycline, an alkylator, and a taxane. Neoadjuvant use is the most common in TNBC versus any other subtype. These modalities are reviewed in (50). Taken together, the poor outcomes, heterogeneity, and lack of targeted therapies for TNBC necessitate a better understanding of the biology that underlies these tumors.

1-2 Epigenetics

The German biologist and cytogeneticist Walter Fleming is credited with first observing chromatin, a complex of DNA, RNA, histone, and non-histone proteins in his studies of eukaryotic mitosis (51). This observation helps explain how billions of base pairs of DNA fit compactly in the cell: not linearly, but wrapped around four pairs of histone proteins (histones H2A, H2B, H3, and H4). This basic unit, which comprises 147 base pairs of DNA is known as a nucleosome (52, 53). Covalent and noncovalent modifications of the nucleosome and methylation of DNA underlie the two main mechanisms of epigenetics, or heritable changes in gene expression that occur outside of changes in the DNA sequence.

In general, epigenetic modifications, such as these post-translational modifications that occur on histone tails, correlate with whether chromatin conforms to an open state (euchromatin) associated with active gene transcription, or a closed state that prevents gene transcription (heterochromatin). These modifications are broadly associated with three classes of proteins: those that place the modifications (writers), those that read the modifications (readers), and those that remove the modifications (erasers) (54). The focus of this dissertation is on a set of proteins responsible for writing these modifications.

1-2.1. Polycomb group and Trithorax group proteins

Polycomb group (PcG) and trithorax group (TrxG) are two of the most well-studied protein complexes responsible for post-translational modifications on histone tails, and consequently, epigenetic regulation. Our earliest hint at understanding these protein complexes dates to 1947, when Pamela Lewis observed that a dominant mutation in *Drosophila* caused additional sex combs to appear on the second and third pairs of legs

of adult males instead of only the first pair. This was referred to as Polycomb (*Pc*) (55). Polycomb was believed to negatively regulate *Hox* genes, which are responsible for anterior-posterior patterning (56). Future screens identified regulatory elements that would when mutated, would ablate gene expression of *Hox* genes: trithorax group (TrxG) proteins.

The canonical perspective of PcG and TrxG proteins is that these regulatory groups are antagonistic, in which they maintain repressed or active states of homeotic patterning, respectively. Both of these protein complexes are evolutionary conserved and maintain their chromatin modifying functions in mammals, and their importance in mammalian development is underscored by embryonic lethality of mice lacking PcG or TrxG genes (57-60). Both PcG and TrxG proteins form multimeric complexes; for the purposes of this dissertation, the focus will be on PcG proteins that form PRC2, although a brief introduction to another PcG complex, PRC1 is described below.

1-2.2. Polycomb Repressive Complex 1

In mammals, the PcG proteins form two major complexes responsible for effecting transcriptional repression: polycomb repressive complexes 1 and 2 (PRC1 and PRC2). Polycomb repressive complexes 1 are generally classified as either canonical or non-canonical (55), and in general comprise four subunit families homologous to the *Drosophila* Sce*,* Psc, Pc, and Ph; these are Ring1, PCGF, CBX, and Phc respectively (61). Common to both canonical and non-canonical complexes are the histone H2AK119 E3 ubiquitin ligase Ring1 and a Polycomb ring-finger domain protein (PCGF1-6). Canonical PRC1 contains one of the PHC1-3 proteins and one of the chromeobox

proteins (CBX2-8), which are responsible for targeting and stabilizing the complex to chromatin by binding H3K27me3 (55, 62). That these canonical PRC1 complexes contain components that bind histone H3 trimethylated at lysine 27 (H3K27me3) suggest that PRC1 functions downstream of PRC2 (discussed below), although there is evidence to suggest that PRC1 can function independent of this mark as well (63). A large number of possible combinations of PRC1 proteins allow for a diverse set of possible functions of PRC1, many of which remain poorly understood. Non-canonical PRC1 members include YAF2, KDM2B, or E2F6 proteins (64).

1-2.3 Polycomb Repressive Complex 2

In contrast to PRC1, PRC2 mediates gene repression by placing methyl marks on lysine 27 of histone H3. (H3K27me, H3K27me2, H3K27me3). Of note, each of these modifications is likely functionally distinct, with H3K27me3 being a stable mark (65). The PRC2 comprises four subunits: with mutual exclusivity, the SET-domain proteins EZH1 or EZH2; embryonic ectoderm development (EED); suppressor of zeste 12 (SUZ12); and the Retinoblastoma protein associated protein 46/48 (RbAp46/48) (65). While other cofactors associate with PRC2, EZH1/2, SUZ12, and EED appear to be minimally required for H3K27 methyltransferase activity in vitro and in vivo (66). PRC2 complexes with EZH1 versus EZH2 show differences in cell type distribution (mitotic and differentiated cells versus mitotic cells, respectively) (65) and methyltransferase activity (lower vs. higher) (67), suggesting non-redundant functions, although PRC2-EZH1 can restore K27 that has been demethylated (67, 68).

Genome-wide ChIP studies have revealed that PRC2 represses transcription of hundreds of genes to maintain pluripotency of embryonic stem cells (69). The catalytic

subunit of the PRC2 are EZH1 or EZH2, the latter of which is better characterized and viewed as the canonical PRC2 member (68). The domain structure of EZH2 and its functions are shown in **Fig 1.4.** A 746 amino acid protein, EZH2 contains a C-terminal SET domain that is well-conserved common to many lysine methyltransferases (70, 71) which catalyzes the exchange of one to three methyl groups from donor SAM onto H3K27. The H3K27me3 form of H3K27 is associated with transcriptional repressive functions and in most contexts, associated with genome-wide distribution of PRC2. Additional domains of EZH2 include its WD-40 binding domain (WDB) responsible for interaction with EED, and domains 1 and 2 thought to mediate protein-protein interactions (72). Two SANT (Swi3, Ada2, N-CoR, TFIIIB) domains are less well characterized but may be important for interaction with histone tails (73). Additionally, a cysteine-rich domain (CXC) sits immediately N-terminal to the SET domain, which is important for methyltransferase activity (73).

Other members of PRC2 contribute to the complex's function. As mentioned previously, the SUZ12 and EED are both minimally required for the methyltransferase activity of EZH2 (66). Recent crystallography studies reveal that the zinc finger protein SUZ12 is also minimally required for the nucleosome binding properties of PRC2. They further find that the different cofactors associated with PRC2, such as PHF19 and AEBP2, may interact with the C2 domain on SUZ12 (74). Cryo-electron microscopy studies have also recently shown that SUZ12 interacts with all other members of PRC2, thereby likely stabilizing the entire complex (75). In contrast, the WD-40 repeat containing protein EED binds H3K27me3, resulting in a conformational change in EZH2 that enhances EZH2 catalytic activity and allows for propagation of the repressive mark (76).

A number of cofactors of PRC2 have been found to associate with PRC2 and its function. The Jumonji AT-rich interactive domain 2 (Jarid2) has a well-studied, albeit complicated role in regulating PRC2 function. On one hand, Jarid2 interacts with PRC2 and increases its methyltransferase activity *in vitro* and in embryonic stem cells (51, 77-80). Jarid2 occupies almost the exact same genomic regions as EZH2, SUZ12, and EED in embryonic stem cells (81), and may play a role in recruiting EZH2 to target genes (81), mediated by interactions with lncRNAs (82). On the other hand, Jarid2 negatively regulates PRC2 methyltransferase activity on core histones from HeLa cells (81). One explanation for these differences might be explained by the recent observation that PRC2 di- and tri-methylates Jarid2 at K116 which allosterically enhances PRC2 methyltransferase activity (78). High-resolution cryo-EM structures of PRC2 in complex with Jarid2 reveal binding of Jarid2 both at allosteric and active sites of PRC2, supporting a model in which Jarid2 is both a substrate of PRC2 and can mimic methylated H3 tails to activate PRC2 (83-85). Thus, it is possible that depending on the methylation of status of Jarid2, it can function to activate or inhibit PRC2 activity.

Other PRC2 cofactors include Adipocyte Enhancer-Binding Protein (AEBP2), a zinc-finger protein that co-occupies a subset of PRC2 genes and enhances PRC2 enzymatic activity in vitro (66). High-resolution cryo-EM structures of AEBP2 show that it interacts with RbAp48 and mimics an unmodified H3 tail (83). A number of other interactors with PRC2 have also been described, but their functions are less clear: the Polycomb-like proteins PHF1, MTF2, and Pcl3 proteins, which may also modulate PRC2 activity and were recently shown to be crucial for PRC2 recruitment to CpG islands (86).

1-3 Role and regulation of EZH2 in cancer

Deregulation of epigenetic proteins are commonly seen in cancer. Alterations in EZH2 have a complex role, exerting both tumor-suppressive and tumor-promoting functions depending on the context. In most cancers where it is deregulated, EZH2 is overexpressed, where its overexpression frequently correlates to poor prognosis; indeed, overexpression of EZH2 has been observed in tumors of the prostate (72, 87-89), breast (89-94), liver (95, 96), lung (97-100), endometrium (89, 101), bladder (102), ovary (103, 104), skin (89), and brain (105). Beyond its role as a biomarker, EZH2 has a well-established role as an oncogene; ectopic expression of EZH2 in benign cells promotes their proliferation (87, 90, 106, 107), and genetic knockdown of EZH2 reduces the proliferation, migration, invasion, and stem properties in multiple cancer cell line and xenograft models (91, 93, 108-110).

How overexpression of EZH2 promotes cancer in each of these individual tumor types is only superficially understood. In prostate cancer, a number of putative tumor suppressors repressed by EZH2 have been described and include repression of E-cadherin (88), DAB2IP (111), PSP94 (112), RUNX3 (113), and others (reviewed nicely in (114). However, for other tumor types, fewer targets have been identified and their regulation by EZH2 may be context-specific, as in the case of tobacco-mediated induction of PRC2 repressing the tumor suppressor Dickkopf-1 in lung cancer (115). For the purposes of this dissertation, the role of EZH2 overexpression in breast cancer and the mechanisms of its action will be explored more fully in the next section.

Activating somatic heterozygous mutations of EZH2 have been observed in up to 30% of non-Hodgkin lymphomas of follicular and germinal center diffuse large B-cell

(GCB-DLBCL) subtypes (116-121). These predominantly occur within the SET domain (hotspot mutations at Y641, A677G, and A687) and alter EZH2 substrate specificity towards di- and tri-methylated H3K27 over mono-methylation (119, 122). The resulting altered specificity, in the case of Y641 for example, effects both a global increase in H3K27me3 and a total redistribution of the repressive mark at PRC2-regulated loci that is sufficient for tumorigenesis (123) and is one rationale for clinical use of EZH2 inhibitors; indeed, to date, three SAM-competitive EZH2 methyltransferase inhibitors (tazemostat/EPZ-6348, GSK2816126, and CPI-1205) have reached phase I/phase II clinical trials for patients with follicular lymphomas, DLBCL harboring these gain-of-function mutations (121). These inhibitors are also being examined in a genetically-defined set of solid tumors harboring inactivating mutations in members of the ATP-dependent chromatin remodeling SWI/SNF complex which results in oncogenic dependency on EZH2 (124-126). A fourth compound, MAK683, is the only EZH2 inhibitor currently in clinical trials that does not target the methyltransferase activity directly, but rather disrupts EZH2-EED interaction, the proof of principle for which is described in Kim et al. (127)

As is the case with many oncogenes, EZH2 can also exert tumor-suppressing functions depending on the cellular context in which it is expressed. Loss of EZH2 in hematopoietic stem cells causes T-cell acute lymphoblastic leukemia in mice (128) and in lung epithelial cells promotes carcinoma in a Kras-driven lung adenocarcinoma model (129). In an inducible EZH2 shRNA mouse glioblastoma model, short-term inhibition of EZH2 is sufficient to reduce glioblastoma tumor growth, but strikingly, long-term depletion

of EZH2 promotes tumor progression and results in more undifferentiated, aggressive tumors, suggesting further context- and temporal-specific roles for EZH2 function (130).

1-3.1 EZH2 in breast cancer

The first study of EZH2 in breast cancer found that it is overexpressed in approximately 55% of invasive breast carcinomas, and its expression is inversely correlated with poor breast cancer survival (90), suggesting a role as a potential biomarker. Since then, the observation has been replicated in other cohorts and supported by meta-analysis (89, 92, 131-134). High expression of EZH2 is significantly associated with ER- status, higher histologic grade, and TNBC status (90, 132) of breast tumors. Additionally, EZH2 may have a role that actually precedes frank tumor dissemination, as higher levels of EZH2 expression in normal breast epithelium correlate with increased risk of breast cancer (135). Together, the data have painted a clear picture of EZH2 as a potential biomarker of breast cancer development and aggressive breast cancers.

Beyond its role as a prognosticating biomarker in breast cancer, gain- and loss-of-function studies have convincingly demonstrated that EZH2 exerts oncogenic functions in breast cells. Overexpression of EZH2 in benign mammary epithelial cells is sufficient to increase their anchorage-independent growth and invasion, and this phenotype is dependent on an intact SET domain (90). Conversely, genetic inhibition of EZH2 using shRNA is sufficient to reduce the proliferation of estrogen-negative breast cancer cells *in vitro* and in vivo by delaying G2/M cell cycle transition (136). Independent of proliferation genetic inhibition with shRNA or pharmacological depletion of EZH2 with 3-

Deazaneplanocin A (DZNep) is sufficient to reduce migration, invasion, and random motility of triple-negative breast cancer cells and is accompanied by the acquisition of an MET phenotype and restoration of E-cadherin. (93). EZH2 also appears to contribute to PARP inhibitor resistance, and pharmacological inhibition of EZH2 with a specific inhibitor can restore PARP inhibitor sensitivity (137). Along these same lines, EZH2 is capable of conferring tamoxifen resistance to ER+ breast cancer cells by repressing the estrogen receptor alpha cofactor GREB1, which causes a redistribution of other ERα cofactors p300 and CBP and explains why tamoxifen can have a paradoxical growth-stimulating effect in tamoxifen-resistant ER+ breast cancer cell lines (134). Thus, the data in breast cancer alone point to EZH2 having a diverse set of oncogenic functions.

The role of EZH2 in initiating tumors is not clear. Overexpression of EZH2 in normal breast cells is associated with an increased risk of invasive carcinoma (135, 138); however, this could just be a consequence, rather than a cause, of increased proliferation. Transgenic mouse models of conditional EZH2 overexpression in mammary epithelial cells (MMTV LTR-driven EZH2) show disrupted TEB development and precocious intraductal epithelial hyperplasia, a precursor to carcinoma in situ. The data also suggest that EZH2 overexpression alone is not sufficient for mammary tumor initiation (139).

A number of putative mechanisms have been posited to explain the precise mechanism by which overexpression of EZH2 confers proliferative, migratory, and invasive potential to breast cancer cells. These include transcriptional repression of tumor suppressors such as RUNX3 (113), CDKN1C (p57) (140), RAD51-paralog proteins (141), RKIP (142), and FOXC1 (143). Separately, EZH2 has been shown to promote EMT by promoting signaling through pro-tumorigenic kinases, such as by activating the p38

MAPK (93). Of note, several recent studies have found that breast cancers display a decoupling of EZH2 and H3K27me3. By immunohistochemistry, TNBCs display higher levels of EZH2 and lower levels of H3K27me3 (144). Stratification of patients by EZH2 and H3K27me3 has shown that this combination (high EZH2/low H3K27me3) portends the worst overall survival in breast cancer patients, irrespsective of ER status (144). These observation may suggest some mechanism of EZH2 HMT regulation, or alternatively, H3K27me3-independent functions of EZH2, such as transactivating functions and nonhistone methylation.

1-3.2 Transcriptional regulation of EZH2

One of the most well-characterized transcriptional regulators of EZH2 across multiple contexts is Myc. In embryonic stem cells c-Myc and n-Myc both bind to the promoters and activate the transcription of Suz12, and EED. In prostate cancer, bladder cancer, and neuroblastoma, Myc binds to the *Ezh2* promoter directly and activates transcription (145-147), although whether Myc coordinately regulates expression of other PcG genes in cancer is not known. In bladder cancer, Bromodomain 4 protein upregulates c-myc, and c-myc also binds to the *Ezh2* promoter and activates its transcription, and this event is abrogated upon inhibition of BRD4 with the small molecule JQ1 or RNA interference against BRD4 (147).

The E2F transcription factors, which regulate cell cycle, also activate EZH2 transcription by binding to the *Ezh2* promoter of 293T and RAT1 cells (148). In mouse models of bladder cancer where the tumor suppressor Rb is inactivated, E2F family members and subsequently EZH2 are expressed (149). The EWS/FLI1 chimeric

transcription factor pathognomonic of Ewing sarcoma also directly binds to *Ezh2* promoter and activates its transcription (150). The TCF4 transcription factor similarly binds directly to the *Ezh2* promoter in HEK293T cells and activates its transcription, suggesting that EZH2 is regulated by Wnt/B-catenin signaling (151). In prostate cancers bearing the TMPRSS2-ERG gene fusion (~50%), ERG binds directly to the promoter of EZH2 and activates its transcription (152, 153). Negative transcriptional regulators include nuclear factor IB (NFIB), which binds directly to the *Ezh2* promoter and represses *Ezh2* transcription (154).

1-3.3 Post-transcriptional regulation of EZH2

Myc also regulates EZH2 post-transcriptionally. In Myc-driven mouse models of lymphoma, Myc downregulates mir-26a leading to subsequent upregulation of EZH2 (155). In prostate cancer, Myc binds to *mir-26a* and *mir-26b* promoters and prevents their transcription, which offers another mechanism of EZH2 mRNA upregulation. Loss of mir-101 has also been found to lead to upregulation of EZH2 across a number of cell and cancer types (156-159). In skeletal muscle, upregulation of mir-214 during muscle differentiation leads to EZH2 mRNA degradation (160).

1-3.4 Post-translational regulation of EZH2

A summary of the post-translational modifications of EZH2 and the contexts in which they have been studied is shown in **Table 1**. To date, the most well-studied modification is S21 phosphorylation, mediated by AKT. Phosphorylation at S21 significantly decreases EZH2 methyltransferase activity on H3K27 by decreasing affinity

of EZH2 for H3 without affecting EZH2 subcellular localization (161). While canonical H3K27me3 activity is reduced, in castration-resistant prostate cancer, S21 phosphorylation promotes interaction with androgen receptor to drive transcription of a number of genes, independent of H3K27me3, and promote growth of castration-resistant prostate cancer cells (72). In multiple myeloma, phosphorylation at this same site underlies cell-adhesion mediated drug resistance (162), while in glioblastoma, it serves as a switch that promotes the non-histone methylation of STAT3 by EZH2, resulting in STAT3 activation (163). Whether the properties of S21 phosphorylation are generalizable across different cancer types, and the role of S21 phosphorylation in normal cells is not known.

Another PTM studied uniquely in the setting of myoblasts and satellite cells is phosphorylation at T367 by the p38 MAPK. In this setting, activation of the p38 signaling pathway via TNFα, as in muscle injury, results in p38α-mediated phosphorylation of EZH2 at T367, and recruitment of EZH2 to the Pax7 promoter (164). In skeletal muscle progenitors, MyoD induces the E3 ubiquitin ligase to ubiquitinate and subsequently degrade EZH2 in response to p38-mediated phosphorylation at T367 (165).

Curated mass-spectrometry datasets of specific post-translational modifications have identified a number of other modifications, including sites of ubiquitylation (K61, K461), dimethylation (K505, K509, K510), and phosphorylation, including some in the C-terminal SET domain (S690, Y696, T718). The origins and functions of these modifications are unknown and therefore require further study (166-168).

1-3.5 Transcriptional activating roles of EZH2

Independent of its H3K27me3 activity, EZH2 can transcriptionally activate genes. Underscoring the importance of cellular context are the disparate roles of EZH2 in studies of ER+ vs. ER- breast cancers with regards to this function. In ER- basal-like breast cancers, EZH2 activates transcription of NF-kB targets independent of other PRC2 members (169). In this setting, EZH2 is forms a complex with RelA and RelB on NF-kB target genes and is associated with activating H3K4 marks rather than H3K27me3 marks (169). Interestingly, EZH2 may itself transcriptionally activate RelB in TNBC, adding an additional layer of complexity to the activating functions of EZH2 (170). In contrast to this, in ER+ breast cancer cell lines, EZH2 can interact with ERα and B-catenin upon E2 treatment. In response to estradiol treatment ERα, B-catenin, and EZH2 form a complex on the *c-Myc* promoter and activate its transcription, also independent of the HMT activity of EZH2 (171). Furthermore, EZH2 was found to interact with the transcription factor TRIM28 and positively regulate transcription of ~100 genes in ER+ cancer cell lines. Through ChIP-QPCR, EZH2 and TRIM28 were found to co-occupy regions within 10kb of the transcription start site (172).

Another example of this transactivating function is in benign mammary epithelial cells in which EZH2 is overexpressed. In this instance, EZH2 binds to the proximal *Notch* promoter with cofactors RelA and RelB to activate transcription. This occurs independent of H3K27me3, is associated with activating H3K4 marks, and is HMT dispensable (173). Likewise, in intestinal stem cells, the DNA repair protein PAF recruits

EZH2 to a B-catenin transcriptional complex to drive transcription of Wnt target genes independent of EED, SUZ12, and the HMT activity of EZH2 (174).

Finally, in castration-resistant prostate cancer, ChIP-seq of EZH2 and H3K27me3 has shown many sites where EZH2 does not colocalize with the repressive mark. These “solo” peaks are instead associated with H3K4me2 and 3 and RNA pol II, and EZH2 knockdown decreases levels of active mark at these sites. These data are interesting because they not only support a transactivating role of EZH2, but also suggest that EZH2 might function as both a transcriptional repressor and activator within the same type of cell (72). Taken together, these studies paint EZH2 as a complex protein capable of exerting repressive and activating functions depending on cellular context.

1-3.6 Nonhistone methylation and extranuclear EZH2 function

Histone lysine methyltransferases can also methylate nonhistone substrates (175). A number of studies have now demonstrated, with varying degrees of evidence, that EZH2 can methylate non-histone substrates (78, 93, 163, 176-184). **Table 1** summarizes these studies. Of note, the 7-amino acid sequence that contains K27 on histone H3 (i.e., the potential consensus for EZH2) is AAR**K**SAP. A cursory glance at the putative nonhistone substrates presented in 1.4, many discovered empirically, reveals sequences that may vary wildly from this H3K27 motif, raising questions on the validity, substrate specificity, cellular context, and role of participating cofactors in these studies. These questions are especially important in light of a recent study that defined the amino acids surrounding K27 required for PRC2 methyltransferase activity by mutation. For example, an arginine or a lysine in the -1 position appears absolutely required for

methylation at K27 (184). Basic questions—for example, whether EZH2 requires SUZ12 and EED for methylation of nonhistone targets—remain to be answered.

1-4 Rationale for this dissertation

It is clear that triple-negative breast cancers remain a significant clinical challenge. The histone methyltransferase EZH2 is overexpressed in ~55% of invasive breast carcinomas and is significantly associated with the triple-negative subtype. However, many questions about what regulates the diverse set of EZH2 functions in cancer remain. Based on observations that p38 binds PRC2 in breast cancer and phosphorylation of EZH2 at T367 (93), we hypothesized that it may be important in breast cancer. In the following chapters, we define EZH2 phosphorylation at T367 in breast cancer (chapter 2), and the functional (chapter 3) and mechanistic (chapter 4) consequences of this phosphorylation on breast cancer cells.

1-5 Figures

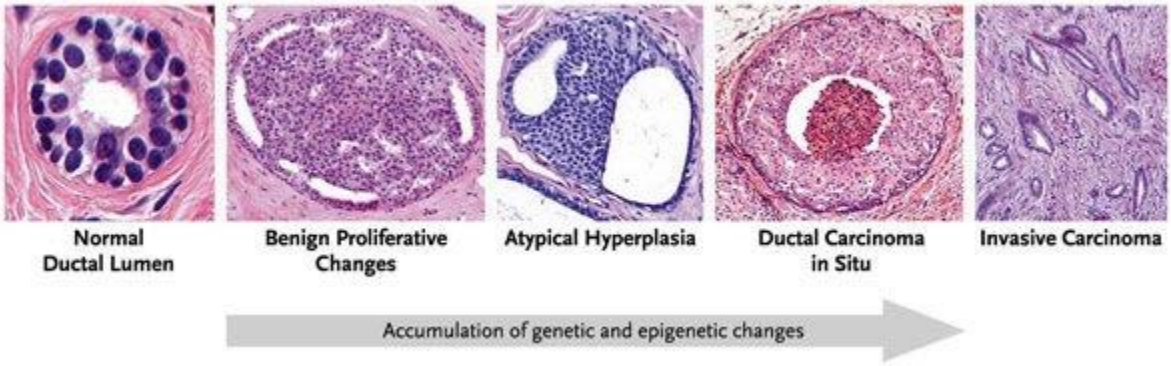

Adapted with permission from (185)

Figure 1.1 The Wellings-Jensen model of breast cancer progression. In this model, normal breast cells of a terminal ductal lobular unit progressively acquire genetic or epigenetic changes, such as gain of oncogene expression (HER2/neu) or loss of tumor suppressors (p53) leading to proliferation. Atypical hyperplasia is considered a precancerous lesion characterized by dysplastic, monotonous epithelial cells and a precursor to ductal carcinoma in situ (DCIS), malignant cells confined to the duct.

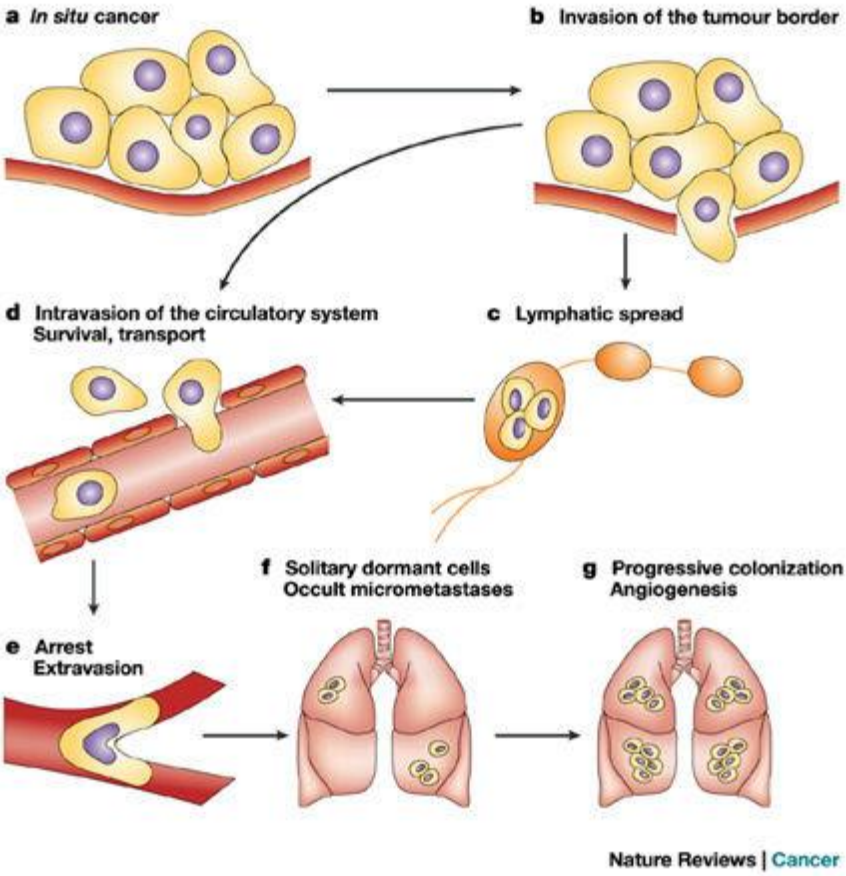

Reproduced with permission from (186)

Figure 1.2 The metastatic cascade. Tumor cells acquire phenotypes that allow them to penetrate the basement membrane and surrounding stroma and intravasate the vasculature either directly or via the lymphatic system. In the vasculature, tumor cells arrest, evade immunosurveillance, and can extravasate at secondary sites to form micrometastases. Some micrometastases will remain dormant while eithers may progress to frank, clinically detectable metastases.

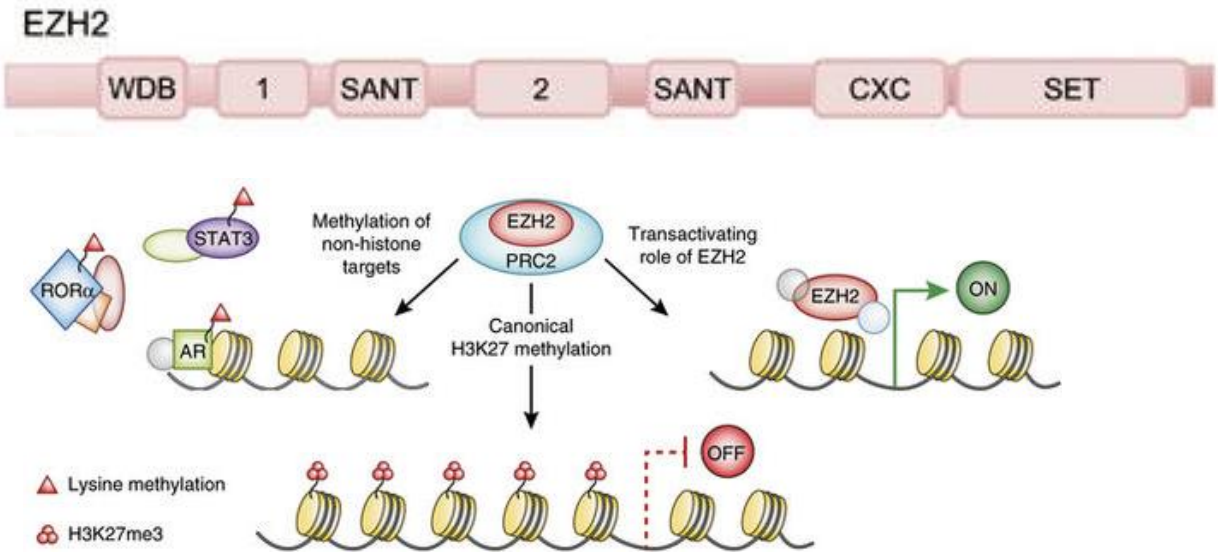

Adapted with permission from (73, 114) (top, bottom)

Figure 1.3 Top, domain structure of EZH2. EZH2 is a 746 amino acid protein with methyltransferase function imparted by its C-terminal SET-domain. The WD-40 binding domain (WDB) is responsible for interaction with EED. Domains 1 and 2 conserved domains thought to mediate protein-protein interactions (72). Two SANT (Swi3, Ada2, N-CoR, TFIIIB) domains are less well characterized but may be important for interaction with histone tails (73). A cysteine-rich domain (CXC) sits immediately N-terminal to the SET domain important for methyltransferase activity. Bottom, functions of EZH2. The canonical function of EZH2 is to mediate gene repression through trimethylation of H3K27. Additional functions include a gene activation and methylation of lysine on nonhistone targets.

Substrate	Site	Peptide	Function and notes	Ref
B-catenin	K49-me3	LSG**(K)**GNP	Promotes repression of Sox1 and Sox3 in ESCs, competes with acetylation at the same site	(183)
EloA	K754-me	TVK**(K)**IAP	Modulates expression of low-expression PRC2 target genes in mouse ESCs.	(184)
Fra-2	K104-me, K104-me2	GVI**(K)**TIG	Prevents Fra-2 from transcriptionally regulating epidermal differentiation genes. The data do not support that PRC2 methylates Fra-2 at these residues.	(178)
GATA4	K299-me	LYM**(K)**LHG	Reduces its transcriptional activity by preventing p300 acetylation in HL-1 cardiac muscle cells	(176)
Histone H2B	K120-me	AVT**(K)**YTS	May compete with H2BK120-ub in vitro and in cancer cell lines	(177)
Jarid2	K116-me3, K116-me2	AQR**(K)**FAQ	Mimics trimethylated histone tail and allosterically activates PRC2 in ESCs	(78, 83)
p38α	K139-me3, K165-me3	RGL**(K)**YIH CEL**(K)**ILD	Based on unpublished in vitro observations from our lab	(93)
PLZF	K430-me	SGM**(K)**TYG	Based only on predictive software, no experimental evidence	(182)
ROR α	K38-me	SAR**(K)**SEP	Promotes ubiquitination and degradation in HEK293 cells	(179)
Stat3	K49-me2	AAS**(K)**ESH	Promotes transcription of STAT3 target genes in response to IL-6 in colon cancer cells	(181)
Stat3	K180-me3	KTL**(K)**SQG	Promotes activation of STAT3 signaling in glioblastoma stem-like cells	(163)
Talin	K2454-me3	EAM**(K)**RLQ	Disrupts binding of Talin to F-actin in neutrophils and dendritic cells	(180)

Table 1. Non-histone targets of EZH2, summarized. Shown are the putative nonhistone targets of EZH2, along with the sequences of the 3 amino acids flanking the lysine on either side. The function and cellular context in which this nonhistone methylation occurs is also noted. Histone H3K27 motif: AAR(K)SAP

Modification	Site	Modifier	Function and notes	Ref
Phosphorylation	S21	AKT	Suppresses EZH2 HMT activity by impeding affinity of EZH2 for nucleosome substrate	(161)
Phosphorylation	S21	AKT	Promotes transcriptional activation by EZH2 and androgen-independent growth of castration-resistant prostate cancer cells.	(72)
Phosphorylation	S21	AKT	Promotes methylation of STAT3 at K180 in glioblastoma cells	(163)
Phosphorylation	Y244	JAK3	Promotes dissociation of PRC2 members; Increases “non-canonical” EZH2 interaction with RNA PolII, promotes proliferation of NK/T-cell lymphoma cells	(187)
Phosphorylation	T261	CDK5-related kinase	Promotes degradation by F-box and WD repeat domain-containing 7	(188)
Phosphorylation	T311	AMPK	Disrupted EZH2 interaction with SUZ12, inhibits EZH2 oncogenic activity and correlates with better survival in breast and ovarian cancers	(189)
Phosphorylation	T345	CDK1/2	Promotes degradation; cell cycle dependent, increases binding to HOTAIR ncRNA and 5’ end of Xist	(190)
Phosphorylation	T345	CDK1/2	Promotes recruitment of EZH2 to target gene loci and maintenance of H3K27me3 levels at these target loci in prostate cells (191)	(191)
Phosphorylation	S363	GSK3B	Not known	(192)
Phosphorylation	T367	p38a	Promotes satellite cell differentiation in response to TNFa through PJA1-mediated degradation of EZH2	(164, 165)
Phosphorylation	T367	GSK3B	Reduces H3K27me3 activity and reduces migratory/invasive properties in MCF12A and MDA-MB-231 overexpressing cells	(192)
Phosphorylation	T416	CDK2	Enhances migration, invasion, stemness in triple-negative breast cancer cells	(193)
Phosphorylation	T416	CDK2	Serves as a docking site for the forkhead-associated domain of NIPP1, which prevents dephosphorylation and is required for EZH2 association with proliferation loci	(194)
Phosphorylation	T487	CDK1	Promotes ubiquitination and degradation by the proteasome; negatively regulates proliferation in PC3 prostate cancer cells	(190)
Phosphorylation	T487	CDK1	Disrupts binding with SUZ12 and EED, thereby suppressing H3K27 methyltransferase activity. Promotes differentiation of mesenchymal stem cells.	(195)
Phosphorylation	T487	PKCλ/ι	Likely regulates EZH2 stability	(196)
Phosphorylation	Y641	JAK2	Promotes B-TrCP (FBXW1)-mediated degradation	(197)
Phosphorylation	S652	ATM	May negatively regulate interaction with PRC2 members SUZ12 and EED and negatively regulate stability	(198)
Phosphorylation	S734	ATM	May negatively regulate interaction with PRC2 members SUZ12 and EED and negatively regulate stability	(198)
O-GlcNacylation	S75	OGT	Likely positively regulates EZH2 protein stability	(199)
Acetylation	K348	PCAF	Decreases phosphorylation at T345 and T487; may enhance transcriptional silencing of HOXA10 in lung carcinoma cells; may enhance lung cancer cell migration and invasion;	(200)
Deacetylation	K348	SIRT1	Opposite of above	(200)
PARylation	D233/ E239	PARP	PRC2 complex dissociation and EZH2 downregulation	(137)

Table 2. Post-translational modifications of EZH2, summarized

Chapter 2: EZH2 is phosphorylated at T367 in human tissue and is overexpressed in breast cancer

2-1 Introduction

The overwhelming majority of breast cancer deaths occur due to metastasis. Breast cancer patients with distant metastases at the time of diagnosis have significantly worse prognosis with a five-year survival rate of 23.4%(3). New effective strategies for inhibiting metastatic spread or blocking the growth of established distant metastasis are needed.

Tumor cells must undergo fundamental changes to their identity to acquire the traits needed for dissemination to distant sites. Dysregulation of factors governing cell type identity is a common feature of metastatic cancer. Enhancer of zeste homologue 2 (EZH2) has been shown to regulate these processes through epigenetic silencing. Our lab and others have demonstrated that EZH2 is overexpressed in human solid and hematopoietic malignancies (87, 90, 114, 117). In breast cancer, EZH2 overexpression is significantly associated with the estrogen receptor-negative (ER-) subtype and worse clinical outcome(90). As the catalytic subunit of the Polycomb repressive complex 2 (PRC2), the methyltransferase EZH2 deposits trimethyl marks on histone tails of lysine 27 of histone H3 (H3K27me3) to effect transcriptional repression. However, the high levels of EZH2 observed in ER- tumors are associated with low H3K27me3(133, 144, 201), suggesting that the oncogenic function of EZH2 may rely on mechanisms other than repression of tumor suppressor genes, which are currently unknown.

Metastatic progression also involves tight regulation of the cellular responses elicited by its microenvironment. p38 MAPK proteins are critical in signaling cascades that transduce extracellular stimuli—inflammation, hypoxia, growth factors, and cytokine stimulation—into biological responses through proline-directed serine/threonine phosphorylation of target substrates commonly involved with gene expression regulation. The most abundant p38 family member, p38α (also known as MAPK14), has a well-documented, albeit complex role in cancer, exerting cell-type dependent tumor-suppressive or tumor-promoting functions (202). In the breast, p38□ promotes breast cancer progression (203-205), and high levels of active p38 MAPK are biomarkers of poor prognosis (202, 206, 207). However, how p38α MAPK activity induces breast cancer progression remains ill-defined.

We have demonstrated that EZH2 and p38α interact in aggressive ER- breast cancer cells(93), and EZH2 has been shown to undergo p38α-mediated T367 phosphorylation during muscle regeneration (164). However, direct demonstration that EZH2 is phosphorylated at T367 in solid tumors has not yet been explored. Here, we develop and validate a novel rabbit polyclonal antibody that can be used to detect report that pEZH2(T367) in tissue. We observe that pEZH2(T367) is upregulated in the cytoplasm of cancer cells in clinical samples of invasive breast carcinoma and distant metastasis in contrast with normal breast epithelium and that cytoplasmic pEZH2(T367) expression is significantly associated with higher histologic grade, ER- status, PR- status, and triple-negative status. Taken together, our data point to pEZH2(T367) as a potential biomarker of aggressive disease.

2-2 Results

2-2.1 Development and validation of a pEZH2(T367) antibody

To investigate whether EZH2 is phosphorylated at T367 in breast cancer and study its biological relevance, we developed and validated a novel rabbit polyclonal anti-phosphorylated T367 EZH2 antibody. In dot blot analyses, the anti-pEZH2(T367) antibody specifically recognized a peptide corresponding to the phosphorylated T367 site but not the unmodified peptide (**Figure 1.1A**). Demonstrating its specificity for the T367 phosphorylated form of the EZH2 protein, the anti-pEZH2(T367) antibody failed to detect dephosphorylated recombinant EZH2 and dephosphorylated EZH2 from breast cancer cell lysate (**Figures 1.1B and C**). Incubation of the antibody with the phosphorylated peptide outcompeted antibody binding in Western blot analysis of whole cell extracts of MDA-MB-231 cells and in immunohistochemistry of breast cancer tissue samples, further demonstrating specificity of the antibody for this site (**Figure 1.1D and E**). Finally, the antibody failed to recognize an unphosphorylatable threonine to alanine (T367A) mutant (**Figure 1.1F**), suggesting that the antibody is specific for phosphorylation at the T367A site.

2-2.2 Phosphorylated EZH2 (T367) is expressed in the cytoplasm of invasive breast carcinoma and distant metastasis.

We evaluated pEZH2(T367) protein expression in situ by immunohistochemistry in a wide range of breast tissue samples from 146 patients, including normal breast (n=19), invasive carcinomas (n=104), and distant metastasis (n=23) arrayed in high density tissue microrrays in triplicate **(Table 3)**. While in normal lobules pEZH2(T367), if

present, was localized to the nucleus, pEZH2(T367) was expressed in the cytoplasm of invasive breast cancer cells (**Figure 1.2A**). The frequency of cytoplasmic pEZH2(T367) increased significantly with breast cancer progression, as it was absent in normal lobules and detected in 57% of invasive carcinomas and in 74% of breast cancer distant metastasis (Chi-square p=0.0001, **Fig. 1.2B**). In the 104 primary invasive carcinomas, high cytoplasmic pEZH2(T367) was significantly associated with higher histological grade (p=0.028), ER- (p=0.0003), PR- (p=0.0002), and triple negative status (p=0.0006) (**Table 4**).

As is the case for clinical samples of breast cancer, in a panel of breast cell lines, we observed that aggressive and metastatic ER- breast cancer cells exhibit higher pEZH2(T367), EZH2, and p-p38 proteins compared to benign and less aggressive ER-positive breast cancer cells and nontumorigenic breast cells (**Fig. 1.2C**).

A survey of pEZH2(T367) expression in a cohort of human normal and cancer tissues showed that cytoplasmic EZH2(T367) is highly expressed in epithelial malignancies including kidney and colon cancer, hepatocellular carcinoma, and thyroid carcinoma compared to normal tissues, and to non-epithelial tumors (**Fig 1.3A**).

Together, these results demonstrate that cytoplasmic pEZH2(T367) is expressed in invasive and metastatic breast carcinomas where it is associated with higher histological grade, a measure of tumor aggressiveness, ER- status, and breast cancer progression. We observe that pEZH2(T367) is upregulated in several types of human carcinoma compared to corresponding normal tissue.

2-3 Summary and Discussion

EZH2 is a bona-fide oncogene in breast cancer, responsible for imparting proliferation, migration, invasion, and stem-like abilities to breast cancer cells (90, 91, 93, 173), but the mechanisms are incompletely understood. As the enzymatic component of PRC2, EZH2 has an established transcriptional repression through its catalysis of histone H3K27 trimethylation. However, the presence of high EZH2 levels in association with low H3K27me3 in aggressive breast cancers suggests that EZH2 may operate via a currently unknown H3K27me3-independent mechanism.

We previously observed that EZH2 and p38 interact in breast cancer (93), and the p38 MAPK was shown to phosphorylate EZH2 at T367 *in vitro (164),* but whether this modification occurs *in vivo* and how it relates to breast cancer was previously unknown. In this chapter, we developed and validated a novel antibody to assess pEZH2(T367) across a wide range of clinical specimens of invasive and metastatic breast carcinoma.

In normal breast lobules, when expressed, pEZH2(T367) was localized to the nucleus of epithelial cells. In contrast, 57% of invasive carcinomas and 74% of breast cancer metastasis exhibit upregulated pEZH2(T367) in the cytoplasm of breast cancer cells (**Fig 2.2A**). Cytoplasmic pEZH2(T367) was significantly associated with higher grade, ER- status, PR- status, and TNBC status, and the pattern of cytoplasmic pEZH2(T367) staining seemed to be common to many tumor types, particularly those of epithelial origin (**Fig 2.3**). The data suggest that EZH2 cytoplasmic localization a cancer-specific phenomenon in epithelial cells. Interestingly, we also observed strong cytoplasmic pEZH2 staining in normal alveolar macrophages (**Fig 2.3**), which may support the idea that the cytoplasmic functions of pEZH2 may occur in normal immune

cells. This observation is in line with previous studies of cytoplasmic EZH2 in immune cells that show that EZH2 can regulate actin polymerization in dendritic cells and migration of neutrophils (180).

Taken together, this chapter establishes the existence of EZH2 phosphorylated at T367 across a wide range of tissues and its cytoplasmic localization as a potential biomarker of aggressive breast cancer.

2-4 Methods

2-4.1 pEZH2 antibody development

Polyclonal pEZH2 (T367) was generated by immunization of KLH-conjugated NNSSRPS[Py]tPTINVLE peptide, corresponding to T367 of EZH2. Crude antibody sera were subjected to repeat affinity purification with phosphorylated peptide and negative adsorption with non-phosphorylated peptide.

2-4.2 Dot Blot

Increasing amounts of NNSSRPS[Py]tPTINVLE and NNSSRPS[nPy]tPTINVLE peptide were added to activated PVDF membrane (GenHunter Cat#B301-50). Membrane was stained with Ponceau S (Sigma P7170) to confirm loading. Membrane was blocked for 1 hour in 5% BSA (Sigma Aldrich, #A3059) in TBS-T (Bio-Rad, #161-0372 with 0.05% Tween 20) and incubated with custom pEZH2(T367) antibody overnight (1:2000), followed by incubation with Secondary antibodies used were Amersham ECL anti-rabbit IgG HRP-linked (GE Healthcare Life Sciences, #NA934). Signal was visualized using Pierce ECL Western Blotting substrate (Pierce Cat#32106).

2-4.3 Western Blot and myc-immunoprecipitation

Western blotting analyses were carried out as previously reported using 50 ug of whole cell extract or 2.5ug recombinant His-GST-EZH2 (BPS Bioscience Cat#50279) as previously reported (91). western blot using recombinant GST-EZH2. Briefly, cells were lysed in RIPA lysis buffer (Pierce #89900) with protease and phosphatase inhibitors (Thermo Scientific #1861281). Samples were resolved by SDS-PAGE, transferred onto PVDF membranes (GenHunter Cat#B301-50), and membranes were blocked and incubated with primary antibodies in 5% BSA (Sigma Aldrich, #A3059) in TBS-T (Bio-Rad, #161-0372 with 0.05% Tween 20) or 5% milk (Bio-Rad #170-6404) in TBS-T at 4°C overnight. Protein signals were detected using enhanced chemiluminescence (Pierce, #32106) as per the manufacturer's instructions. Primary antibodies used in this chapter included Cell Signaling antibodies: EZH2 (#5246), myc-tag (#2276), and B-Actin HRP (Santa Cruz, #sc47778) was used as for loading control. Secondary antibodies used were Amersham ECL anti-rabbit IgG HRP-linked (GE Healthcare Life Sciences, #NA934) or Amersham ECL anti-mouse IgG HRP-linked (GE Healthcare Life Sciences, #NA931).

Immunoprecipitations of myc-tagged proteins were performed using anti c-myc agarose resin (Pierce #20168) following the manufacturer's instructions.

2-4.4 Lambda Phosphatase and peptide competition assay

For cell lysate dephosphorylation assays, cells were lysed in RIPA buffer and lysate was treated with lambda phosphatase (NEB Cat#P0753) following manufacturer's

instructions. For peptide competition assay, lysate was incubated with non-phospho and competing phospho peptides (200-fold molar excess).

2-4.5 Cell lines

Breast cancer cell lines MDA-MB-231, MDA-MB-468 were purchased from the American Type Culture Collection and grown under recommended conditions. Stable knockdown and rescue of EZH2 was achieved by lentiviral transduction of EZH2 with pBabe-myc-EZH2 (wild-type) or pBabe-myc-EZH2 (T367A), both kind gifts from the laboratory of PL Puri (164). After transduction, cells were selected for antibiotic resistant with 2 ug/ml puromycin (Sigma Aldrich, #P9620), followed by knockdown using stable short-hairpin interfering RNA (MISSION shRNA, Sigma Aldrich) targeting the 3'UTR of Ezh2 (TRCN0000286227), as previously reported.(91) Oligos in the pLKO.1 vector were packaged into lentiviral particles at the University of Michigan Vector Core.

2-4.6 Tissue samples and immunohistochemistry

Tissues from 104 invasive carcinomas arranged in triplicate samples in a high density tissue microarray (TMA), 19 normal breast tissues, and 23 tissue samples of distant metastasis, previously characterized by our group were employed (208-210). Five micron-thick paraffin-embedded sections were de-paraffinized in xylene and rehydrated through graded alcohols to water. Heat Induced Epitope Retrieval (HIER) was performed in the Decloaking Chamber (Biocare Medical) with Target Retrieval, pH 6.0 (DakoCytomation). Slides were incubated in 3% hydrogen peroxide for 5 minutes to quench endogenous peroxidases. Anti-pEZH2(T367) (1:8000) developed by our lab and

anti-H3K27me3 (Cell Signaling Tri-Methyl-Histone H3 (Lys27) (C36B11) Rabbit mAb #9733, 1:200) were incubated with the tissue sections for 1.5 hours at room temperature. Antibodies were detected with Envision+ HRP Labeled Polymer (DakoCytomation) for 30 minutes at room temperature. HRP staining was visualized with the DAB+ Kit (DakoCytomation). Negative control slides were run. Slides were counterstained in hematoxylin, blued in running tap water, dehydrated through graded alcohols, cleared in xylene and then mounted with Permount. Expression of pEZH2 (T367) and H3K27me3 was analyzed blindly by two observers, at least twice. pEZH2 (T367) staining was categorized as nuclear or cytoplasmic, and as high and low based on the presence or absence of protein expression. The expression of H3K27me3 in the nucleus of cancer cells was scored using a four-tiered system based on intensity of staining and percentage of staining cells, with scores 1-2 categorized as low, and 3-4 as high (208, 211)

2-5. Figures

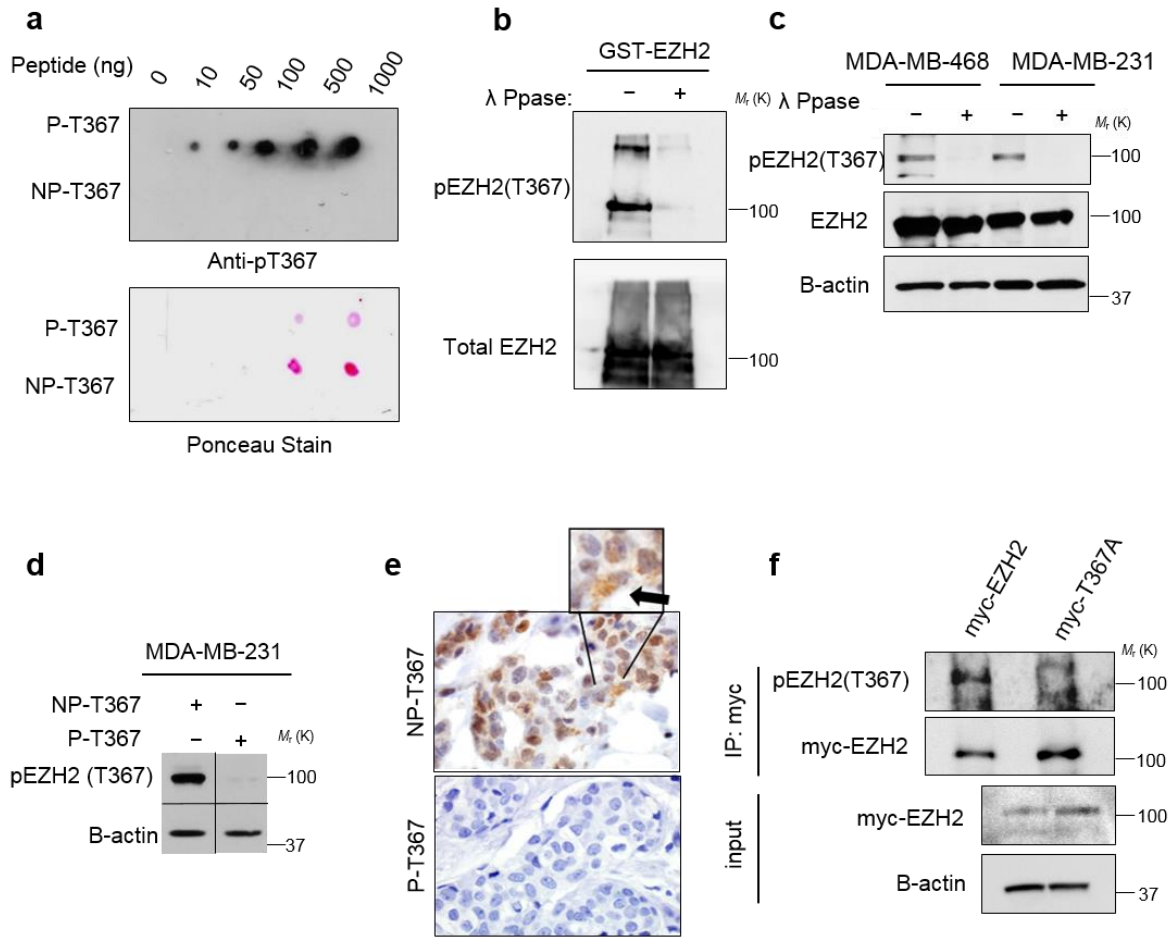

Figure 2.1 pEZH2(T367) can be detected *in vitro* and *in vivo*. a. Dot-blot assays performed using increasing quantities of phosphorylated (NSSRPS(pT)PTINVL) or non-phosphorylated (NSSRPSTPTINVL) peptides after incubation with affinity purified pEZH2 (T367) antibody. Ponceau stain shown as loading control. **b**. Western blot of recombinant His-GST-EZH2 treated with lambda phosphatase to dephosphorylate protein. **c.** Western blot using MDA-MB-468 and MDA-MB-231 whole cell lysates treated with lambda phosphatase to dephosphorylate protein. **d.** Peptide competition western blot of MDA-MB-231 whole cell lysates using pEZH2 antibody pre-incubated with 200-fold molar excess of either non-phosphorylated or phosphorylated peptide. **e.** Peptide competition immunohistochemistry of an invasive breast carcinoma using pEZH2 antibody pre-incubated with 200-fold molar excess of either non-phosphorylated or phosphorylated peptide. **f.** Immunoprecipitation myc antibody in MDA-MB-231 cells transduced to express myc-WT-EZH2 or myc-T367A-EZH2 followed by western blot with pEZH2(T367) (top), with input (bottom).

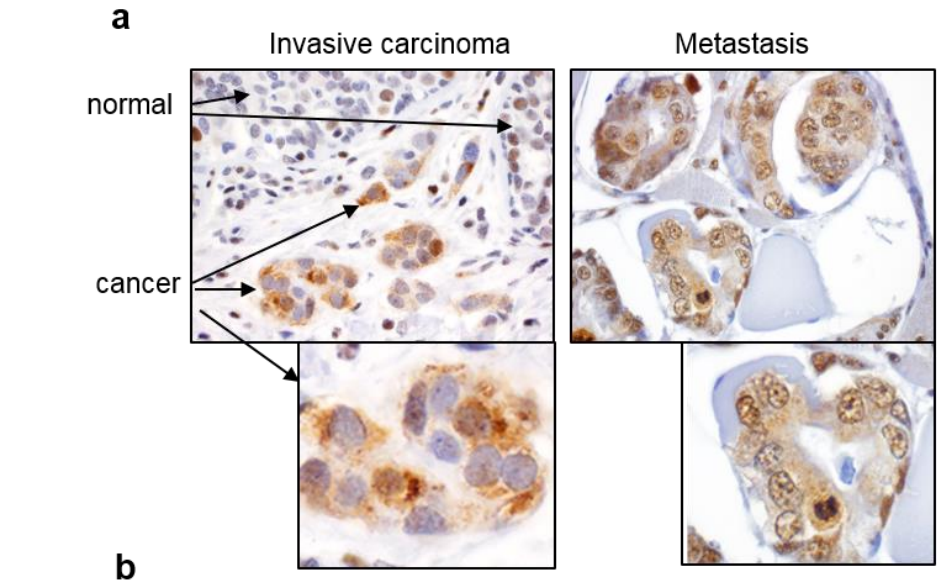

b

Diagnosis	Cyto pEZH2 Low, n (%)	Cyto pEZH2 High, n (%)
Normal	19 (100%)	0 (0%)
Invasive ca	45 (43%)	59 (57%)
Metastasis	6 (26%)	17 (74%)

Chi-square p<0.00001

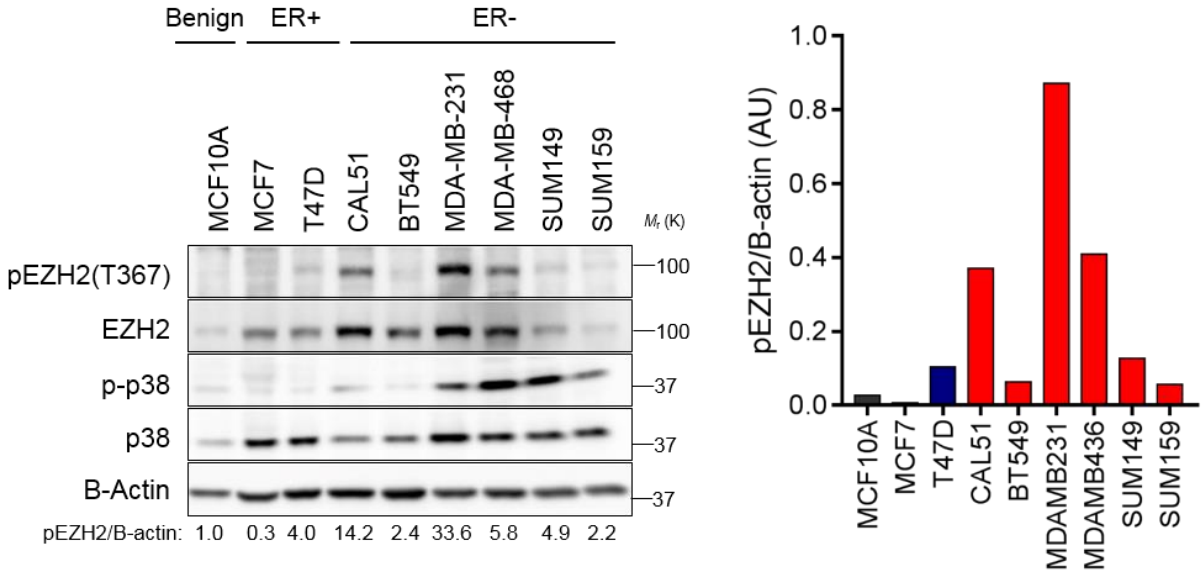

Figure 2.2. Phosphorylated EZH2 (T367) is expressed in the cytoplasm of invasive breast carcinoma and distant metastases. a. Immunohistochemical analysis of pEZH2(T367) expression using a novel, specific antibody in human tissue samples of 193 patients. Pictures show a representative invasive breast carcinoma with adjacent normal breast (left) and metastasis (right) (400x magnification). Insets show expression of pEZH2(T367) in cancer cells (600x magnification). **b**. Results are tabulated. Cytoplasmic

pEZH2 is significantly associated with invasive carcinoma and metastasis compared to normal and fibrocystic changes (Chi-square $p<0.00001$).

Variable	N	%
Cytoplasmic pEZH2(T367)		
Low	45	43.3
High	59	56.7
T-stage		
1	46	44.2
2	33	31.7
3	13	12.5
4	3	2.9
Missing	9	8.7
N Stage		
0	45	43.3
1	28	26.9
2	10	9.6
3	6	5.8
Missing	15	14.4
Histological Tumor Grade		
1	6	5.8
2	36	34.6
3	53	51.0
Missing	9	8.7
Estrogen Receptor		
Negative	40	38.5
Positive	51	49.0
Missing	13	12.5
Progesterone Receptor		
Negative	54	51.9
Positive	37	35.6
Missing	13	12.5
HER2/neu overexpression		
Negative	76	73.1
Positive	11	10.6
Missing	17	16.3

Table 3. Clinical and pathological characteristics of the invasive carcinomas.

Variable	Cytoplasmic pEZH2(T367)				
	Low		High		
	n	%	n	%	p-value
T Stage					
1	23	53.5	24	45.3	0.47
2	15	34.9	18	34.0	
3-4	5	11.6	11	20.8	
N Stage					
0	17	46.0	28	53.8	0.69
1	12	32.4	16	30.8	
2-3	8	21.6	8	15.4	
Histological Tumor Grade					
1	5	12.5	1	1.8	0.028
2	18	45.0	18	32.7	
3	17	42.5	36	65.5	
Estrogen Receptor					
Negative	9	22.5	31	60.8	0.0003
Positive	31	77.5	20	39.2	
Progesterone Receptor					
Negative	15	37.5	39	76.5	0.0002
Positive	25	62.5	12	23.5	
HER2/neu overexpression					
Negative	37	92.5	39	83.0	0.18
Positive	3	7.5	8	17.0	
Triple Negative					
No	34	85.0	23	50.0	0.0006
Yes	6	15.0	23	50.0	

Table 4. Associations between pEZH2(T367) cytoplasmic expression and clinical and pathological characteristics on the invasive carcinomas.

Epithelial origin	Cyto pEZH2
Lung (n)	
normal (1)	-
adenocarcinoma (5)	+
Intestine (n)	
colon (3)	-
adenocarcinoma (3)	+
Kidney (n)	
normal (2)	-
renal cell carcinoma (3)	+
Prostate (n)	
normal (1)	-
adenocarcinoma (2)	-
Liver (n)	
normal (3)	-
carcinoma (1)	+
Thyroid (n)	
normal (1)	-
carcinoma (5)	+

Non-epithelial origin	Cyto pEZH2
Brain (n)	
normal (2)	-
glioma (2)	-
Smooth muscle (n)	
normal (5)	-
leiosarcoma (1)	-
Testis (n)	
normal (1)	+
seminoma (1)	-
Lymphocytes (n)	
lymph node (2)	-
Hodgkin's lymphoma (3)	+
Thymus (n)	
normal (2)	-
thymoma (1)	-

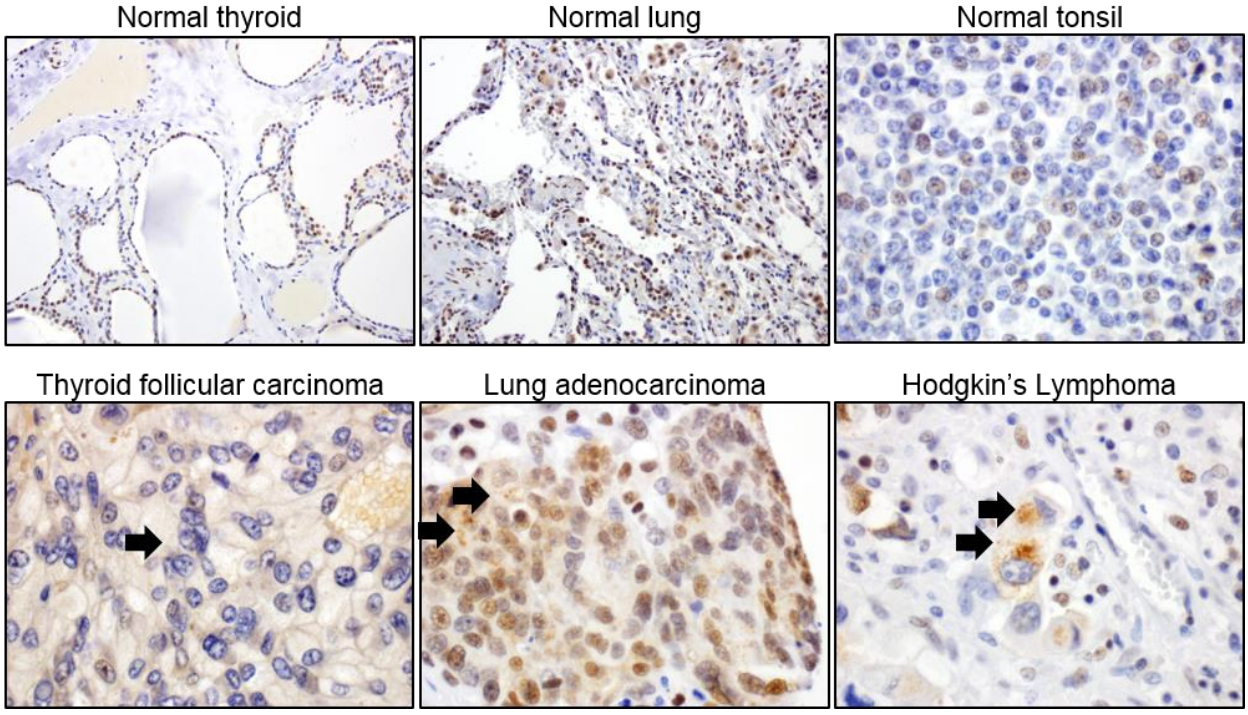

Figure 2.3. Survey of pEZH2(T367) expression in normal and malignant tissue. (Table, top) pEZH2(T367) expression in normal and neoplastic tissues of epithelial (left) and non-epithelial (right) origin. The presence of cytoplasmic pEZH2(T367) tissue is noted. (Bottom) Example immunohistochemical images of pEZH2(T367) expression

patterns in normal thyroid, lung, and tonsil, and thyroid follicular carcinoma, lung adenocarcinoma, and Hodgkin's lymphoma. Images taken at 400X magnification. Arrows delineate cells with pEZH2 in the cytoplasm.

Chapter 3: p38-mediated phosphorylation at T367 induces EZH2 cytoplasmic localization to promote breast cancer metastasis

3-1 Introduction

In chapter 2, we observed EZH2 phosphorylated at T367 was expressed in the cytoplasm of invasive breast carcinomas and that this was associated with higher grade, ER- status, PR- status, and TNBC subtype. Here, we establish the functional relevance of phosphorylation at this site.

We have demonstrated that EZH2 and p38α interact in aggressive ER- breast cancer cells (93), and EZH2 has been shown to undergo p38α -mediated T367 phosphorylation during muscle regeneration (164). However, direct demonstration that p38α phosphorylates EZH2 in solid tumors, the biological consequences of EZH2 T367 phosphorylation in breast cancer, and the mechanisms of pEZH2(T367) function are still unclear. Despite evidence of cytoplasmic EZH2 in aggressive breast cancers (92), studies have focused on the nuclear functions of EZH2, and the functions of EZH2 in the cytoplasm have remained elusive.

Here, we find that phosphorylation of EZH2 at T367 plays a critical role in breast cancer invasion and metastasis. In human invasive carcinomas and distant metastasis, cytoplasmic EZH2 phosphorylated at T367 is inversely correlated with global levels of H3K27me3. We uncover a previously unrecognized PRC2-independent mechanism by which phosphorylation of EZH2 at T367 promotes its cytoplasmic localization. Cytoplasmic localization is sufficient for conferring the migratory and invasive properties

of EZH2. Ectopic expression of a phospho-deficient mutant of EZH2 where T367 has been replaced with Ala is sufficient to inhibit EZH2 cytoplasmic expression, to disrupt binding to cytoskeletal regulators, and to reduce EZH2-mediated adhesion, migration, invasion, and the development of spontaneous metastasis. These results point to a novel non-canonical mechanism for EZH2 pro-metastatic function and suggest a new therapeutic approach for metastatic breast cancer.

3-2 Results

3-2.1 p38 phosphorylates EZH2 at T367 in breast cancer.

To examine the function and regulation of pEZH2(T367) in breast tumorigenesis, we used MDA-MB-231, MDA-MB-468, and SUM159 breast cancer cell lines which exhibit p38-EZH2 binding, high endogenous levels of p-p38 (93), and high pEZH2(T367) (**Fig 2.2C**). Quantitative Bio-Layer Interferometry (BLI) data with recombinant proteins indicated a strong binding affinity of EZH2 for p38α with binding affinity KD of 5.54 nM and kinetic constants: association rate of k_{on} = 4.68 x 106 [M-1s-1], and dissociation rate, k_{off} = 2.59 x 10-2 [s-1]. Affinity constant obtained from the kinetic analysis was in excellent agreement with the steady state analysis, KD of 3.4 nM, confirming the direct and strong binding interaction between EZH2 for p38α (**Fig. 3.1A**).

We next investigated the effect of p38α -mediated T367 phosphorylation on EZH2 function, through complementary and independent approaches to inhibit and to activate p38MAPK. Both p38α knockdown using stable lentiviral-mediated short hairpin RNA interference (shRNA) and chemical inhibition of p38α/β activity with SB202190 significantly reduced pEZH2(T367) protein in breast cancer cells without affecting total

levels of EZH2 and was accompanied by increased H3K27me3 levels (**Fig. 3.1B**). Activation of p38α, the most abundant isoform, occurs through a dual phosphorylation event at T180/T182 by upstream kinases MKK3 and MKK6(212). Transduction with an inducible, constitutively activated mutant MKK6 (MKK6EE)(213) resulted in increased p-p38 and pEZH2(T367) (**Fig. 3.1C**).

Demonstrating the significance of these results, clinical samples of invasive breast carcinoma showed a significant inverse association between cytoplasmic pEZH2(T367) and H3K27me3 levels (Chi-square $p<0.00001$, **Figs. 3.1D-E**). Taken together, these data show a direct interaction between p38α and EZH2, that p38α phosphorylates EZH2 at T367 in breast cancer cells and human tissues, and suggest that p38α -mediated phosphorylation reduces EZH2-mediated trimethylation of H3K27.

3-2.2 p38α-mediated phosphorylation at T367 is sufficient to promote EZH2 cytoplasmic localization.

Dox-induced MKK6 activation of p38α was sufficient to promote cytoplasmic localization of GFP-EZH2 expressed in MDA-MB-231 cells compared to controls (**Fig. 3.2A**). To directly investigate the relevance of phosphorylation at T367 to the subcellular localization of EZH2, we generated a GFP-tagged EZH2 mutant by replacing T367 with Ala (T367A). In MDA-MB-231, SUM159, and MDA-MB-468 cells, ectopic GFP-EZH2-T367A was nuclear and showed reduced localization to the cytoplasm (**Fig. 3.2B-C**), demonstrating that T367 phosphorylation is required for the cytoplasmic expression of EZH2. Further supporting this observation, fractionation of MDA-MB-231 and MDA-MB-

468 cells showed an enrichment of pEZH2(T367) in the cytoplasmic compartment and an absence in the chromatin-bound compartment compared to total EZH2 (**Fig. 3.2D**).

To test the relevance of cytoplasmic EZH2 to the neoplastic functions of breast cancer we developed an EZH2 mutant lacking the nuclear localization domain (ΔNLS-EZH2) (**Fig. 3.3A**). To avoid the contribution of endogenous EZH2 we first generated MDA-MB-231 cells with stable 3'UTR EZH2 knockdown followed by rescue with full length (WT-EZH2) and ΔNLS-EZH2 mutant adenoviral constructs (**Fig. 3.3B**). Rescue ΔNLS-EZH2 was sufficient to restore the reduced invasion and migration of MDA-MB-231 shEZH2 breast cancer cells to similar levels that WT-EZH2 (**Fig. 3.3C-D**). ΔNLS-EZH2 expression was cytoplasmic and retained the ability to interact with SUZ12 and EED but had no effect on H3K27me3 (**Fig 3.4**). Collectively, these data show that T367 phosphorylation is required for EZH2 cytoplasmic localization in breast cancer cells, and reveal that cytoplasmic EZH2 expression is sufficient to promote breast cancer cell migration and invasion.

3-2.3 pEZH2(T367) is essential for breast cancer migration and invasion in vitro, and metastasis in vivo.

We hypothesized that in the cytoplasm, pEZH2(T367) may regulate the migratory and invasive abilities of breast cancer cells, and set out to rescue the expression of WT-EZH2 and the phospho-deficient T367A-EZH2 mutant in MDA-MB-231, -468, and SUM159 cells with EZH2 3'UTR knockdown (**Fig. 4.5A**). In contrast with WT-EZH2, ectopic expression of T367A-EZH2 was unable to rescue breast cancer cell invasion (**Fig. 4.5B**). Based on the observation that T367A-EZH2 expressing cells adhered strongly to

the substrate during culture, we reasoned that EZH2 phosphorylation may regulate this function. Our studies demonstrate that T367A-EZH2 significantly increased attachment of breast cancer cells in adhesion assays compared to WT-EZH2 (**Fig. 4.5C**).

Ectopic expression of T367A-EZH2 was able to restore the proliferative abilities of knockdown-rescue cells as effectively as WT-EZH2 (**Fig. 4.5D-F**), demonstrating that T367 phosphorylation is dispensable for EZH2 proliferative functions. Our data also reveal that T367 phosphorylation did not significantly affect the stability of EZH2 protein or its ability to bind with other PRC2 proteins SUZ12 and EED (**Fig 4.6**).

As expected based on our previous results (91), MDA-MB-231 expressing shRNA against EZH2 formed smaller tumors than controls. Validating the dispensable role for T367 phosphorylation on cell proliferation observed in vitro, primary tumors formed by T367-EZH2 and WT-EZH2 were of similar size (**Fig. 4.7A**). Despite no differences in primary tumor growth kinetics (**Fig. 4.7B)**, T367A-EZH2 signficantly reduced the lung metastatic burden and ability to metastasize compared to WT-EZH2 (**Fig. 4.7C-E**). Together, these data document that T367 phosphorylation is critical for the metastasis-promoting function of EZH2 in breast cancer.

3-3. Summary and Discussion

EZH2 is a bona-fide oncogene in breast cancer, responsible for imparting proliferation, migration, and invasion abilities to breast cancer cells(90, 91, 93), but the mechanisms are incompletely understood. As the enzymatic component of PRC2, EZH2 has an established transcriptional repression through its catalysis of histone H3K27 trimethylation. However, the presence of high EZH2 levels in association with low

H3K27me3 in aggressive breast cancers suggests that EZH2 operates via a currently unknown H3K27me3-independent mechanism. Here, we discover the presence of upregulated phosphorylated EZH2 at T367 in clinical samples of invasive and metastatic breast carcinoma. Our study shows that p38-mediated phosphorylation at T367 promotes EZH2 cytoplasmic localization and binding to cytoskeletal regulatory proteins and is essential for breast cancer metastasis.

While most studies have focused on the role of EZH2 as a transcriptional repressor in cancer, there is mounting evidence that EZH2 has non-canonical functions involving transcriptional activation and methylation of non-histone proteins. We recently reported that in aggressive ER- breast cancer, EZH2 complexes with RelA/RelB and binds to the *Notch1* promoter to activate transcription independent of its methyltransferase activity (173). In castration-resistant prostate cancer EZH2 was also found to activate transcription of genes in a methyltransferase-independent manner(214). EZH2 has also been shown to methylate non-histone substrates; EZH2-mediated methylation of STAT3 leads to STAT3 activation and increased glioblastoma tumorigenicity(215). The present study reveals a previously undescribed oncogenic mechanism by which p38-mediated EZH2 phosphorylation at T367 promotes breast cancer progression by inducing EZH2 cytoplasmic function and reducing nuclear EZH2 methyltransferase activity on histone H3K27. These conclusions are supported by in vitro and in vivo functional and mechanistic studies and are validated in human breast cancer tissue samples.

Our lab and other investigators have established a role for EZH2 in breast cancer proliferation, migration, and invasion. We have demonstrated that EZH2 shRNA knockdown reduced the size of primary breast cancer xenografts compared to

controls(91). In this study, we show that phosphorylation of EZH2 at T367 specifically regulates the adhesive, migratory, and invasive properties of breast cancer cells without affecting their proliferation abilities. A phospho-deficient EZH2 mutant promoted proliferation to similar levels of wild type EZH2 but failed to promote breast cancer cell migration, invasion, and adhesion. Demonstrating an essential role for T367 phosphorylation on the ability of breast cancer cells to move and invade, mutation of T367 to alanine resulted in a significant decrease in distant metastatic burden without affecting primary tumor volume, and led to significantly improved metastasis free survival of mice.

In chapter 2 of this dissertation, we observed that in normal breast lobules, when expressed, EZH2 phosphorylated at T367 is localized to the nucleus of epithelial cells. In contrast, 57% of invasive carcinomas and 74% of breast cancer metastasis exhibited upregulated pEZH2 T367 in the cytoplasm of breast cancer cells. In this chapter, we found that phosphorylation of EZH2 at T367 is sufficient and necessary for cytoplasmic EZH2 localization in breast cancer cells in cell lines and clinical samples of invasive carcinoma. Cytoplasmic EZH2 has been observed previously in murine fibroblasts where it retains methyltransferase activity and regulates actin polymerization(216). In leukocytes, EZH2 was shown to methylate the cytoplasmic protein talin-1 to enhance migration by inhibiting the binding of talin-1 to F-actin (180). In breast cancer, we have reported cytoplasmic EZH2 protein in 16% of invasive ER- breast carcinomas from Ghanaian patients(92). Likewise, EZH2 expression has been observed in prostate cancer cells(217). Despite evidence that EZH2 is expressed in the cytoplasm of human malignancies, the mechanism has remained unexplored. Using EZH2 mutants with a deletion in the nuclear localization signal and a T367 phosphorylation deficient mutant, we directly demonstrate

that cytoplasmic localization and T367 phosphorylation are sufficient for EZH2-mediated breast cancer progression.

In muscle stem cells, injury induced p38-mediated EZH2 T367 phosphorylation leads to enhanced recruitment EZH2 to the *Pax7* promoter to promote muscle differentiation and subsequent EZH2 degradation(164),(165). In breast cancer, however, we observe that T367 phosphorylation appears to favor an H3K27me3-independent oncogenic mechanism without significantly affecting EZH2 protein stability. Our data are in agreement with a recent study showing that inhibition of EZH2 phosphorylation at T367 resulted in increased levels of H3K27me3 as well as similarly negligible changes in proliferation with expression of a T367A mutant. However, the authors observed increased migration and invasion with expression of the T367A mutant in MDA-MB-231 and benign MCF12A cells(192). The discordant functional findings might be explained by the approach used as well as the cellular context; the authors overexpressed wild-type or T367A EZH2 in MDA-MB-231 cells, which express high endogenous levels of EZH2, while we employed a knockdown-rescue approach. The association and mechanistic link between p38-mediated phosphorylation of EZH2 at T367, cytoplasmic localization, and breast cancer progression was validated in vitro, in vivo, and in human breast cancer samples.

Taken together, the findings in this chapter provide strong evidence for a critical function of pEZH2(T367) in breast cancer metastasis and uncover a novel mechanism whereby phosphorylation promotes cytoplasmic localization of EZH2 to promote the metastatic properties of breast cancer cells.

3-4 Methods

3-4.1 Cell culture.

Breast cancer cell lines MDA-MB-231, MDA-MB-468, MCF7, and non-tumorigenic breast epithelial cells, MCF10A, were purchased from the American Type Culture Collection and grown under recommended conditions. The CAL51 breast cancer cell line was purchased from German Collection of Microorganism and Cell Cultures (DSMZ GmbH; Cat. No. DSMZ ACC 302) and also grown as recommended. The SUM149 breast cancer cell line was obtained from the laboratory of S. Either (Karmanos Cancer Institute, Detroit) and maintained as reported previously.(218) Cell lines were tested for mycoplasma infection using Sigma LookOut Mycoplasma PCR Detection Kit (Cat MP0035).

Stable knockdown and rescue of EZH2 was achieved by lentiviral transduction of EZH2 with pBabe-myc-EZH2 (wild-type) or pBabe-myc-EZH2 (T367A), both kind gifts from the laboratory of PL Puri (164). After transduction, cells were selected for antibiotic resistant with 2 ug/ml puromycin (Sigma Aldrich, #P9620), followed by knockdown using stable short-hairpin interfering RNA (MISSION shRNA, Sigma Aldrich) targeting the 3'UTR of Ezh2 (TRCN0000286227), as previously reported.(91) Oligos in the pLKO.1 vector were packaged into lentiviral particles at the University of Michigan Vector Core.

Inducible activation of p38 MAPK was used using the pBabe pSLIK 3xHA-MKK6-EE neo plasmid, a kind gift from Kevin Janes (Addgene plasmid #47546). Cells were lentivirally transduced and selected with Geneticin (Gibco #10131) and treated with 2ug/ml doxycycline (Sigma Aldrich, #D3072) to induce activation of MKK6 as previously reported(164). Cells were treated The p38 inhibitors SB202190 (Cell Signaling #8158)

and SB203580 (Cell Signaling #5633) and were used at 20 uM for 48 hours as previously reported(93) p38a knockdown was achieved using stable short-hairpin interfering RNA (MISSION shRNA, Sigma Aldrich) (TRCN0000000510).

3-4.2 Western blotting and Immunoprecipitations

Western blotting analyses were carried out as previously reported using 50ug of whole cell extract, as previously reported(91). Briefly, cells were lysed in RIPA lysis buffer (Pierce #89900) with protease and phosphatase inhibitors (Thermo Scientific #1861281). Samples were resolved by SDS-PAGE, transferred onto PVDF membranes, and membranes were blocked and incubated with primary antibodies in 5% BSA (Sigma Aldrich, #A3059) in TBS-T (Bio-Rad, #161-0372 with 0.05% Tween 20) or 5% milk (Bio-Rad #170-6404) in TBS-T at 4°C overnight. Protein signals were detected using enhanced chemiluminescence (Pierce, #32106) as per the manufacturer's instructions. Primary antibodies used included Cell Signaling antibodies: EZH2 (#5246), Histone H3 (#9715), myc-tag (#2276), p38α MAPK (9218), trimethyl-histone H3 (Lys27) (#9733), SP1 (#9389) SUZ12 (#3737), phospho-p38 MAPK (#4511) phospho-Hsp27 (#2401); Abcam antibodies: EED (#ab4469), vinculin (#ab18058); Thermo Antibody: phospho-vinculin Y100 (Catalog #44-1074G); B-Actin HRP (Santa Cruz, #sc47778) was used as for loading control. Secondary antibodies used were Amersham ECL anti-rabbit IgG HRP-linked (GE Healthcare Life Sciences, #NA934) or Amersham ECL anti-mouse IgG HRP-linked (GE Healthcare Life Sciences, #NA931).

Immunoprecipitations of endogenous proteins was performed using magnetic Dynabeads following protocol instructions (Invitrogen, #10007D). Briefly, cells were lysed

in IP lysis buffer (Pierce #87788) with protease and phosphatase inhibitors (Thermo Scientific #1861281). Dynabeads were washed and incubated for 10 minutes with rotation with supplied antibody-washing buffer containing antibody for bead-antibody conjugation. Antibodies used for immunoprecipitation included EZH2 (Cell Signaling #5246), pEZH2 (custom antibody), and vinculin (#ab18058). After conjugation, beads were washed with supplied antibody-washing buffer and incubated with protein extract overnight at 4C. The next day, dynabead-antibody-antigen complexes were washed in stringent conditions and eluted with SDS-Laemmli Sample Buffer. Immunoprecipitations of myc-tagged proteins were performed using anti c-myc agarose resin (Pierce #20168) following the manufacturer's instructions.

For fractionation, the Thermo Subcellular Fractionation Kit for Cultured Cells (Catalog 78840) was used.

3-4.5 Wound healing, invasion, microfluidic migration, and cell attachment assays

Wound healing assays were performed by seeding cells in complete media a 6-well plate for 24-48 hours until a confluent monolayer had formed. Linear scratches were made using a sterile 200 ul pipette tip. Monolayers were washed three times with PBS to remove detached cells, and then complete media was added. Photographs of the wound were taken immediately after wound formation and 24h after with phase contrast microscopy. Wound area was measured over time using ImageJ.

In vitro invasion assays were performed using a 24-well matrigel invasion chamber (BD Biosciences, #354480), per manufacturer's instructions. All invasion experiments were performed with technical triplicates, and repeated at least three times with biological

replicates. Cells that had invaded through the matrigel membrane were fixed with methanol, stained with crystal violet, photographed at high resolution, and counted manually using ImageJ. The representative whole inserts were imaged under the same conditions, and are shown in this paper after increasing brightness by 20% across all images in Microsoft Powerpoint.

Microfluidic migration assays were performed using a previously published microfluidic migration platform(219, 220). To achieve higher throughput, the design was modified to have 450 migration channels per device, and the migration channel was designed to be 5 μm in height, 30 μm in width, and 1 mm in length. Before cell loading, collagen solution (1.45 mL Collagen (Collagen Type 1, 354236, BD Biosciences) and 0.1 mL acetic acid in 50 mL DI Water) was used to prime the device for one hour, and the cell culture medium flowed through the channel for one hour for better cell adhesion and viability. The cells were trypsinized, centrifuged, and then re-suspended to a concentration of 4 X 10^5 cells/ml for loading into the device. After cell loading, the cell suspension in the inlet was replaced by serum-free cell culture media, and 10% FBS serum cell culture media was applied to the other inlet to induce chemotactic migration. The microfluidic chip was then put into an incubator, and migration distance was measured based on the final cell position after 24 hours of incubation without medium replenishment. For data collection, cells were stained by LIVE/DEAD® Viability/Cytotoxicity Kit (Invitrogen, L3224) to distinguish live and dead cells. To have consistent results, we only use the data from central 300 (out of 450) migration channels. The images were analyzed by custom MATLAB code automatically (221). Cells were identified based on their fluorescence, and debris was ignored by their small size. For all

conditions in this work, 4 replicates (a total of 1,200 channels) were performed. Box graphs were plotted using Origin 9.0. The bottom and top of the box are the first and third quartiles, and the band inside the box is always the second quartile (the median). The ends of the whiskers represent the 5th percentile and the 95th percentile. The square inside the box indicates the mean, and the x outside the box indicates the minimum and maximum of all of the data.

Cell attachment assays were performed by trypsinizing 70% confluent cell dishes and seeding 1 x 10^5 cells in a 12 well plate. After 30 minutes, non-adherent cells were removed by washing wells with PBS three times. Adherent cells were then imaged and entire wells were counted using ImageJ.

3-4.6 Determination of binding affinity using Bio-Layer Interferometry (BLI) technology

Recombinant EZH2 (GST-EZH2 aa 2-end; MW = 114kDa; Bioscience) protein was biotinylated using the Thermo EZ-link Sulpho-NHS-LC-biotin biotinylation kit (cat. 21435). EZH2 protein and biotin were mixed in a 1:1 molar ratio in HBS buffer (10mM HEPES pH 7.4, 150mM NaCl) on ice for 2 hours. Reaction mixture was dialyzed in HBS buffer to remove excess biotin.

BLI experiments were performed using an OctetRED96 instrument from PALL/ForteBio. All assays were run at 30°C using HBS-P buffer (10mM HEPES pH 7.4, 150mM NaCl, 0.005% tween-20) with continuous 1000 rpm shaking. Biotinylated EZH2 was immobilized on Super Streptavidin (SSA) biosensors (ForteBio) by dipping sensors in 20 µg/mL protein solutions. Biotin labeled streptavidin protein was immobilized on SSA

sensors and used as inactive reference controls. Recombinant p38α (His-p38α aa 1-360; MW = 43kDa; Abcam) allowed to associate for 2 minutes and dissociate for 2 minutes. Collected raw kinetic data collected were processed with the Data Analysis software provide by ForteBio using double referencing in which both the buffer only sensors and inactive protein sensors were subtracted. Resulting data were analyzed based on the 1:1 binding model and kinetic parameters k_{on}, k_{off} and K_d were determined as well as steady state binding affinity.

3.4-7 Spontaneous metastasis model and xenograft immunohistochemistry

Eight-week old severe combined immunodeficiency mice (Jackson Laboratories) were used for examining tumorigenicity as previously reported(93). Briefly, GFP-Firefly-luciferase expressing MDA-MB-231 shVector, shEZH2 + pBabe, shEZH2 + WT-EZH2 or shEZH2 + T367A-EZH2 cells were orthotopically injected into the right inguinal mammary fat pad of anesthetized mice at a concentration of 10^6 cells resuspended in 50 ul of matrigel (n = 10 mice per group). Primary tumor growth was monitored semiweekly by caliper measurement as strong BLI signals quickly become saturated by rapid growth of primary MDA-MB-231 tumors. Metastases were monitored using bioluminescence imaging as previously described. Briefly, mice were anesthetized and injected i.p. with 75 mg/kg D-Luciferin (Xenogen) resuspended in PBS. Bioluminescence images were acquired using the IVIS imaging system (Xenogen) within approximately 2-5 minutes after injection. Analysis was performed using the Living Image software platform (Xenogen) by measuring photon flux, measured in photons/s/cm2/sr, by using a region of interest (ROI)

drawn around the bioluminescence signal to be measured and subtracting background measurements. All mice were sacrificed when the first primary tumor size reached 2 cm^3.

3-4.8 Immunohistochemistry, immunofluorescence, and proximity-ligation assays

Tumors, lungs, and bones of mice were collected, fixed in 10% neutral buffered formalin, and embedded in paraffin for immunohistochemistry. Immunofluorescence was performed by seeding cells into 2-well chambered slides (Thermo Fisher Lab-Tek #154461). 24 hr after seeding, cells were fixed with 4% PFA diluted in PBS for 15 minutes at room temperature, rinsed three times with PBS, and blocked for 1 hour using blocking buffer, 5% normal goat serum containing 0.3% Triton X-100 in PBS). After blocking, slides were incubated with primary antibody diluted in antibody buffer (5% bovine serum albumin containing 0.3% Triton X-100 in PBS) at 4C overnight. Next day, slides were washed 3 times with PBS and incubated with fluorescent secondary antibodies (Alexafluor goat-anti Rabbit 488 Cat # A-11008 or goat anti-mouse 594 Cat A-11005). Slides were washed 3 times with PBS and coverslipped using ProLong Diamond Antifade Mountant with DAPI (Thermo Fisher, Cat# P36962). Slides were imaged using Leica SP5 Inverted 2-Photon FLIM Confocal, and image analysis was performed using ImageJ.

3-4.9 Tissue samples and immunohistochemistry

Tissues from 104 invasive carcinomas arranged in triplicate samples in a high density tissue microarray (TMA), 19 normal breast tissues, and 23 tissue samples of distant metastasis, previously characterized by our group were employed (208-210). Five micron-thick paraffin-embedded sections were de-paraffinized in xylene and rehydrated

through graded alcohols to water. Heat Induced Epitope Retrieval (HIER) was performed in the Decloaking Chamber (Biocare Medical) with Target Retrieval, pH 6.0 (DakoCytomation). Slides were incubated in 3% hydrogen peroxide for 5 minutes to quench endogenous peroxidases. Anti-pEZH2(T367) (1:8000) developed by our lab and anti-H3K27me3 (Cell Signaling Tri-Methyl-Histone H3 (Lys27) (C36B11) Rabbit mAb #9733, 1:200) were incubated with the tissue sections for 1.5 hours at room temperature. Antibodies were detected with Envision+ HRP Labeled Polymer (DakoCytomation) for 30 minutes at room temperature. HRP staining was visualized with the DAB+ Kit (DakoCytomation). Negative control slides were run. Slides were counterstained in hematoxylin, blued in running tap water, dehydrated through graded alcohols, cleared in xylene and then mounted with Permount. Expression of pEZH2 (T367) and H3K27me3 was analyzed blindly by two observers, at least twice. pEZH2 (T367) staining was categorized as nuclear or cytoplasmic, and as high and low based on the presence or absence of protein expression. The expression of H3K27me3 in the nucleus of cancer cells was scored using a four-tiered system based on intensity of staining and percentage of staining cells, with scores 1-2 categorized as low, and 3-4 as high (208, 211)

3-4.9 Statistics

Results are presented as mean ± SD or mean ± SEM, unless otherwise noted. Comparisons between two groups were performed using an unpaired two-sided Student's t test for continuous variables or Chi-square test for categorical variables. A p value of < 0.05 was considered statistically significant.

3-4.10 Study Approval

All procedures using animals were conducted in accordance with the NIH Guide for the Care and Use of Laboratory Animals and were approved by the Institutional Animal Care and Use Committee at the University of Michigan (UCUCA#PRO 00005009).

3-5 Figures

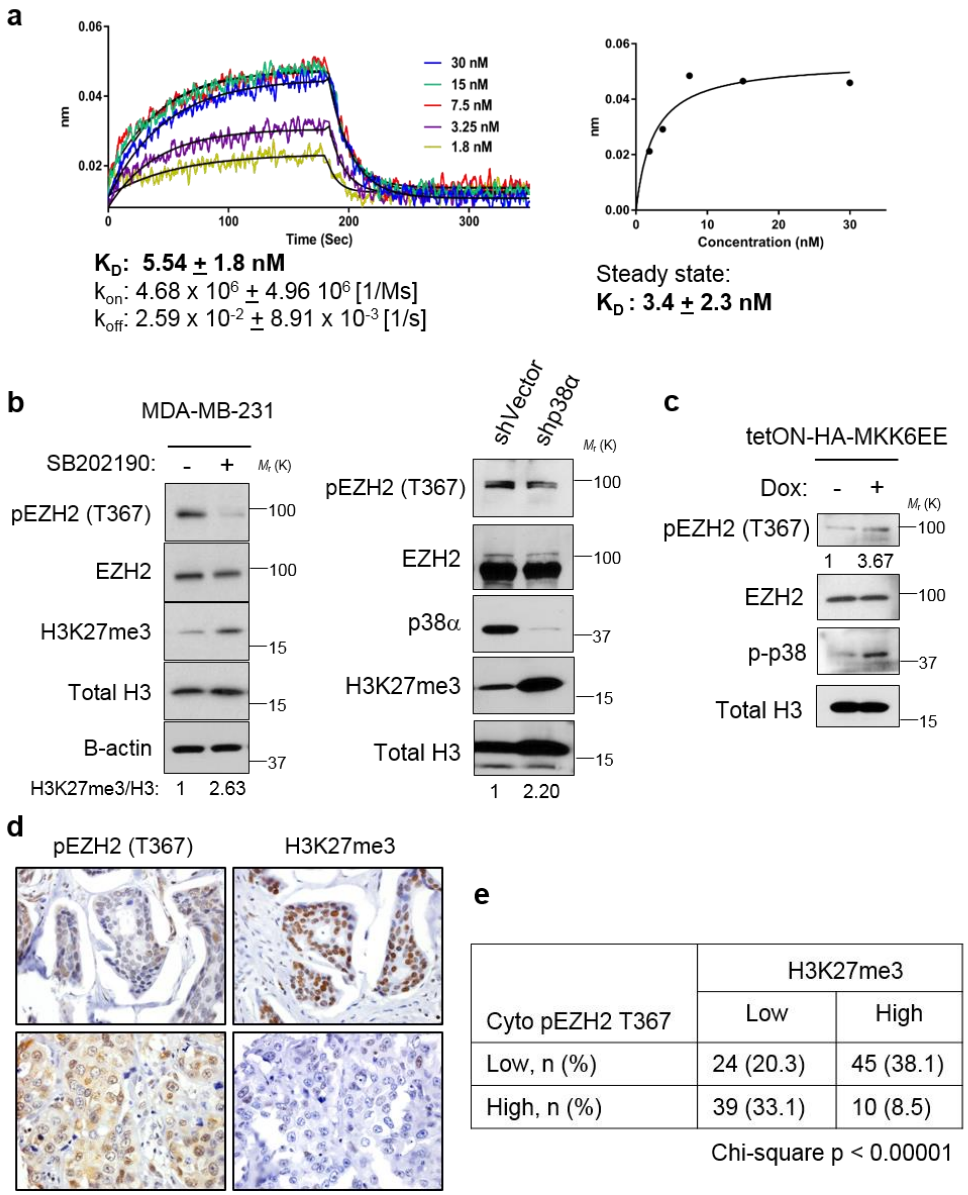

Cyto pEZH2 T367	H3K27me3	
	Low	High
Low, n (%)	24 (20.3)	45 (38.1)
High, n (%)	39 (33.1)	10 (8.5)

Chi-square p < 0.00001

Figure 3.1. p38 phosphorylates EZH2 in breast cancer. a. Quantitative analysis of the direct interaction between recombinant EZH2 and p38α proteins using BLI. EZH2 was immobilized on a sensor chip and a concentration series of p38α protein was added. Sensorgrams and corresponding fitting curves for kinetics constants and affinity determination (left) and corresponding plot of steady state response against concentration (right) for determination of binding affinity. b. Western blot of MDA-MB-231 cells treated with 20uM SB202190 for 48 hr (left panel) or with p38 shRNA (right panel) to pharmacologically and genetically inhibit p38 activity, respectively. c. Western blot of MDA-MB-231 cells transduced with dox-inducible MKK6EE to activate p38α. d-e. Immunohistochemical staining of 118 samples of human invasive breast carcinomas using pEZH2(T367) and H3K27me3 antibodies demonstrating a significant inverse association (Chi-square, p<0.00001) (400x magnification).

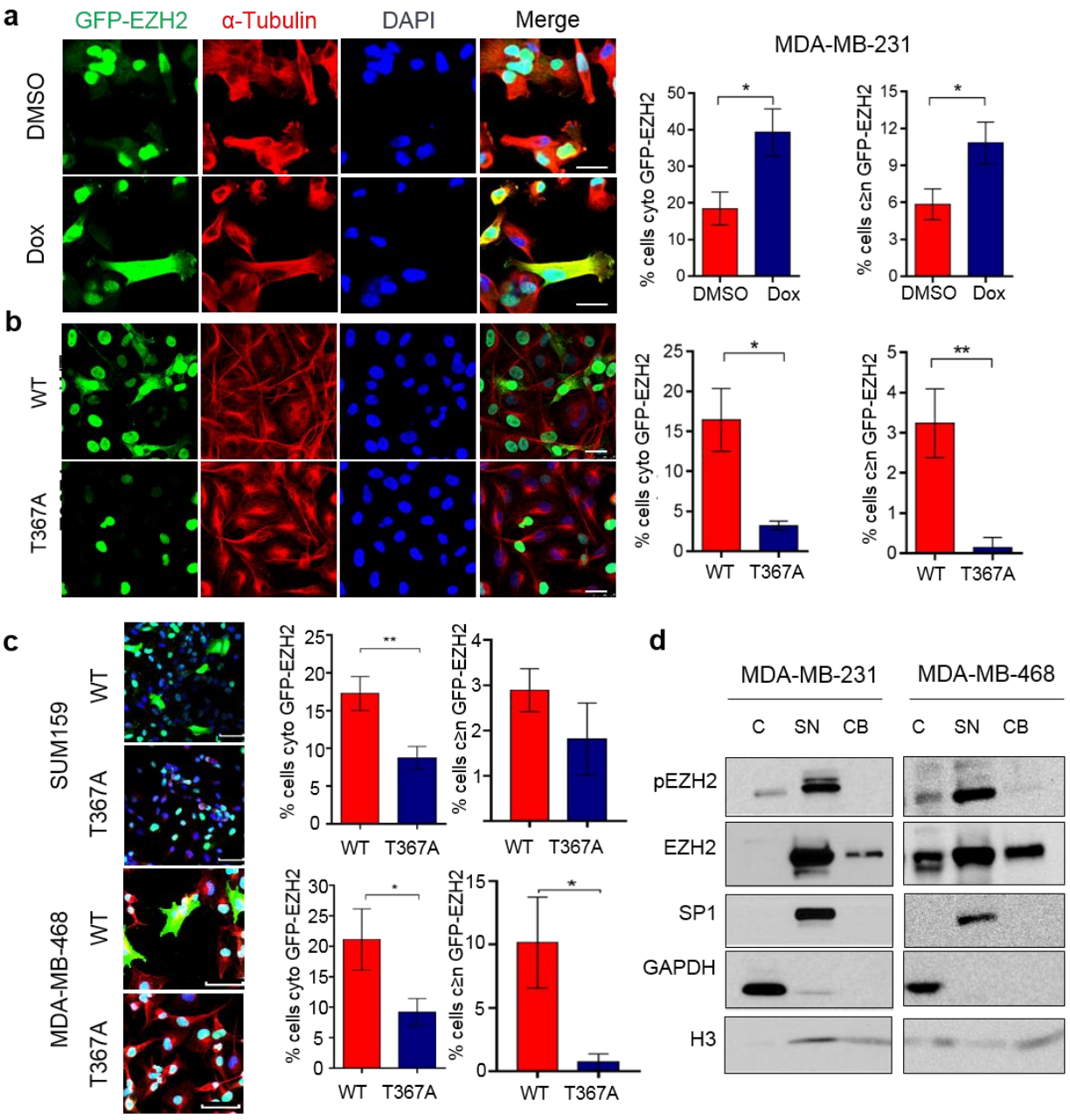

Figure 3.2 p38-mediated phosphorylation at T367 promotes EZH2 cytoplasmic localization. a. Immunofluorescence images of MDA-MB-231 cells transduced with lentiviruses to express GFP-EZH2 and a dox-inducible, constitutively active MKK6 kinase. The percentage of non-mitotic cells expressing cytoplasmic EZH2 and cytoplasmic GFP-EZH2 ≥nuclear expression was quantified. Scale bars, 25 um. b. Immunofluorescence images of MDA-MB-231 cells transduced with lentivirus to express GFP-EZH2 wild-type or T367A protein. The percentage of non-mitotic cells expressing cytoplasmic EZH2 was quantified. Scale bars, 25 um. c. Immunofluorescence images of SUM159 and MDA-MB-468 cells transduced with lentivirus to express GFP-EZH2 wild-type, or T367A protein. The number of non-mitotic cells expressing cytoplasmic EZH2 was quantified from ≥50

cells for each condition in three fields and graphicized on the right. Red, alpha-Tubulin, blue, DAPI. Scale bars, 50 um. d. Western blot analysis of MDA-MB-231 and MDA-MB-468 cell lines subjected to fractionation into cytoplasmic (C), soluble nuclear (SN), and chromatin-bound (CB) fractions. SP1, GAPDH, and Histone H3 used as subcellular fractionation compartment controls.

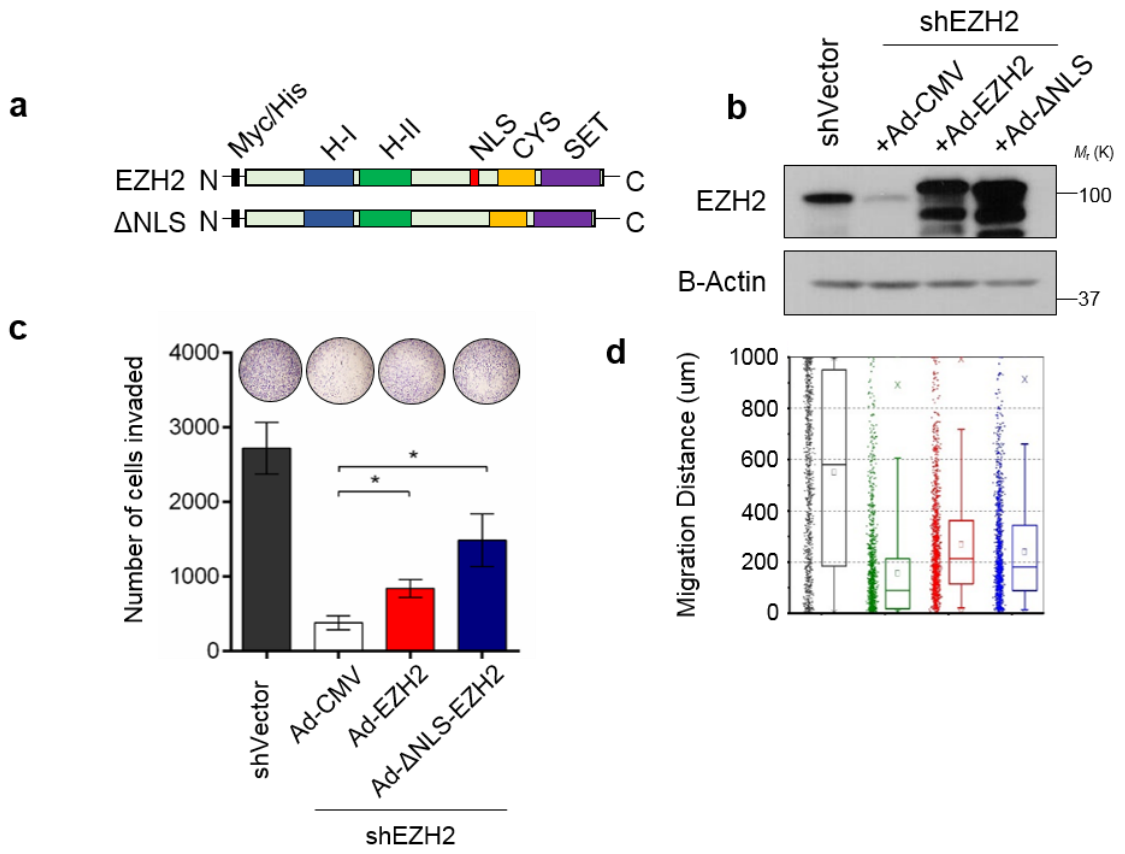

Figure 3.3 Cytoplasmic localization and is sufficient for migration and invasion of breast cancer cells. a. Schematic diagram of myc-tagged EZH2 and nuclear localization signal (NLS) mutant (top left). b. Western blot analysis of MDA-MB-231 cells showing EZH2 knockdown after lentiviral transduction with control shRNA (shVector) or 3' UTR EZH2-targeting shRNA (shEZH2) and rescue with myc-tagged Ad-EZH2 or Ad-ΔNLS mutant (top right). Ad-CMV, adenovirus control vector. c. Cell invasion assay of cells in (b) using a reconstituted Boyden basement membrane invasion chamber assay. d. Cell migration assays were performed in cells described in (b) using a high-throughput microfluidic migration platform to measure migration distance after 24 hr. Data are from at least three independent experiments carried out in at least triplicate and are presented as mean ± SD *p≤0.05; **p≤0.01

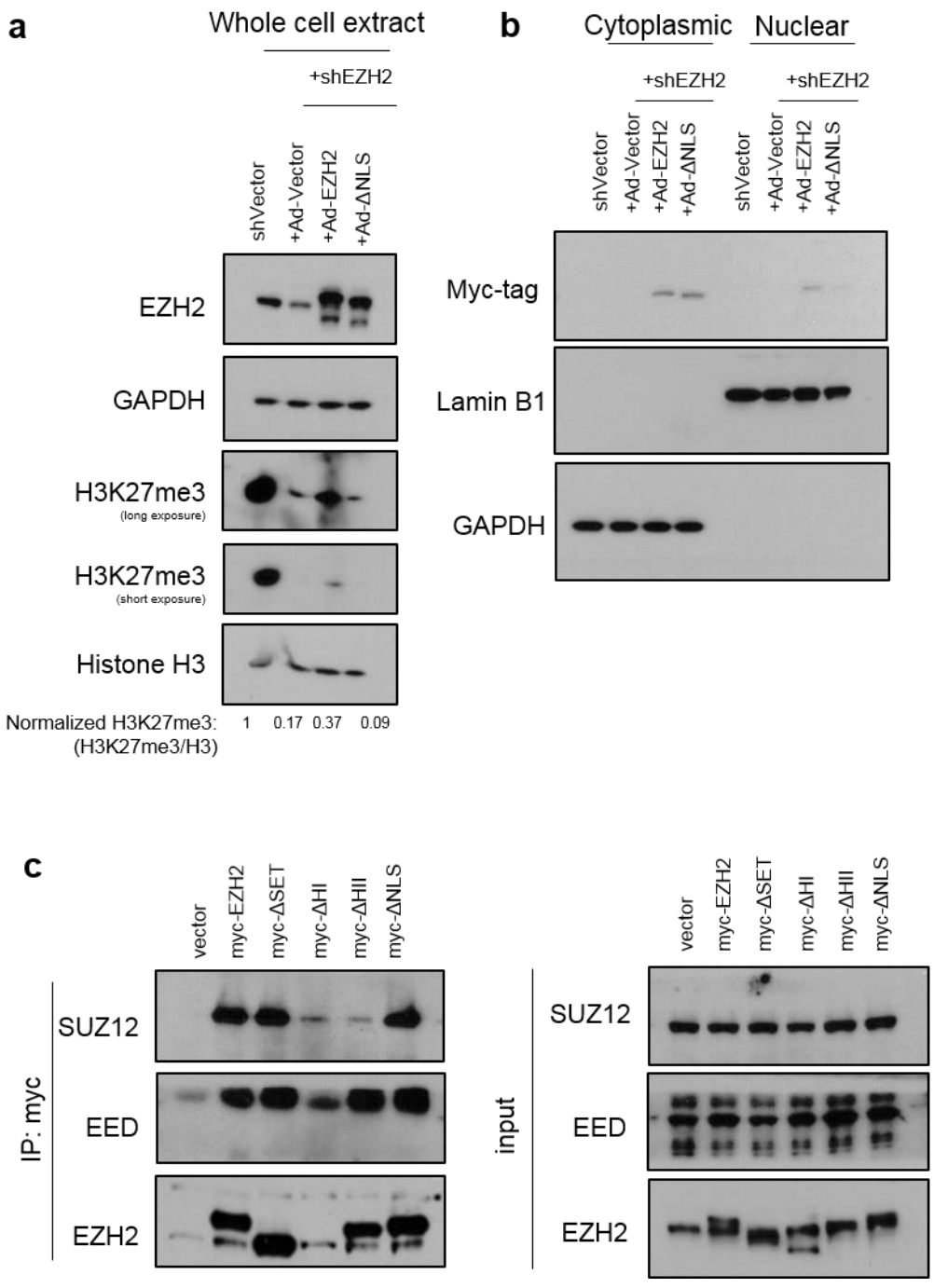

Figure 3.4. ΔNLS-EZH2 can incorporate into PRC2. a. Western blot analysis of MDA-MB-231 transduced with lentivirus to knockdown EZH2 and rescue with Ad-EZH2 or Ad-ΔNLS EZH2 whole cell lysate (a) and fractionated cells (b). c. Immunoprecipitation of myc-tag from MDA-MB-231 cells transduced with adenovirus to express vector, wild-type EZH2, or ΔSET, ΔHI, ΔHII, or ΔNLS domain deletion constructs. Western blot performed on immunoprecipitated protein for PRC2 members SUZ12 and EED. Right, input.

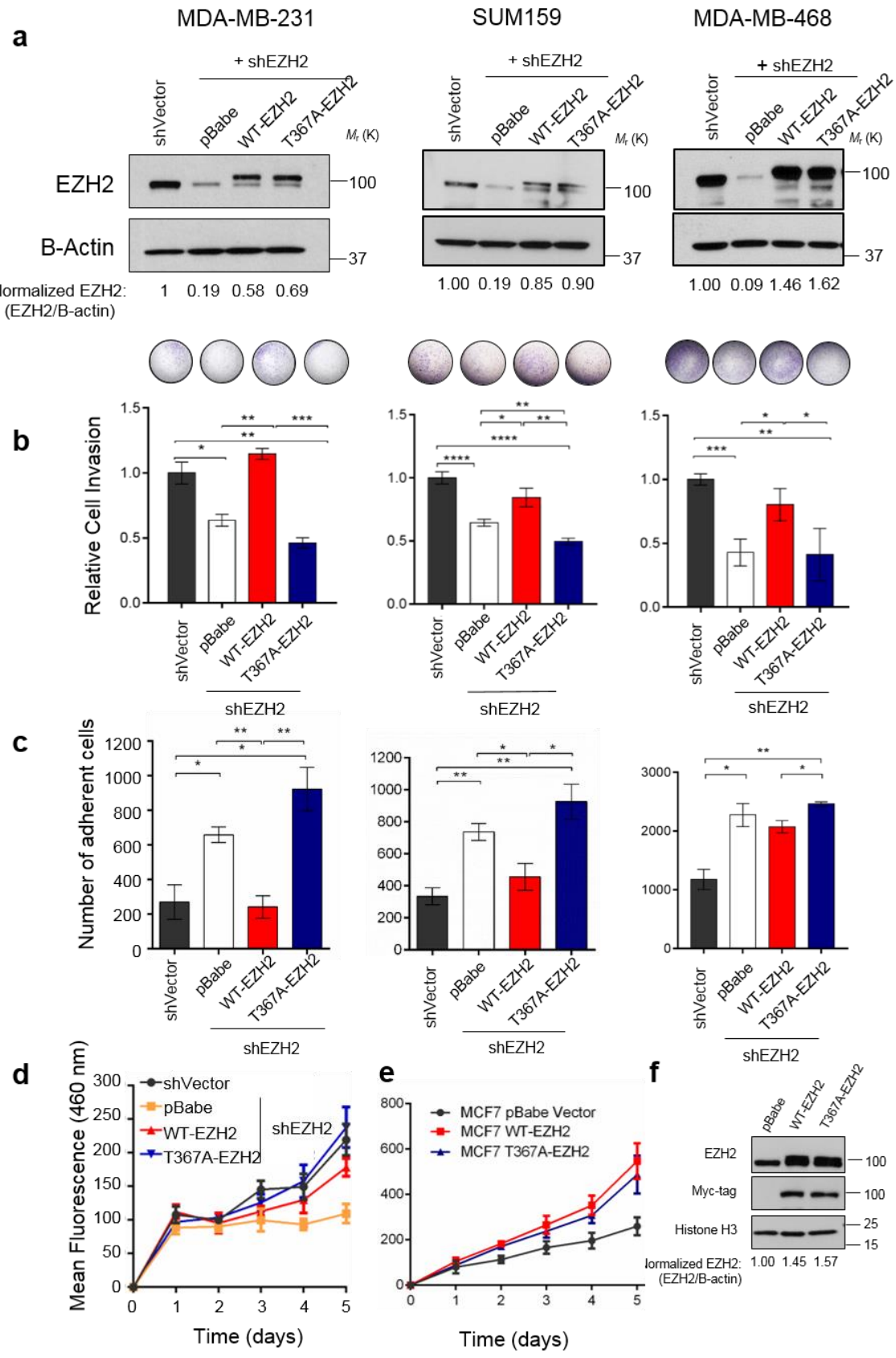

Figure 3.5. pEZH2(T367) promotes breast cancer cell invasion, and adhesion

without affecting cell proliferation. a. Western blot analysis of indicated breast cancer cells showing EZH2 knockdown after lentiviral transduction with control shRNA (shVector) or 3' UTR EZH2-targeting shRNA (shEZH2) and rescue with myc-tagged WT-EZH2 or T367A-EZH2. b. Reconstituted Boyden basement membrane invasive chamber assay of cells in (A). Representative chambers after crystal violet staining shown above bars. c. Cells described in (A) employed in a cell attachment assay. d. MDA-MB-231 cells described in (A) subjected to time course proliferation assay using Hoescht 33258 to quantify dsDNA. e. Data are from at least three independent experiments carried out in at least triplicate and are presented as mean ± SD. *p≤0.05; **p≤0.01; ***p≤0.005; ****p≤0.0001

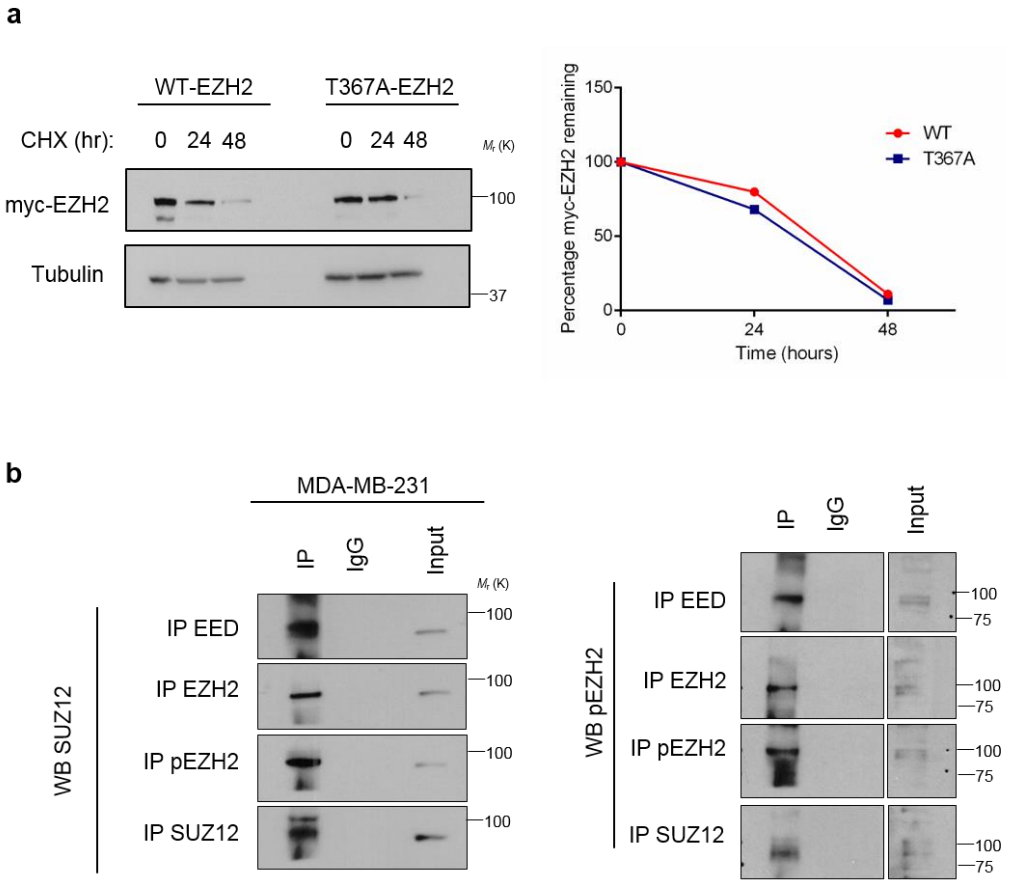

Figure 3.6. T367A-EZH2 not associated with stability, and pEZH2 can bind PRC2 members SUZ12 and EED. Related to Figures 2 and 3. a. Cycloheximide (CHX) pulse chase assay in MDA-MB-231 cells transduced with lentivirus to express myc-WT-EZH2 or myc-T367A-EZH2. Cells were seeded in a 6-well plate and treated with 100ug/ml CHX for 0, 24, and 48 hours. Left, immunoblot of myc-tag. Right, plotted quantified immunoblot, with myc-EZH2 stability over time normalized to tubulin expression. b. Co-immunoprecipitation followed by western blot experiments using the indicated antibodies from MDA-MB-231 whole cell lysates showing interaction of pEZH2 with SUZ12 and EED.

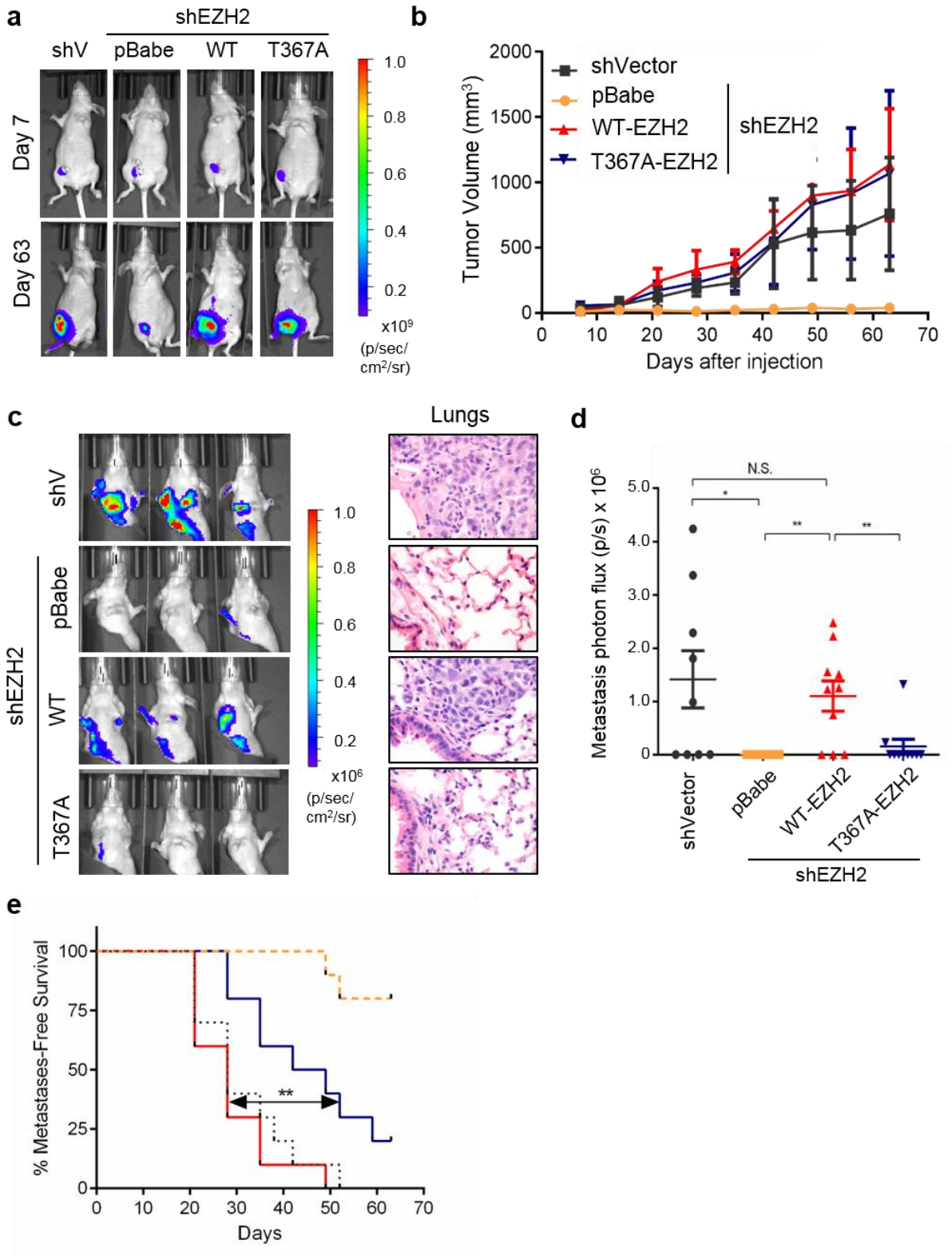

Figure 3.7. Inhibition of EZH2 T367 phosphorylation reduces breast cancer metastasis. a. Representative bioluminescence images of primary tumors at one and nine weeks post tumor implantation. b. Primary tumor growth curves of NOD/SCID mice

orthotopically-implanted with MDA-MB-231 EZH2 knockdown rescue cells (n=10 per condition) expressing GFP-Luciferase. Primary tumor growth as determined by caliper measurements, shown as mean ± SD. c. Representative bioluminescence images of metastases (primary tumor shielded), imaged at four weeks post tumor implantation (left) with representative H&E staining of lung tissue from each of the four groups at nine weeks post implantation (right, 600x magnification) d. Metastatic lung burden assessed by measuring photon flux measured four weeks post tumor implantation using Live Image Pro after shielding primary tumors. Data are presented as means ± SEM. e. Kaplan-Meier metastasis-free survival curve of mice as determined by presence of lung metastases with bioluminescence imaging showing difference between WT-EZH2 (red) and T367A-EZH2 (blue) knockdown-rescue groups. *p≤0.05; **p≤0.01

Chapter 4: EZH2 phosphorylation at T367 alters its interactome and promotes its binding to cytoplasmic partners

4.1 Introduction

In the previous chapter, we observed that p38-mediated phosphorylation of EZH2 at T367 contributes to the migration, invasion and metastasis of breast cancer cells. Mechanistically, we observed that this phosphorylation promoted a fraction of EZH2 to translocate to the cytoplasm. The cytoplasmic localization of EZH2 is sufficient to impart these migratory and invasive phenotypes. These data, taken with our observations from chapter 1 that cytoplasmic pEZH2(T367) significantly associated with tumor grade, ER-status, PR- status, and HER2- status in invasive breast carcinomas suggest that EZH2 exerts oncogenic functions in the cytoplasm.

In order to determine these functions, we employ an unbiased proteomics approach and uncover a phosphorylation-dependent ability of EZH2 to interact with cytoskeletal regulators in breast cancer cells. The data presented in this chapter pave the way for many new potential studies on EZH2 function in breast cancer.

4.2 Results

4.2.1 Phosphorylation at T367 changes the EZH2 interactome in breast cancer to promote binding to cytoplasmic proteins.

Based on the significant association between cytoplasmic pEZH2(T367) and breast cancer invasion and metastasis in clinical samples, and its critical role in promoting breast cancer progression, we hypothesized that pEZH2(T367) may interact with cytoplasmic and cytoskeletal regulatory proteins. To map pEZH2(T367) interactors, whole cell lysates of knockdown-rescue MDA-MB-231 cells expressing FLAG vector, FLAG-WT, or FLAG-T367A were affinity purified using FLAG immunoprecipitation. We then performed liquid chromatography/tandem mass spectrometry (LC/MS/MS) analysis of proteins that coprecipitated with wild-type or mutant EZH2 from MDA-MB-231 cell lysates. We scored wild-type and mutant EZH2 interactions using MS/MS spectral counting to calculate the Significance Analysis of Interactome (SAINT) probability and empirical fold-change scores (FC) for each prey protein using the CRAPome resource(222). Validating the robustness of the assay, we calculated the SAINT probabilities of the three biological replicates for known interactors of EZH2 (**Table 5**). Comparative analyses revealed 45 proteins that coprecipitated significantly more with FLAG-EZH2 than with FLAG-T367A, suggesting a requirement for T367 phosphorylation in regulating these potential interactions (**Fig. 4.1a**). Consistent with our subcellular localization studies, DAVID functional analysis showed enrichment for FLAG-EZH2 interactors in the cytoplasm and actin-binding functional annotations compared to FLAG-T367A (**Fig 4.1b**), which included important regulators of cell migration, adhesion, and invasion (**Fig 4.1c**).

4-2.2 pEZH2(T367) binds with vinculin in a p38-dependent manner in the cytoplasm of estrogen receptor-negative breast cancer cells.

Among the top differential interactors of pEZH2(T367) in the actin-binding set was vinculin, a cytoplasmic membrane and cytoskeletal protein found at focal adhesions with roles in breast cancer migration and invasion (223, 224). We validated and investigated the mechanistic details of the interaction between pEZH2(T367) and vinculin using multiple independent and complementary strategies. By immunofluorescence, pEZH2(T367) colocalized with vinculin in the cytoplasm of MDA-MB-231, -468, and SUM159 cells (**Fig 4.2a**). These data are further supported by immunofluorescence studies using GFP-T367A-EZH2 and ΔNLS-EZH2 in MDA-MB-231 cells (**Fig 4.2b-c**). Using proximity ligation assays (PLA) with confocal imaging, we detected pEZH2(T367)-vinculin interaction (<40 nm apart) in the cytoplasm of breast cancer cells (**Fig 4.2d-e**).

To investigate the details of the novel EZH2-vinculin interaction, we evaluated real-time interactions and quantified the binding affinity using BLI. Recombinant vinculin protein showed strong binding affinity of immobilized EZH2 with K_D of 15 nM and kinetic constants: association rate of k_{on} = 2.94 x 10^5 $\pm$ 3.80 x 10^5 [1/Ms] and dissociation rate, k_{off} = 3.85 x 10^{-3} $\pm$ 8.39 x 10^{-4} [1/s]. Affinity constant obtained from the kinetic analysis was in agreement with the steady state analysis with K_D value of 42 nM, confirming the direct and strong binding interaction between EZH2 and vinculin (**Fig. 4.2f**).

4-2.3 pEZH2(T367) promotes phosphorylation of vinculin at Y100

To determine whether p38 activation was required for EZH2-vinculin binding in breast cancer cells, we induced p38 MAPK signaling in MDA-MB-231 cells using the

tetON-HA-MKK6EE system. Activation of p38 led to an approximate 10-fold increase pEZH2(T367)-vinculin binding compared to uninduced controls (**Fig. 4.3a**).

We next investigated the consequences of the novel interaction between EZH2 and vinculin. Although our data demonstrate that pEZH2(T367) binds to PRC2 by co-immunoprecipitation and PLA studies, we found that vinculin does not interact with EED and SUZ12 (**Fig 4.2e**). Further supporting a PRC2-independent mechanism, we were unable to detect vinculin methylation after incubation with PRC2 by mass spectrometry (data not shown). These data coupled with the reported role of phosphorylation in vinculin activation at sites of focal adhesions (225, 226), suggested the hypothesis that p38-induced pEZH2(T367)-vinculin interaction may enhance vinculin phosphorylation and activation. We observed that induction of p38 activation increased vinculin Y100 phosphorylation (**Fig. 4.3b**), and that WT-EZH2 but not EZH2-T367A rescued phosphorylated vinculin Y100 levels and localization at sites of focal adhesions in MDA-MB-231 cells, suggesting that T367 phosphorylation of EZH2 is required for this function (**Fig. 4.3c**).

Taken together the data suggest that p38-mediated T367 phosphorylation of EZH2 in ER- breast cancer cells promotes a PRC2-independent interaction with cytoplasmic vinculin, leading to phosphorylation of vinculin at Y100 and localization at focal adhesions. Our data document that pEZH2(T367) interacts with cytoplasmic proteins in breast cancer cells uncovering a largely unexplored oncogenic mechanism in solid tumors. **Fig. 4.3d** shows our working model of pEZH2(T367) oncogenic functions.

4-3 Summary and Discussion

In this chapter, we investigated potential mechanisms of EZH2 function in the cytoplasm. Through an unbiased proteomics approach, we uncovered a phosphorylation-dependent ability of EZH2 to interact with cytoskeletal regulators in breast cancer cells. From our dataset we infer that phosphorylation promotes binding to proteins associated with actin-binding, cell adhesion, and cytosolic functions (**Fig. 4.1**). Among the top pEZH2(T367) actin-binding interactors is vinculin, an F-actin binding protein important for cell-cell and cell-matrix interactions through focal adhesion stabilization (227),(228). Vinculin is overexpressed in human malignancies, including breast cancer, where it regulates cell adhesion and migration (223, 224, 229-232). Through several complementary approaches, we find that EZH2 binds with vinculin at high affinity and regulates its activation at Y100 in a T367 phosphorylation-dependent manner. Phosphorylation of vinculin at this site is one of two events critical for cell spreading (226) and cellular transmission of force (225), which likely result from local conformational rearrangements that promote a more open and active state of vinculin (233). The data suggest one possible mechanism whereby EZH2 regulates this active state through direct interaction. How precisely the interaction of EZH2 and vinculin—which appears to be SUZ12- and EED- independent—promotes phosphorylation at this site requires further study.

Our proteomics analyses also uncovered other novel pEZH2(T367) interactors in breast cancer with roles in cytoskeletal organization that have not been previously studied in this context. Among these interactors are SYNE2, EPS8, EPS8 related protein 2, MLPH, and DBNL. SYNE2 (nesprin-2), an actin-binding nuclear envelope protein that

tethers the nucleus to the cytoskeleton, has been shown to promote pancreatic cancer metastasis (234). EPS8 (Epidermal Growth Factor Receptor Pathway Substrate 8) is a regulator of actin cytoskeleton dynamics with putative oncogenic functions in breast cancer(235). EPS8L2 is an EPS8 related protein which links growth factor signaling to actin reorganization(236). MLPH forms a complex with Rab effector proteins and regulates the movement of melanosomes in the cytoskeleton. DBNL is a cytosolic adaptor protein and putative suppressor of breast cancer metastasis (237). The contribution of vinculin and other pEZH2(T367) binding proteins to pEZH2 pro-metastatic functions may lead to new diagnostic, prognostic and therapeutic targets, and warrants in depth further investigations.

4-4 Methods

4-4.1 Affinity-Purification Mass Spectrometry

MDA-MB-231 knockdown rescue cells expressing FLAG-EZH2 or FLAG-T367A were washed three times with PBS, harvested, and lysed in Pierce IP Lysis Buffer (#87797) containing protease and phosphatase inhibitors (Thermo Scientific #1861281) and immunoprecipitated with anti-FLAG antibody beads (Sigma M8823). On-bead digestion followed by LC-MS/MS analysis was performed following the protocol optimized at the Proteomics Resource Facility at the University of Michigan. Briefly, the beads were resuspended in 50 ml of 100 mM ammonium bicarbonate buffer (pH ~8). Upon reduction (10 mM DTT) and alkylation (65 mM 2-chloroacetamide) of the cysteines, proteins were digested with 500 ng of sequencing grade, modified trypsin (Promega). Resulting peptides were resolved on a nano-capillary reverse phase column (Acclaim PepMap C18,

2 micron, 50 cm, ThermoScientific) using 0.1% formic acid/acetonitrile gradient at 300 nl/min (2-25% acetonitrile in 105 min; 25-40% in 20 min, followed by a 90% acetonitrile wash for 10 min and a further 25 min re-equilibration with 2% acetonitrile) and directly introduced in to *Q Exactive HF* mass spectrometer (Thermo Scientific, San Jose CA). MS1 scans were acquired at 120K resolution. Data-dependent high-energy C-trap dissociation MS/MS spectra were acquired with top speed option (3 sec) following each MS1 scan (relative CE ~28%). Proteins were identified by searching the data against *Homo sapiens* database (UniProtKB, v2014-4-13) using Proteome Discoverer (v2.1, Thermo Scientific). Search parameters included MS1 mass tolerance of 10 ppm and fragment tolerance of 0.1 Da; two missed cleavages were allowed; carbamidimethylation of cysteine was considered fixed modification and oxidation of methionine; deamidation of aspergine and glutamine; phosphorylation of Serine, Threonine and Tyrosine were considered as variable modifications. Percolator algorithm was used for discriminating between correct and incorrect identification and peptides/proteins with <1% FDR (false discovery rate) were retained for further analysis.

Interactions with EZH2 and mutant EZH2 were scored using empirical fold-change scores (FC) and significance analysis of interactome (SAINT) probabilities for each interaction calculated using the CRAPome resource(222). To calculate the FC scores (the primary FC-A score) and SAINT probabilities (using SAINTexpress (238)), the three FLAG-IP replicates of cells expressing only the empty vector were used as negative controls. Replicates were combined in FC scoring and in SAINT probability calculation using average values of the three biological replicates. Briefly, the FC scores represent the increase (or decrease) in protein abundances (estimated using MS/MS spectral

counts) in bait IPs relative to the control samples. SAINT calculates the probability that an interaction is a true positive using a model where true-positive and false-positive interactions for each bait are modeled statistically as distinct Poisson distributions. A value of 1 indicates a high probability of a bona-fide interaction (239).

PANTHER cellular component (gene ontology) analyses were performed on protein sets that were filtered using a SAINT probability cutoff of ≥0.7 and an FC score of ≥2. DAVID functional analysis was performed using a stricter SAINT cutoff of 0.9. (https://david.ncifcrf.gov/content.jsp?file=citation.htm; http://pantherdb.org/citePanther.jsp) . The background for these analyses were set as all of the proteins identified in the LC-MS/MS experiment (5800 proteins).

Venn diagrams were generated using the VennDiagram package in R version 3.3.2. Data-framing was performed using RStudio version 0.98. Graphs of enrichment analyses were generated in Prism6.

4-4.2 Western blotting and Immunoprecipitations

Western blotting analyses were carried out as previously reported using 50ug of whole cell extract, as previously reported(91). Briefly, cells were lysed in RIPA lysis buffer (Pierce #89900) with protease and phosphatase inhibitors (Thermo Scientific #1861281). Samples were resolved by SDS-PAGE, transferred onto PVDF membranes, and membranes were blocked and incubated with primary antibodies in 5% BSA (Sigma Aldrich, #A3059) in TBS-T (Bio-Rad, #161-0372 with 0.05% Tween 20) or 5% milk (Bio-Rad #170-6404) in TBS-T at 4°C overnight. Protein signals were detected using enhanced chemiluminescence (Pierce, #32106) as per the manufacturer's instructions.

Primary antibodies used included Cell Signaling antibodies: EZH2 (#5246), Histone H3 (#9715), myc-tag (#2276), p38α MAPK (9218), trimethyl-histone H3 (Lys27) (#9733), SP1 (#9389) SUZ12 (#3737), phospho-p38 MAPK (#4511) phospho-Hsp27 (#2401); Abcam antibodies: EED (#ab4469), vinculin (#ab18058); Thermo Antibody: phospho-vinculin Y100 (Catalog #44-1074G); B-Actin HRP (Santa Cruz, #sc47778) was used as for loading control. Secondary antibodies used were Amersham ECL anti-rabbit IgG HRP-linked (GE Healthcare Life Sciences, #NA934) or Amersham ECL anti-mouse IgG HRP-linked (GE Healthcare Life Sciences, #NA931).

Immunoprecipitations of endogenous proteins was performed using magnetic Dynabeads following protocol instructions (Invitrogen, #10007D). Briefly, cells were lysed in IP lysis buffer (Pierce #87788) with protease and phosphatase inhibitors (Thermo Scientific #1861281). Dynabeads were washed and incubated for 10 minutes with rotation with supplied antibody-washing buffer containing antibody for bead-antibody conjugation. Antibodies used for immunoprecipitation included EZH2 (Cell Signaling #5246), pEZH2 (custom antibody), and vinculin (#ab18058). After conjugation, beads were washed with supplied antibody-washing buffer and incubated with protein extract overnight at 4C. The next day, dynabead-antibody-antigen complexes were washed in stringent conditions and eluted with SDS-Laemmli Sample Buffer. Immunoprecipitations of myc-tagged proteins were performed using anti c-myc agarose resin (Pierce #20168) following the manufacturer's instructions.

4-4.3 Immunohistochemistry, immunofluorescence, and proximity-ligation assays

Tumors, lungs, and bones of mice were collected, fixed in 10% neutral buffered formalin, and embedded in paraffin for immunohistochemistry. Immunofluorescence was performed by seeding cells into 2-well chambered slides (Thermo Fisher Lab-Tek #154461). 24 hr after seeding, cells were fixed with 4% PFA diluted in PBS for 15 minutes at room temperature, rinsed three times with PBS, and blocked for 1 hour using blocking buffer, 5% normal goat serum containing 0.3% Triton X-100 in PBS). After blocking, slides were incubated with primary antibody diluted in antibody buffer (5% bovine serum albumin containing 0.3% Triton X-100 in PBS) at 4C overnight. Next day, slides were washed 3 times with PBS and incubated with fluorescent secondary antibodies (Alexafluor goat-anti Rabbit 488 Cat # A-11008 or goat anti-mouse 594 Cat A-11005). Slides were washed 3 times with PBS and coverslipped using ProLong Diamond Antifade Mountant with DAPI (Thermo Fisher, Cat# P36962). Slides were imaged using Leica SP5 Inverted 2-Photon FLIM Confocal, and image analysis was performed using ImageJ. For immunofluorescence imaging and quantitation of phospho-vinculin Y100 focal adhesion, 8-well chambered slides (Thermo Fisher Lab-Tek Cat #154534) were first coated with fibronectin (Sigma Fibronectin F0895) per the manufacturer's coating protocol at a dilution of 2 ug/ml, and immunofluorescence was carried out as outlined above. For post-imaging analysis, we followed a previously published protocol from Horzum et al., which details a step-by-step quantitative analysis of focal adhesions from MDA-MB-231 breast cancer cells,(240) quantifying focal adhesions from 70-100 cells per condition across at least 5 separate fields.

For proximity ligation assays, cells were seeded in 8-well chambered slides (Thermo Fisher Lab-Tek Cat #154534). 24 hr after seeding, cells were fixed with 4% PFA diluted in PBS for 15 minutes at room temperature, rinsed three times with PBS, and blocked for 1 hour using blocking buffer, 5% normal goat serum containing 0.3% Triton X-100 in PBS). After blocking, slides were incubated with primary antibody diluted in antibody buffer (5% bovine serum albumin containing 0.3% Triton X-100 in PBS) at 4C overnight. Next day, slides were washed 3 times with PBS and incubated with DuoLink PLA probes (Sigma, Cat #DUO92101) and protocol for PLA secondary antibody incubation, ligation, amplification, and washes were performed following the manufacturer's protocol. Slides were imaged using Leica SP5 Inverted 2-Photon FLIM Confocal. Positive signals were normalized to single-primary antibody control (pEZH2, 1:500) and image analysis was performed using ImageJ. Images were taken under the same conditions, and if manipulated for representative images, brightness was increased across all images equally.

4-4.4 Determination of binding affinity using Bio-Layer Interferometry (BLI) technology

Recombinant EZH2 (GST-EZH2 aa 2-end; MW = 114kDa; Bioscience) protein was biotinylated using the Thermo EZ-link Sulpho-NHS-LC-biotin biotinylation kit (cat. 21435). EZH2 protein and biotin were mixed in a 1:1 molar ratio in HBS buffer (10mM HEPES pH 7.4, 150mM NaCl) on ice for 2 hours. Reaction mixture was dialyzed in HBS buffer to remove excess biotin.

BLI experiments were performed using an OctetRED96 instrument from PALL/ForteBio. All assays were run at 30°C using HBS-P buffer (10mM HEPES pH 7.4, 150mM NaCl, 0.005% tween-20) with continuous 1000 rpm shaking. Biotinylated EZH2 was immobilized on Super Streptavidin (SSA) biosensors (ForteBio) by dipping sensors in 20 µg/mL protein solutions. Biotin labeled streptavidin protein was immobilized on SSA sensors and used as inactive reference controls. Recombinant human vinculin (His-vinculin Cat: 10019-H08H) allowed to associate for 2 minutes and dissociate for 2 minutes. Collected raw kinetic data collected were processed with the Data Analysis software provide by ForteBio using double referencing in which both the buffer only sensors and inactive protein sensors were subtracted. Resulting data were analyzed based on the 1:1 binding model and kinetic parameters k_{on}, k_{off} and K_d were determined as well as steady state binding affinity.

4-5. Figures

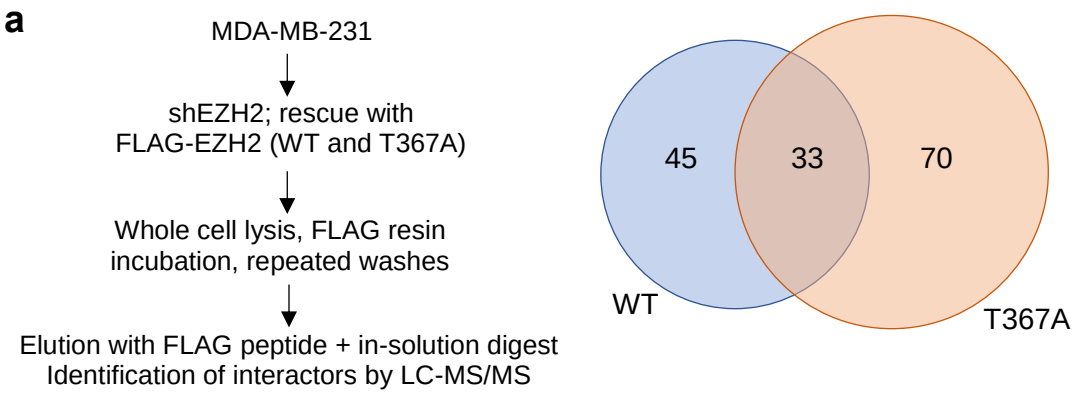

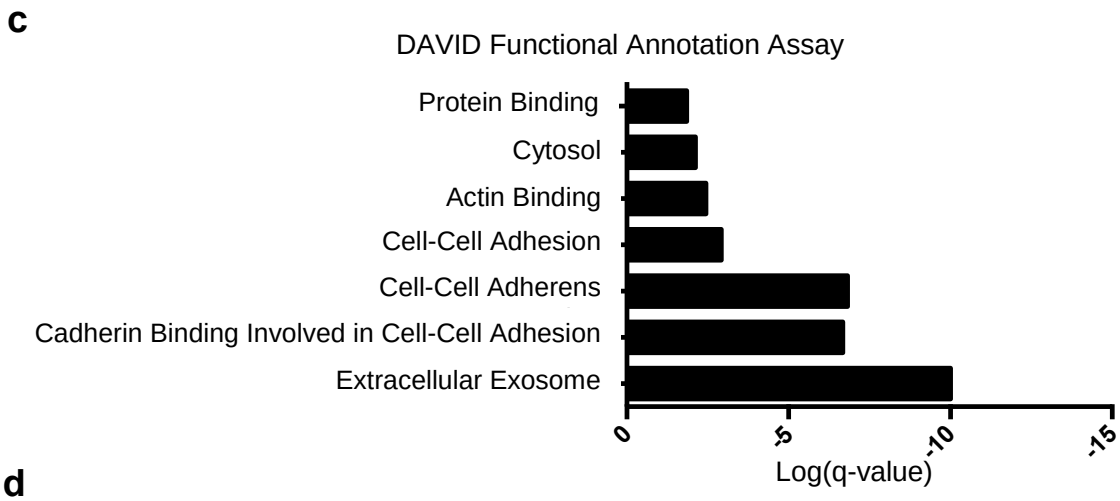

d

GENE_ID	WT_FC_A	T367A_FC_A	AVERAGE_WT_SC	AVERAGE_T367A_SC	AVERAGE_control_SC	WT_SP	T367A_SP
SYNE2	22.9	4.8	27	4	0	1	0.7
EPS8	7.2	0.6	22	0.3	2	0.9	0
MLPH	5.3	1.1	16	2	1.7	1	0.2
MYO1F	5.14	4.97	16	13.3	2	0.94	0.67
VCL	4.2	3.1	26.3	16.7	4	1	0.8
DBNL	3.9	3	3.7	2.3	0	1	0.7
EPS8L2	3.5	1.7	10.3	4	1.3	1	0.5

Figure 4.1. The interactome of pEZH2(T367) reveals new cytoplasmic binding proteins. a. Schematic of mass spectrometry experiment to identify binding partners of EZH2 in MDA-MB-231 cells. Experiment was performed in triplicate. **b.** Venn diagram displaying interactors overlap in proteins co-immunoprecipitating with WT- or T367A-EZH2 from the three biological replicates analyzed. **c.** DAVID functional annotation analysis of processes enriched in WT-EZH2 over T367A-EZH2. **d.** List of differential interactors identified from actin-binding set with fold-change (FC) scores and normalized FC scores based on total EZH2 pulldown. Average WT and T367A spectral counts (SC) and SAINT probabilities (SP) are also tabulated.

WT-EZH2 and T367A-EZH2 known interactors

Gene ID	WT FC-A	T367A FC-A	WT Normalized FC-A	T367A Normalized FC-A	Average WT SC	Average T367A SC	Average Control SC	WT-SP	T367A-SP
EZH2	71.2	270.9	1.0000	1.0000	92.7	338.7	0.0	1.0	1.0
SUZ12	39.3	106.1	0.5519	0.3918	52.0	131.7	0.0	1.0	1.0
EED	38.2	224.8	0.5363	0.8297	49.3	298.0	0.0	1.0	1.0
PHF19	4.8	17.0	0.0670	0.0628	5.0	20.0	0.0	1.0	1.0
PHF1	4.4	18.1	0.0624	0.0666	4.3	20.3	0.0	1.0	1.0
JARID2	3.9	10.4	0.0553	0.0385	4.0	11.0	0.0	1.0	1.0
TK1	3.0	4.8	0.0426	0.0179	2.7	4.7	0.0	0.7	1.0
CTNNB1	2.7	3.2	0.0375	0.0117	11.0	12.3	2.3	0.5	0.6
PHB2	2.4	1.4	0.0337	0.0050	11.0	4.3	3.7	0.3	0.0
RASA1	2.3	2.1	0.0320	0.0076	1.3	1.0	0.0	0.3	0.3
SMS	2.2	1.4	0.0302	0.0050	1.3	0.3	0.0	0.6	0.0
USP7	1.5	2.0	0.0212	0.0072	9.7	13.3	4.3	0.1	0.3
GNAS	1.4	1.2	0.0195	0.0044	4.0	3.3	1.7	0.3	0.3
WDR61	1.4	2.3	0.0190	0.0085	0.3	1.3	0.0	0.0	0.3
RBBP4	1.4	2.3	0.0190	0.0083	20.7	32.7	10.3	0.1	0.7
CDK1	1.3	1.6	0.0178	0.0058	8.3	10.7	4.7	0.1	0.4
RELA	0.7	1.4	0.0097	0.0052	1.0	3.3	1.3	0.0	0.5
STAT3	0.7	1.7	0.0095	0.0063	5.3	13.3	5.0	0.0	0.4
MTF2	0.0	3.8	0.0000	0.0139	0.0	3.7	0.0	0.0	0.7

Table 5. WT- and T367A-EZH2 known interactors identified by mass spectrometry. List of differential interactors identified from actin-binding set with fold-change A (FC-A) scores and normalized FC-A scores based on total EZH2 pulldown. Average WT- and T367A spectral counts (SC) and SAINT probabilities (SP) are also displayed.

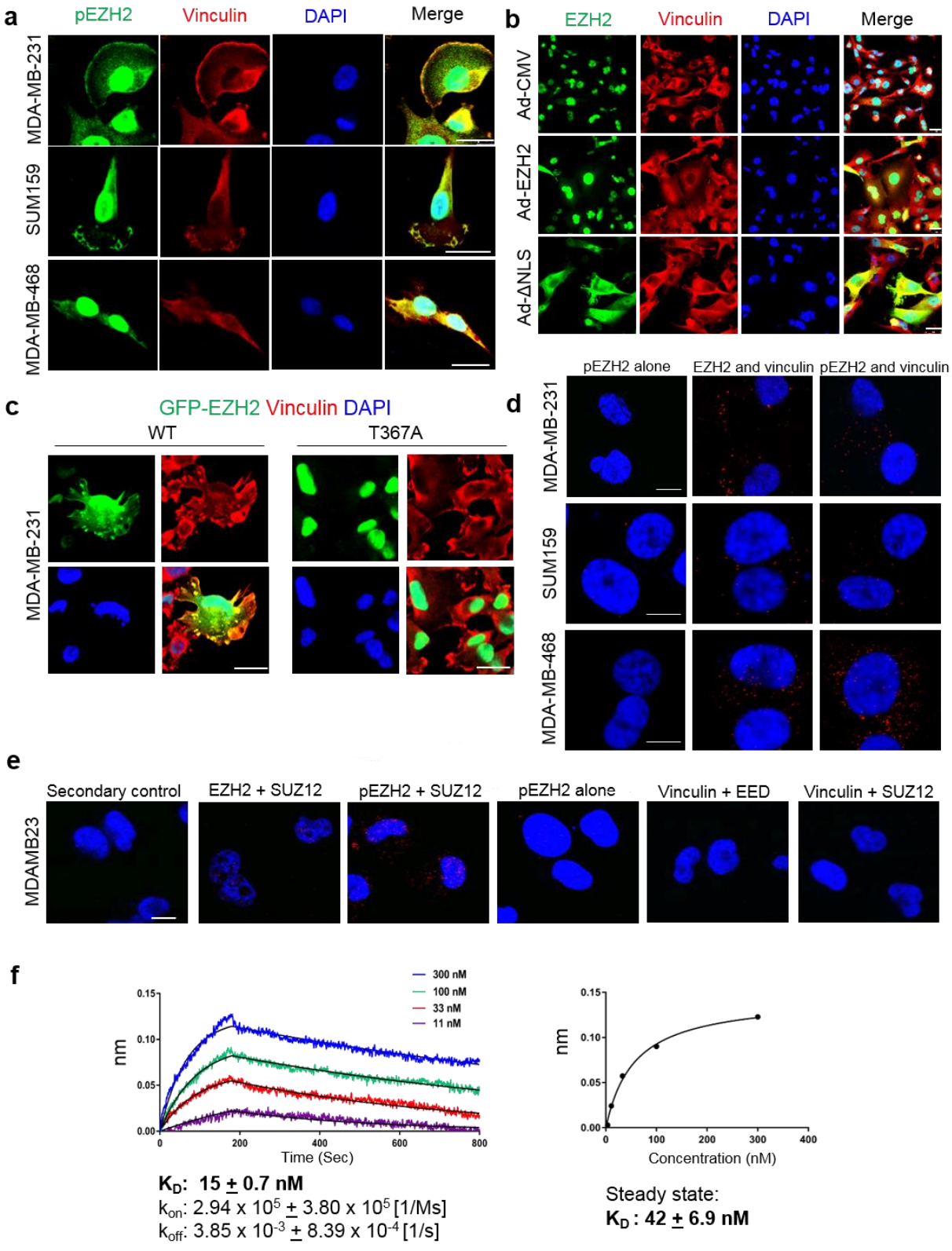

K_D: 15 ± 0.7 nM

k_{on}: 2.94 x 10^5 ± 3.80 x 10^5 [1/Ms]

k_{off}: 3.85 x 10^{-3} ± 8.39 x 10^{-4} [1/s]

Figure 4.2. EZH2 and vinculin interact. a. Immunofluorescence staining of pEZH2(T367) and vinculin counterstained with DAPI imaged by confocal microscopy in the indicated breast cancer cell lines. Scale bars, 25 um. **b.** Immunofluorescence imaging of MDA-MB-231 cells transduced with Ad-vector, Ad-EZH2, or Ad-ΔNLS mutant. Cells were stained for EZH2 (green) and vinculin (red), and counterstained with DAPI. Scale bars, 25 uM. **c.** Immunofluorescence images of MDA-MB-231 cells transduced with GFP-WT-EZH2 or GFP-T367A-EZH2 (green); vinculin (red). Scale bars, 25 um. **d-e.** Proximity ligation images depicting co-localization with the indicated proteins by red fluorescent dots in the indicated cell lines. Scale bars, 10 um. **f.** Quantitative analysis of the direct interaction between recombinant EZH2 and vinculin proteins using BLI. EZH2 was immobilized on a sensor chip, and a concentration series of vinculin protein was added. Sensorgrams and corresponding fitting curves for kinetics constants and affinity determination (left) and corresponding plot of steady state response against concentration (right) for determination of binding affinity.

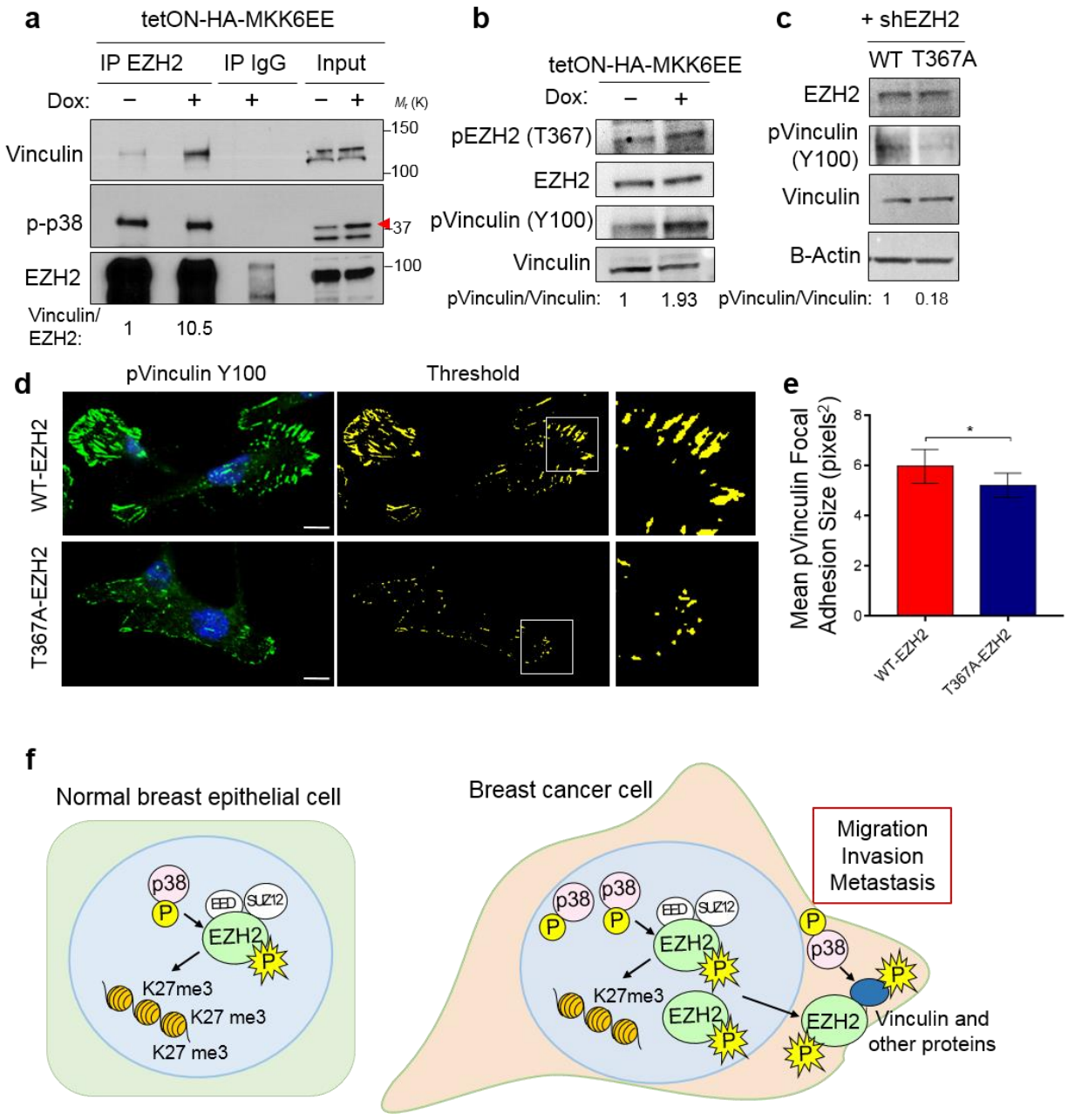

Figure 4.3. pEZH2 promotes vinculin phosphorylation at Y100. a. Co-immunoprecipitation experiment from whole cell extracts demonstrating interaction between endogenous EZH2 and vinculin after treatment with doxycycline to induce p38 activation.**b**. Western blot of MDA-MB-231 cells transduced with dox-inducible MKK6EE to activate p38α activity. **c.** Western blot analysis comparing phospho-vinculin(Y100) in MDA-MB-231 knockdown-rescue WT-EZH2 and T367A-EZH2 cells **d.**Immunofluorescence imaging of MDA-MB-231 knockdown-rescue cells expressing WT-EZH2 or T367-EZH2 and seeded on fibronectin stained with pVinculin (Y100) (left), with example threshold image use for quantitation of focal adhesion size. **e.** The data are quantified. *p≤0.05. **f**. Our working model of pEZH2(T367) function in breast cancer.

Chapter 5: Summary and Future Directions

5-1 Summary of work

Despite improvement in its early detection and treatment, breast cancer remains a significant clinical challenge and source of cancer-associated deaths worldwide. The majority of deaths occur due to metastatic dissemination to distant sites. The broad aims of this dissertation were to examine how the histone methyltransferase EZH2—an epigenetic protein significantly associated with metastatic dissemination of breast cancer and poor breast cancer outcomes—is regulated. Previous studies find that EZH2 is coordinately overexpressed with the activated form of the p38 MAPK in breast cancer patients, and p38 phosphorylates EZH2 at T367 in vitro and interacts with EZH2 in breast cancer cells (93, 164). However, whether EZH2 is phosphorylated in breast cancer at T367 and the biological relevance of this event were previously unknown. This work identifies phosphorylation of EZH2 at T367 as a critical event in regulating the metastatic functions of EZH2 in breast cancer.

In the first part of this dissertation (chapter 2), we developed and validated a novel antibody to detect for the first time pEZH2(T367) expression across a range of cell lines and tissues, normal and malignant. We observed a unique pattern of expression in which pEZH2(T367) shows nuclear expression in most normal tissues and cytoplasmic expression in tumors of epithelial origin. We find a significant correlation between pEZH2(T367) expression and invasive breast carcinoma grade, ER- status, PR- status,

and TNBC status. In the second part of this dissertation (chapter 3), we observe phosphorylation of EZH2 at T367 specifically regulates the adhesive, migratory, and invasive properties of breast cancer cells without affecting their proliferation abilities. A phospho-deficient EZH2 mutant promoted proliferation to similar levels of wild type EZH2 but failed to promote breast cancer cell migration, invasion, and adhesion. Demonstrating an essential role for T367 phosphorylation on the ability of breast cancer cells to move and invade, mutation of T367 to alanine resulted in a significant decrease in distant metastatic burden without affecting primary tumor volume, and led to significantly improved metastasis free survival of mice. These findings provide strong evidence for a critical function of pEZH2(T367) in breast cancer metastasis.

Our mechanistic studies (chapter 4) identify novel cytoplasmic EZH2 binding partners using proteomics. We validate that the F-actin binding protein vinculin interacts with EZH2 and that phosphorylation at T367 is important for vinculin activation. Prior to these observations, the existence and role of pEZH2 T367 in the cytoplasm and in the metastatic ability of breast cancer were unknown. Our data show that EZH2 is a phosphorylation substrate of p38 in breast cancer, and that pEZH2(T367) promotes metastasis, at least in part by cytoplasmic localization and interaction with cytoskeletal proteins.

5-2 Limitations and considerations from this work

There are a number of limitations to the work presented in this dissertation. First, we developed a rabbit polyclonal antibody to assess pEZH2(T367) across a wide range of normal and malignant tissues and cell lines (**Figs 2.1 – 2.3, Tables 3-4**). Although we

observe pEZH2 expression to varying levels of expression across these tissues, it is still not known exactly what percentage of EZH2 is actually phosphorylated at any given time. Although proportionally, a higher amount of EZH2 is phosphorylated in more aggressive cell lines, this may be a fraction of the total pool of EZH2. Additional LC MS/MS studies of the post-translational modifications on EZH2 across different cell lines, such as those performed in leukemic stem cell models (241) may help elucidate this problem. The data in this dissertation support that abrogating phosphorylation at this threonine significantly affects breast cancer cell migration and invasion.

To support data observed from phosphodeficient mutants, it is common to generate phosphomimetic (e.g., aspartic or glutamic acids (242)) mutants. We generated both T367D and T367E phosphomimetic mutants to test the hypothesis that constitutive phosphorylation of EZH2 at this residue but were unable to detect significant phenotypic changes when it was used to rescue EZH2 knockdown (not shown). However, aspartic and glutamic acid often fail to fully recapitulate the effects of phosphorylation, particularly in facilitating adaptor interactions, due to differences in size, geometry, and degree of negative charge between phospho-groups and these amino acids (243). This is especially true for instances in which phosphorylation serves as a recognition signal for 14-3-3-, FHA- (244), and SH2- (245) domain containing proteins (reviewed in (242)). Another recent study demonstrated that a phosphoserine, but not a phosphomimetic protein, can compete for binding with an adjacent lysine, which results in partial unfolding and promotes new protein-protein interactions (246). It is possible that EZH2 is serving some adapter function in the cytoplasm, in which case phosphomimetic mutants would fail to truly mimic phosphorylation.

Phosphorylation of EZH2 at T367 has been observed previously in muscle stem cells, where it causes recruitment of EZH2 to the *Pax7* promoter to promote muscle differentiation and subsequent EZH2 degradation through the E3 ubiquitin ligase Praja-1(164),(165). In this study, we observed no significant effect of phosphorylation on EZH2 protein stability. Little is known about Praja1, especially in the setting of cancer, so future studies should attempt to reconcile these differences: for example, is the Praja1-mediated ubiquitination of EZH2 a muscle-specific phenomenon? Praja1 is MyoD induced, suggesting muscle specificity, but do normal breast cells show ubiquitination of EZH2 by Praja1, and is there deregulation of the Praja1 pathway in breast cancer?

Our data are in agreement with a recent study showing that inhibition of EZH2 phosphorylation at T367 resulted in increased levels of H3K27me3 as well as similarly negligible changes in proliferation with expression of a T367A mutant. However, the authors observed increased migration and invasion with expression of the T367A mutant in MDA-MB-231 and benign MCF12A cells(192). The discordant functional findings might be explained by the approach used as well as the cellular context; the authors overexpressed wild-type or T367A EZH2 in MDA-MB-231 cells, which express high endogenous levels of EZH2, while we employed a knockdown-rescue approach. The association and mechanistic link in our study between p38-mediated phosphorylation of EZH2 at T367, cytoplasmic localization, and breast cancer progression was validated in vitro, in vivo, and in human breast cancer samples. Nevertheless, this warrants future studies that employ mutagenesis of endogenous EZH2 (e.g., as in (247, 248)).

5-3 Remaining questions and future directions

Across all normal tissues stained with our novel pEZH2(T367) antibody, we observed predominantly nuclear staining. For our mechanistic studies, we focused on the cytoplasmic function of pEZH2 because we found that it was associated with tumor grade, ER- status (a marker of more aggressive disease), PR- status, and TNBC status. However, there is still a possibility that pEZH2(T367) in the nucleus contributes to EZH2 function. We observed a near absence of pEZH2(T367) in chromatin bound fractions of breast cancer cells in comparison to all EZH2 and an enrichment in soluble nuclear and cytoplasmic fraction. In short what is pEZH2(T367) doing in the nucleus, and do ChIP studies support the idea that phosphorylation alters EZH2 localization?

One immediate mechanistic question that remains from our work is whether phosphorylation promotes increased migration and invasion in a mechanism independent of the translocation of EZH2? Put another way, does EZH2 need to be phosphorylated once it is in the cytoplasm, or is merely the translocation sufficient? Assays similar to those used in **Fig 3.5** with a double ΔNLS-T367A mutant would answer this question.

Along similar lines, is the methyltransferase activity required for the cytoplasmic functions of EZH2? The H689 amino acid is required for the methyltransferase of EZH2 (249). Knockdown rescue studies using a genetic approach with a double EZH2 non-phosphorylatable catalytically dead T367A-H689A mutant may answer this question and could be supported by pharmacological inhibition studies with GSK343 (250). Furthermore, does pEZH2(T367) retain its methyltransferase activity? Comparison of immunoprecipitated WT-EZH2 and T367A-EZH2 in a methyltransferase assay may assist in answering this question.

Finally, is all of PRC2 sequestered into the cytoplasm in a T367-phosphorylation dependent manner? We were unable to detect vinculin colocalization with PRC2 members EED and SUZ12 (**4.2e**), but did observe a number of cytosolic interactions between pEZH2 and SUZ2/EED. Others have also reported the existence of cytosolic PRC2 complexes (216). Comparing the subcellular localization of PRC2 components by fractionation or immunofluorescence in cells expressing WT-EZH2 and T367A-EZH2 would clarify this question. These mechanistic questions are important for delineating how exactly EZH2 functions in triple-negative breast cancer.

5-4 Additional EZH2 binding partners

The data presented from our proteomic studies in chapter 4 opens the door for many future studies. As mentioned above, our studies revealed a phosphorylation-dependent enrichment in F-actin and cytoplasmic proteins. We chose to pursue vinculin for validation given its known role in mediating breast cancer cell adhesion and migration. However, it is highly unlikely that the phenotypic differences we observe between WT-EZH2- and T367A-EZH2-expressing cells are solely due to this protein-protein interaction. Rather, EZH2 likely interacts with a number of extranuclear proteins to effect this change.

For example, also in the list of differential interactors is nesprin-2 (SYNE2). Nesprin 2 is a member of the Linker of the Nucleoskeleton and Cytoskeleton (LINC) complex and contributes to tethering the nuclear envelope to the cytoskeleton. Nesprin was recently demonstrated to interact with the F-actin bundling protein Fascin through F-actin. Disrupting this interaction abrogates F-actin binding to the nuclear envelope and

abrogates cell movement through confined spaces (251). Knockdown of Nesprin 2 in A375 melanoma cells alters the adhesive properties of invadopodia (252). Matsumota et al found loss of the LINC complex, including Nesprin 2 in a cohort of breast tissues compared to surrounding normal tissues (253). These observations make nesprin-2 a promising potential interactor.

Another target worth pursuing is MYO18A. MYO18A is an unconventional mysosin characterized by its N-terminal PDZ domain (254) that may regulate its interactors (255). Proteomic and loss-of-function experiments have revealed a diverse set of functions of MYO18A, including actin treadmilling and golgi function (256). In myoblasts, MYO18A is required for cell adhesion to extracellular-matrix and F-actin organization (255). Higher expression of MYO18A correlates with prostate cancer invasiveness, and its genetic inhibition using RNA interference significantly decreases directional persistence (257). In a quantitative proteomics screen using SILAC affinity purification mass-spectrometry in mouse embryonic stem cells, MYO18A was identified as a novel interactor of EZH2 in a proteomics screen (258), and MYO18A was also observed as an overlapping interactor of EZH2 in our proteomic studies. It is tempting to speculate that EZH2 may regulate MYO18A function through this interaction to promote breast cancer cell migration and metastasis; however, future studies will be needed to first validate this interaction and determine its role in breast cancer.

Finally, a recent study used a positional screening methyltransferase assay to determine which amino acids surrounding H3K27 are essential for EZH2-mediated methylation. From this data, they performed a Scansite database search and identified 339 potential non-histone substrates of EZH2 (184). Interestingly, 12 of these 339

substrates were observed in our mass-spectrometry data set. The overlapping potential substrates are summarized in **Table 6**. Of particular interest is the poly ADP ribose polymerase PARP1, responsible for single stranded DNA repair. As PARP inhibitors are used clinically (MK-4827, olaparib, veliparib), for tumors with BRCA1, BRCA2, or PALB mutations, investigating whether PARP is a target of EZH2 could be directly translatable (259, 260). Also of biological interest is EXOSC8, a member of the cellular exosome complex. This is a conserved complex responsible for processing, degrading, and turning over coding and noncoding RNA (261). The concept of PRC2 binding RNA and its promiscuity for doing so (262, 263) has been the subject of several studies, although the function is unclear. Many have posited that the function of RNA binding PRC2 is recruitment to certain loci (reviewed in (264)), while others have proposed a model in which PRC2's promiscuity allows it to "scan" for genes that have escaped repression (262, 263). Additionally, the binding appears to be size-dependent, and it appears to prefer short repeats of consecutive guanines (265). We observed phosphorylation-dependent binding of exosome complex members in our mass spectrometry analysis. It is tempting to speculate that PRC2 may play some role in mediating RNA processing through the exosome, or that its promiscuity to RNA is functionally enabled by binding with the exosome complex and associated RNAs. Many more studies are needed to understand the nature of these interactions and the relevance to biology and disease.

5-5 Towards targeting EZH2 in triple-negative breast cancer

That oncogenic alterations in pathways directly involving EZH2 are frequent across multiple types of cancer make targeting EZH2 a tantalizing option for cancer treatment.

Indeed, overexpression of EZH2 is commonly observed in a number of solid tumors (87, 90, 95, 96, 101, 102) , and activating mutations are observed in hematological malignancies (116, 119). Inactivation of UTX, an H3K27 demethylase responsible for antagonizing EZH2 canonical function is also observed in several cancer types including multiple myeloma, esophageal squamous cell carcinomas, renal cell carcinomas (266) and pancreatic cancer (114, 267). Recurrent mutations in the chromatin remodeling SWI/SNF complex members ARID1A, PBRM1, and SMARCA4 are also common (~20%(268, 269)) across multiple tumor types and render tumor cells dependent on EZH2 catalytic and non-catalytic activity (125, 268). Taken together, these factors make EZH2 a tantalizing target for the treatment of cancer.

Several potent S-adenosylmethionine (SAM)-competitive EZH2 inhibitors have been developed over the past five years and have reached phase I-II clinical trials for patients with a defined set of genetic alterations in EZH2 or in SWI/SNF complex members. EZH2 is overexpressed in ~55% invasive breast carcinomas, and this overexpression is significantly associated with the triple-negative subtype (90). Inhibition of EZH2 function, assessed by global levels of H3K27me3, using one of these compounds at low micromolar concentrations GSK126, appears to have no effect on cell proliferation of three triple-negative breast cancer cell lines, despite de-repression of at least two canonical EZH2 targets, CDKN1A and CDKN1C, and may even promote invasion of breast cancer cells through de-repression of MMPs (270). These data are largely in line with unpublished observations from our lab, in which treatment of breast cancer cell lines with GSK126 or GSK343 (another potent and selective SAM-competitive EZH2 inhibitor (271)) failed to significantly decrease proliferation and showed only minor

effects on triple-negative breast cancer cell invasion, suggesting that inhibition of the methyltransferase activity of EZH2 alone is not sufficient to abrogate EZH2 oncogenic functions in triple-negative breast cancer cell lines.

Interestingly, Scott et al. recently found that combined treatment of primary chronic myeloid leukemia cells with an EZH2 inhibitor and the tyrosine kinase inhibitor (dasatanib or nilotinib) significantly decreased leukemic stem cells compared to either treatment alone (272). p38 inhibitors have been widely explored in clinical trials for rheumatoid arthritis, chronic obstructive pulmonary disease, and cardiovascular disease (273). In our proposed model (**Fig 4.3f**), phosphorylation of EZH2 at T367 promotes its cytoplasmic localization, and conversely, inhibition of phosphorylation promotes nuclear retention and increased global levels of H3K27me3 (**Fig. 3.1b** and (192)). It will be exciting to continue preliminary studies which show that p38 and EZH2 inhibitors can work in concert to abrogate the tumorigenic properties of breast cancer cells.

5-6 Figures

Protein	PRC2 Methylated Peptide from (184)	WT FC_B	T367A FC_B	Function
MYCBP2	AMKQALR**K**SACRVFA	0.41	0.39	E3 ubiquitin ligase(274)
STAU2	PNKKIAK**K**NAAEAML	0.99	0.89	mRNA degradation (275)
SPO11	DSPKSVK**K**FALILKV	1.18	0	Double-stranded breaks in meiotic recombination (276)
LYAR	GTIKAVL**K**QAPDNEI	1.29	0.63	Cell growth regulation? (277)
DHX9	RELLPVK**K**FEAEILE	0.95	0.93	ATP-dependent RNA helicase (278)
DTX2	EPEQVIR**K**YTEELKV	1.01	0.62	Probable E3 ubiquitin ligase (279)
PARP1	GQMRLSK**K**MVDPEKP	4.12	1.57	NAD+ ADP-ribosyltransferase 1 (280)
APTX	LESQAVI**K**MVQEAGR	1.18	0	RNA/DNA deadenylase (281)
IWS1	QKKPALK**K**LTLLPTV	1.27	1.19	RNA PolII elongation complex and mRNA processing (282)
WRN	IIYCPSR**K**MTEQVTA	1.27	1.19	RecQ DNA helicase (283)
EXOSC8	SRDICLK**K**FVKPIFT	0.49	0.44	Exosome complex member, RNA processing (284)
DEF6	FYDRVSK**K**EAKPQIC	3.29	1.33	Guanine exchange factor for RAC and CDC42 (285)

Table 6. List of potential EZH2 substrates. Based on hits overlapping from (131) and our own mass spectrometry data set. Shown are the gene name, the lysine methylated, WT and T367A fold change scores, and a description of gene function.

References

1. Siegel RL, Miller KD, and Jemal A. Cancer statistics, 2018. *CA: A Cancer Journal for Clinicians.* 2018;68(1):7-30.

2. Global Burden of Disease Cancer C. Global, regional, and national cancer incidence, mortality, years of life lost, years lived with disability, and disability-adjusted life-years for 32 cancer groups, 1990 to 2015: A systematic analysis for the global burden of disease study. *JAMA Oncology.* 2017;3(4):524-48.

3. Howlader N NA, Krapcho M, Miller D, Bishop K, Altekruse SF, Kosary CL, Yu M, Ruhl J, Tatalovich Z, Mariotto A, Lewis DR, Chen HS, Feuer EJ, Cronin KA (eds). SEER Cancer Statistics Review, 1975-2013, National Cancer Institute. Bethesda, MD, http://seer.cancer.gov/csr/1975_2013/, based on November 2015 SEER data submission, posted to the SEER web site, April 2016. 2016.

4. Iqbal J, Ginsburg O, Rochon PA, Sun P, and Narod SA. Differences in breast cancer stage at diagnosis and cancer-specific survival by race and ethnicity in the united states. *JAMA.* 2015;313(2):165-73.

5. Cunningham JE, and Butler WM. Racial disparities in female breast cancer in South Carolina: clinical evidence for a biological basis. *Breast Cancer Research and Treatment.* 2004;88(2):161-76.

6. DeSantis CE, Ma J, Sauer AG, Newman LA, and Jemal A. Breast cancer statistics, 2017, racial disparity in mortality by state. *CA: A Cancer Journal for Clinicians.* 2017;67(6):439-48.

7. Li CI, Anderson BO, Daling JR, and Moe RE. Trends in incidence rates of invasive lobular and ductal breast carcinoma. *JAMA.* 2003;289(11):1421-4.

8. Colleoni M, Rotmensz N, Maisonneuve P, Mastropasqua MG, Luini A, Veronesi P, Intra M, Montagna E, Cancello G, Cardillo A, et al. Outcome of special types of luminal breast cancer. *Annals of Oncology.* 2012;23(6):1428-36.

9. Acevedo C, Amaya C, and López-Guerra J-L. Rare breast tumors: Review of the literature. *Reports of Practical Oncology & Radiotherapy.* 2014;19(4):267-74.

10. Wellings SR, and Jensen HM. On the Origin and Progression of Ductal Carcinoma in the Human Breast2. *JNCI: Journal of the National Cancer Institute.* 1973;50(5):1111-8.

11. Allred DC, Wu Y, Mao S, Nagtegaal ID, Lee S, Perou CM, Mohsin SK, O'Connell P, Tsimelzon A, and Medina D. Ductal Carcinoma In situ and the Emergence of Diversity during Breast Cancer Evolution. *Clinical Cancer Research.* 2008;14(2):370-8.

12. Narod SA, and Sopik V. Is invasion a necessary step for metastases in breast cancer? *Breast Cancer Research and Treatment.* 2018.

13. Hanahan D, and Weinberg RA. Hallmarks of cancer: the next generation. *Cell.* 2011;144(

14. Seyfried TN, and Huysentruyt LC. On the Origin of Cancer Metastasis. *Critical reviews in oncogenesis.* 2013;18(1-2):43-73.

15. Lambert AW, Pattabiraman DR, and Weinberg RA. Emerging Biological Principles of Metastasis. *Cell.* 2017;168(4):670-91.

16. Valastyan S, and Weinberg RA. Tumor metastasis: molecular insights and evolving paradigms. *Cell.* 2011;147(

17. Kalluri R, and Weinberg RA. The basics of epithelial-mesenchymal transition. *The Journal of Clinical Investigation.* 2009;119(6):1420-8.

18. Hay ED. An overview of epithelio-mesenchymal transformation. *Acta anatomica.* 1995;154(1):8-20.

19. Hugo H, Ackland ML, Blick T, Lawrence Mitchell G, Clements Judith A, Williams Elizabeth D, and Thompson Erik W. Epithelial—mesenchymal and mesenchymal—epithelial transitions in carcinoma progression. *Journal of Cellular Physiology.* 2007;213(2):374-83.

20. Anwar TE, and Kleer CG. Tissue-based identification of stem cells and epithelial-to-mesenchymal transition in breast cancer. *Human Pathology.* 2013;44(8):1457-64.

21. Thiery JP, Acloque H, Huang RYJ, and Nieto MA. Epithelial-Mesenchymal Transitions in Development and Disease. *Cell.* 2009;139(5):871-90.

22. Krebs AM, Mitschke J, Lasierra Losada M, Schmalhofer O, Boerries M, Busch H, Boettcher M, Mougiakakos D, Reichardt W, Bronsert P, et al. The EMT-activator Zeb1 is a key factor for cell plasticity and promotes metastasis in pancreatic cancer. *Nature Cell Biology.* 2017;19(518.

23. Graham TR, Zhau HE, Odero-Marah VA, Osunkoya AO, Kimbro KS, Tighiouart M, Liu T, Simons JW, and O'Regan RM. Insulin-like Growth Factor-I–Dependent Up-regulation of ZEB1 Drives Epithelial-to-Mesenchymal Transition in Human Prostate Cancer Cells. *Cancer Research.* 2008;68(7):2479-88.

24. Moody SE, Perez D, Pan T-c, Sarkisian CJ, Portocarrero CP, Sterner CJ, Notorfrancesco KL, Cardiff RD, and Chodosh LA. The transcriptional repressor Snail promotes mammary tumor recurrence. *Cancer Cell.* 2005;8(3):197-209.

25. Yook JI, Li X-Y, Ota I, Hu C, Kim HS, Kim NH, Cha SY, Ryu JK, Choi YJ, Kim J, et al. A Wnt–Axin2–GSK3β cascade regulates Snail1 activity in breast cancer cells. *Nature Cell Biology.* 2006;8(1398.

26. Trimboli AJ, Fukino K, de Bruin A, Wei G, Shen L, Tanner SM, Creasap N, Rosol TJ, Robinson ML, Eng C, et al. Direct Evidence for Epithelial-Mesenchymal Transitions in Breast Cancer. *Cancer Research.* 2008;68(3):937-45.

27. Zheng X, Carstens JL, Kim J, Scheible M, Kaye J, Sugimoto H, Wu C-C, LeBleu VS, and Kalluri R. Epithelial-to-mesenchymal transition is dispensable for metastasis but induces chemoresistance in pancreatic cancer. *Nature.* 2015;527(525.

28. Fischer KR, Durrans A, Lee S, Sheng J, Li F, Wong STC, Choi H, El Rayes T, Ryu S, Troeger J, et al. Epithelial-to-mesenchymal transition is not required for lung metastasis but contributes to chemoresistance. *Nature.* 2015;527(472.

29. Brabletz T, Kalluri R, Nieto MA, and Weinberg RA. EMT in cancer. *Nature Reviews Cancer.* 2018;18(128.

30. Aiello NM, Brabletz T, Kang Y, Nieto MA, Weinberg RA, and Stanger BZ. Upholding a role for EMT in pancreatic cancer metastasis. *Nature.* 2017;547(E7.

31. Fischer KR, Altorki NK, Mittal V, and Gao D. Fischer et al. reply. *Nature.* 2017;547(E5.

32. Nieto MA. Context-specific roles of EMT programmes in cancer cell dissemination. *Nature Cell Biology.* 2017;19(416.

33. Scully OJ, Bay B-H, Yip G, and Yu Y. Breast Cancer Metastasis. *Cancer Genomics - Proteomics.* 2012;9(5):311-20.

34. Jin X, and Mu P. Targeting Breast Cancer Metastasis. *Breast Cancer : Basic and Clinical Research.* 2015;9(Suppl 1):23-34.

35. Gupta GP, Nguyen DX, Chiang AC, Bos PD, Kim JY, Nadal C, Gomis RR, Manova-Todorova K, and Massagué J. Mediators of vascular remodelling co-opted for sequential steps in lung metastasis. *Nature.* 2007;446(765.

36. Chen L, Yang S, Jakoncic J, Zhang JJ, and Huang X-Y. Migrastatin analogues target fascin to block tumour metastasis. *Nature.* 2010;464(1062.

37. Sørlie T, Perou CM, Tibshirani R, Aas T, Geisler S, Johnsen H, Hastie T, Eisen MB, van de Rijn M, Jeffrey SS, et al. Gene expression patterns of breast carcinomas distinguish tumor subclasses with clinical implications. *Proceedings of the National Academy of Sciences.* 2001;98(19):10869-74.

38. Perou CM, Sørlie T, Eisen MB, van de Rijn M, Jeffrey SS, Rees CA, Pollack JR, Ross DT, Johnsen H, Akslen LA, et al. Molecular portraits of human breast tumours. *Nature.* 2000;406(747.

39. Penault-Llorca F, and Viale G. Pathological and molecular diagnosis of triple-negative breast cancer: a clinical perspective. *Annals of Oncology.* 2012;23(suppl_6):vi19-vi22.

40. Dai X, Li T, Bai Z, Yang Y, Liu X, Zhan J, and Shi B. Breast cancer intrinsic subtype classification, clinical use and future trends. *American Journal of Cancer Research.* 2015;5(10):2929-43.

41. Cheang MCU, Chia SK, Voduc D, Gao D, Leung S, Snider J, Watson M, Davies S, Bernard PS, Parker JS, et al. Ki67 Index, HER2 Status, and Prognosis of Patients With Luminal B Breast Cancer. *JNCI: Journal of the National Cancer Institute.* 2009;101(10):736-50.

42. Muaiad K, Alberto JM, and Stefan G. Molecular Profiling for Breast Cancer: A Comprehensive Review. *Biomarkers in Cancer.* 2013;5(BIC.S9455.

43. Brewster AM, Chavez-MacGregor M, and Brown P. Epidemiology, biology, and treatment of triple-negative breast cancer in women of African ancestry. *The Lancet Oncology.*15(13):e625-e34.

44. Costa RLB, and Gradishar WJ. Triple-Negative Breast Cancer: Current Practice and Future Directions. *Journal of Oncology Practice.* 2017;13(5):301-3.

45. Lin NU, Vanderplas A, Hughes ME, Theriault RL, Edge SB, Wong YN, Blayney DW, Niland JC, Winer EP, and Weeks JC. Clinicopathologic features, patterns of recurrence, and survival among women with triple-negative breast cancer in the National Comprehensive Cancer Network. *Cancer.* 2012;118(22):5463-72.

46. Azim HA, Michiels S, Bedard PL, Singhal SK, Criscitiello C, Ignatiadis M, Haibe-Kains B, Piccart MJ, Sotiriou C, and Loi S. Elucidating Prognosis and Biology of Breast Cancer Arising in Young Women Using Gene Expression Profiling. *Clinical Cancer Research.* 2012;18(5):1341-51.

47. Lund MJ, Trivers KF, Porter PL, Coates RJ, Leyland-Jones B, Brawley OW, Flagg EW, O'Regan RM, Gabram SGA, and Eley JW. Race and triple negative threats to breast cancer survival: a population-based study in Atlanta, GA. *Breast Cancer Research and Treatment.* 2009;113(2):357-70.

48. Criscitiello C, Azim JHA, Schouten PC, Linn SC, and Sotiriou C. Understanding the biology of triple-negative breast cancer. *Annals of Oncology.* 2012;23(suppl_6):vi13-vi8.

49. Lehmann BD, Bauer JA, Chen X, Sanders ME, Chakravarthy AB, Shyr Y, and Pietenpol JA. Identification of human triple-negative breast cancer subtypes and preclinical models for selection of targeted therapies. *The Journal of Clinical Investigation.* 2011;121(7):2750-67.

50. Gadi VK, and Davidson NE. Practical Approach to Triple-Negative Breast Cancer. *Journal of Oncology Practice.* 2017;13(5):293-300.

51. Aranda S, Mas G, and Di Croce L. Regulation of gene transcription by Polycomb proteins. *Science Advances.* 2015;1(11).

52. Kornberg RD. Chromatin Structure: A Repeating Unit of Histones and DNA. *Science.* 1974;184(4139):868-71.

53. Luger K, Mäder AW, Richmond RK, Sargent DF, and Richmond TJ. Crystal structure of the nucleosome core particle at 2.8 Å resolution. *Nature.* 1997;389(251.

54. Arrowsmith CH, Bountra C, Fish PV, Lee K, and Schapira M. Epigenetic protein families: a new frontier for drug discovery. *Nature Reviews Drug Discovery.* 2012;11(384.

55. Schuettengruber B, Bourbon H-M, Di Croce L, and Cavalli G. Genome Regulation by Polycomb and Trithorax: 70 Years and Counting. *Cell.*171(1):34-57.

56. Schwartz YB, and Cavalli G. Three-Dimensional Genome Organization and Function in Drosophila. *Genetics.* 2017;205(1):5-24.

57. O'Carroll D, Erhardt S, Pagani M, Barton SC, Surani MA, and Jenuwein T. The Polycomb-Group GeneEzh2 Is Required for Early Mouse Development. *Molecular and Cellular Biology.* 2001;21(13):4330-6.

58. Faust C, Lawson KA, Schork NJ, Thiel B, and Magnuson T. The Polycomb-group gene eed is required for normal morphogenetic movements during gastrulation in the mouse embryo. *Development.* 1998;125(22):4495-506.

59. Pasini D, Bracken AP, Jensen MR, Denchi EL, and Helin K. Suz12 is essential for mouse development and for EZH2 histone methyltransferase activity. *The EMBO Journal.* 2004;23(20):4061-71.

60. Yu BD, Hanson RD, Hess JL, Horning SE, and Korsmeyer SJ. MLL, a mammalian trithorax-group gene, functions as a transcriptional maintenance factor in morphogenesis. *Proceedings of the National Academy of Sciences.* 1998;95(18):10632.

61. Kerppola TK. Polycomb group complexes – many combinations, many functions. *Trends in Cell Biology.*19(12):692-704.

62. Bernstein E, Duncan EM, Masui O, Gil J, Heard E, and Allis CD. Mouse Polycomb Proteins Bind Differentially to Methylated Histone H3 and RNA and Are Enriched in Facultative Heterochromatin. *Molecular and Cellular Biology.* 2006;26(7):2560-9.

63. Schoeftner S, Sengupta AK, Kubicek S, Mechtler K, Spahn L, Koseki H, Jenuwein T, and Wutz A. Recruitment of PRC1 function at the initiation of X inactivation independent of PRC2 and silencing. *The EMBO Journal.* 2006;25(13):3110-22.

64. Gil J, and O'Loghlen A. PRC1 complex diversity: where is it taking us? *Trends in Cell Biology.* 2014;24(11):632-41.

65. Margueron R, and Reinberg D. The Polycomb Complex PRC2 and its Mark in Life. *Nature.* 2011;469(7330):343-9.

66. Cao R, and Zhang Y. SUZ12 Is Required for Both the Histone Methyltransferase Activity and the Silencing Function of the EED-EZH2 Complex. *Molecular Cell.*15(1):57-67.

67. Margueron R, Li G, Sarma K, Blais A, Zavadil J, Woodcock CL, Dynlacht BD, and Reinberg D. Ezh1 and Ezh2 Maintain Repressive Chromatin through Different Mechanisms. *Molecular Cell.*32(4):503-18.

68. Shen X, Liu Y, Hsu Y-J, Fujiwara Y, Kim J, Mao X, Yuan G-C, and Orkin SH. EZH1 Mediates Methylation on Histone H3 Lysine 27 and Complements EZH2 in Maintaining Stem Cell Identity and Executing Pluripotency. *Molecular Cell.* 2008;32(4):491-502.

69. Lee TI, Jenner RG, Boyer LA, Guenther MG, Levine SS, Kumar RM, Chevalier B, Johnstone SE, Cole MF, Isono K-i, et al. Control of Developmental Regulators by Polycomb in Human Embryonic Stem Cells. *Cell.*125(2):301-13.

70. Holoch D, and Margueron R. Mechanisms Regulating PRC2 Recruitment and Enzymatic Activity. *Trends in Biochemical Sciences.*42(7):531-42.

71. Rea S, Eisenhaber F, O'Carroll D, Strahl BD, Sun Z-W, Schmid M, Opravil S, Mechtler K, Ponting CP, Allis CD, et al. Regulation of chromatin structure by site-specific histone H3 methyltransferases. *Nature.* 2000;406(593.

72. Xu K, Wu ZJ, Groner AC, He HH, Cai C, Lis RT, Wu X, Stack EC, Loda M, Liu T, et al. EZH2 Oncogenic Activity in Castration-Resistant Prostate Cancer Cells Is Polycomb-Independent. *Science.* 2012;338(6113):1465-9.

73. Tan J-z, Yan Y, Wang X-x, Jiang Y, and Xu HE. EZH2: biology, disease, and structure-based drug discovery. *Acta Pharmacologica Sinica.* 2013;35(161.

74. Chen S, Jiao L, Shubbar M, Yang X, and Liu X. Unique Structural Platforms of Suz12 Dictate Distinct Classes of PRC2 for Chromatin Binding. *Molecular Cell.*69(5):840-52.e5.

75. Ciferri C, Lander GC, Maiolica A, Herzog F, Aebersold R, and Nogales E. Molecular architecture of human polycomb repressive complex 2. *eLife.* 2012;1(e00005.

76. Jiao L, and Liu X. Structural basis of histone H3K27 trimethylation by an active polycomb repressive complex 2. *Science.* 2015;350(6258).

77. Li G, Margueron R, Ku M, Chambon P, Bernstein BE, and Reinberg D. Jarid2 and PRC2, partners in regulating gene expression. *Genes & Development.* 2010;24(4):368-80.

78. Sanulli S, Justin N, Teissandier A, Ancelin K, Portoso M, Caron M, Michaud A, Lombard B, da Rocha Simao T, Offer J, et al. Jarid2 Methylation via the PRC2 Complex Regulates H3K27me3 Deposition during Cell Differentiation. *Molecular Cell.* 2015;57(5):769-83.

79. Zhang Z, Jones A, Sun C-W, Li C, Chang C-W, Joo H-Y, Dai Q, Mysliwiec MR, Wu L-C, Guo Y, et al. PRC2 Complexes with JARID2, MTF2, and esPRC2p48 in ES Cells to Modulate ES Cell Pluripotency and Somatic Cell Reprograming. *Stem cells (Dayton, Ohio).* 2011;29(2):229-40.

80. Son J, Shen SS, Margueron R, and Reinberg D. Nucleosome-binding activities within JARID2 and EZH1 regulate the function of PRC2 on chromatin. *Genes & Development.* 2013;27(24):2663-77.

81. Peng JC, Valouev A, Swigut T, Zhang J, Zhao Y, Sidow A, and Wysocka J. Jarid2/Jumonji Coordinates Control of PRC2 Enzymatic Activity and Target Gene Occupancy in Pluripotent Cells. *Cell.*139(7):1290-302.

82. Kaneko S, Bonasio R, Saldaña-Meyer R, Yoshida T, Son J, Nishino K, Umezawa A, and Reinberg D. Interactions between JARID2 and noncoding RNAs regulate PRC2 recruitment to chromatin. *Molecular cell.* 2014;53(2):290-300.

83. Kasinath V, Faini M, Poepsel S, Reif D, Feng XA, Stjepanovic G, Aebersold R, and Nogales E. Structures of human PRC2 with its cofactors AEBP2 and JARID2. *Science.* 2018;359(6378):940-4.

84. Margueron R, Justin N, Ohno K, Sharpe ML, Son J, Drury Iii WJ, Voigt P, Martin SR, Taylor WR, De Marco V, et al. Role of the polycomb protein EED in the propagation of repressive histone marks. *Nature.* 2009;461(762.

85. Hansen KH, Bracken AP, Pasini D, Dietrich N, Gehani SS, Monrad A, Rappsilber J, Lerdrup M, and Helin K. A model for transmission of the H3K27me3 epigenetic mark. *Nature Cell Biology.* 2008;10(1291.

86. Li H, Liefke R, Jiang J, Kurland JV, Tian W, Deng P, Zhang W, He Q, Patel DJ, Bulyk ML, et al. Polycomb-like proteins link the PRC2 complex to CpG islands. *Nature.* 2017;549(287.

87. Varambally S, Dhanasekaran SM, Zhou M, Barrette TR, Kumar-Sinha C, Sanda MG, Ghosh D, Pienta KJ, Sewalt RGAB, Otte AP, et al. The polycomb group protein EZH2 is involved in progression of prostate cancer. *Nature.* 2002;419(6907):624-9.

88. Cao Q, Yu J, Dhanasekaran SM, Kim JH, Mani RS, Tomlins SA, Mehra R, Laxman B, Cao X, Yu J, et al. Repression of E-cadherin by the polycomb group protein EZH2 in cancer. *Oncogene.* 2008;27(7274.

89. Bachmann IM, Halvorsen OJ, Collett K, Stefansson IM, Straume O, Haukaas SA, Salvesen HB, Otte AP, and Akslen LA. EZH2 Expression Is Associated With High Proliferation Rate and Aggressive Tumor Subgroups in Cutaneous Melanoma and Cancers of the Endometrium, Prostate, and Breast. *Journal of Clinical Oncology.* 2006;24(2):268-73.

90. Kleer CG, Cao Q, Varambally S, Shen R, Ota I, Tomlins SA, Ghosh D, Sewalt RGAB, Otte AP, Hayes DF, et al. EZH2 is a marker of aggressive breast cancer and promotes neoplastic transformation of breast epithelial cells. *Proceedings of the National Academy of Sciences.* 2003;100(20):11606-11.

91. Gonzalez ME, DuPrie ML, Krueger H, Merajver SD, Ventura AC, Toy KA, and Kleer CG. Histone Methyltransferase EZH2 Induces Akt-Dependent Genomic Instability and BRCA1 Inhibition in Breast Cancer. *Cancer Research.* 2011;71(6):2360-70.

92. Pang J, Toy KA, Griffith KA, Awuah B, Quayson S, Newman LA, and Kleer CG. Invasive breast carcinomas in Ghana: high frequency of high grade, basal-like histology and high EZH2 expression. *Breast Cancer Research and Treatment.* 2012;135(1):59-66.

93. Moore HM, Gonzalez ME, Toy KA, Cimino-Mathews A, Argani P, and Kleer CG. EZH2 inhibition decreases p38 signaling and suppresses breast cancer motility and metastasis. *Breast Cancer Research and Treatment.* 2013;138(3):741-52.

94. Chang C-J, Yang J-Y, Xia W, Chen C-T, Xie X, Chao C-H, Woodward WA, Hsu J-M, Hortobagyi GN, and Hung M-C. EZH2 promotes expansion of breast tumor initiating cells through activation of RAF1-β-catenin signaling. *Cancer cell.* 2011;19(1):86-100.

95. Sudo T, Utsunomiya T, Mimori K, Nagahara H, Ogawa K, Inoue H, Wakiyama S, Fujita H, Shirouzu K, and Mori M. Clinicopathological significance of EZH2 mRNA expression in patients with hepatocellular carcinoma. *British Journal Of Cancer.* 2005;92(1754.

96. Sasaki M, Ikeda H, Itatsu K, Yamaguchi J, Sawada S, Minato H, Ohta T, and Nakanuma Y. The overexpression of polycomb group proteins Bmi1 and EZH2 is associated with the progression and aggressive biological behavior of hepatocellular carcinoma. *Laboratory Investigation.* 2008;88(873.

97. Behrens C, Solis LM, Lin H, Yuan P, Tang X, Kadara H, Riquelme E, Galindo H, Moran CA, Kalhor N, et al. EZH2 Protein Expression Associates with the Early Pathogenesis, Tumor Progression, and Prognosis of Non–Small Cell Lung Carcinoma. *Clinical Cancer Research.* 2013;19(23):6556-65.

98. Zhang H, Qi J, Reyes JM, Li L, Rao PK, Li F, Lin CY, Perry JA, Lawlor MA, Federation A, et al. Oncogenic deregulation of EZH2 as an opportunity for targeted therapy in lung cancer. *Cancer Discovery.* 2016.

99. Kikuchi J, Kinoshita I, Shimizu Y, Kikuchi E, Konishi J, Oizumi S, Kaga K, Matsuno Y, Nishimura M, and Dosaka-Akita H. Distinctive expression of the polycomb group proteins Bmi1 polycomb ring finger oncogene and enhancer of zeste homolog 2 in nonsmall cell lung cancers and their clinical and clinicopathologic significance. *Cancer.* 2010;116(12):3015-24.

100. Wang X, Zhao H, Lv L, Bao L, Wang X, and Han S. Prognostic Significance of EZH2 Expression in Non-Small Cell Lung Cancer: A Meta-analysis. *Scientific Reports.* 2016;6(19239.

101. Zhou J, Roh J-W, Bandyopadhyay S, Chen Z, Munkarah AR, Hussein Y, Alosh B, Jazaerly T, Hayek K, Semaan A, et al. Overexpression of enhancer of zeste homolog 2 (EZH2) and focal adhesion kinase (FAK) in high grade endometrial carcinoma. *Gynecologic Oncology.* 2013;128(2):344-8.

102. Arisan S, Buyuktuncer ED, Palavan-Unsal N, Çaşkurlu T, Çakir OO, and Ergenekon E. Increased Expression of EZH2, a Polycomb Group Protein, in Bladder Carcinoma. *Urologia Internationalis.* 2005;75(3):252-7.

103. Rao Z-Y, Cai M-Y, Yang G-F, He L-R, Mai S-J, Hua W-F, Liao Y-J, Deng H-X, Chen Y-C, Guan X-Y, et al. EZH2 supports ovarian carcinoma cell invasion and/or metastasis via regulation of TGF-β1 and is a predictor of outcome in ovarian carcinoma patients. *Carcinogenesis.* 2010;31(9):1576-83.

104. Lu C, Han HD, Mangala LS, Ali-Fehmi R, Newton CS, Ozbun L, Armaiz-Pena GN, Hu W, Stone RL, Munkarah A, et al. Regulation of Tumor Angiogenesis by EZH2. *Cancer Cell.* 2010;18(2):185-97.

105. Crea F, Hurt EM, and Farrar WL. Clinical significance of Polycomb gene expression in brain tumors. *Molecular Cancer.* 2010;9(1):265.

106. Bracken AP, Pasini D, Capra M, Prosperini E, Colli E, and Helin K. EZH2 is downstream of the pRB-E2F pathway, essential for proliferation and amplified in cancer. *The EMBO Journal.* 2003;22(20):5323-35.

107. Karanikolas BDW, Figueiredo ML, and Wu L. Polycomb Group Protein Enhancer of Zeste 2 Is an Oncogene That Promotes the Neoplastic Transformation of a Benign Prostatic Epithelial Cell Line. *Molecular Cancer Research.* 2009;7(9):1456-65.

108. Lv Y-F, Yan G-N, Meng G, Zhang X, and Guo Q-N. Enhancer of zeste homolog 2 silencing inhibits tumor growth and lung metastasis in osteosarcoma. *Scientific Reports.* 2015;5(12999.

109. Li H, Cai Q, Godwin AK, and Zhang R. Enhancer of Zeste Homolog 2 Promotes the Proliferation and Invasion of Epithelial Ovarian Cancer Cells. *Molecular Cancer Research.* 2010;8(12):1610-8.

110. Murai F, Koinuma D, Shinozaki-Ushiku A, Fukayama M, Miyaozono K, and Ehata S. EZH2 promotes progression of small cell lung cancer by suppressing the TGF-β-Smad-ASCL1 pathway. *Cell Discovery.* 2015;1(15026.

111. Chen H, Tu S-w, and Hsieh J-T. Down-regulation of Human DAB2IP Gene Expression Mediated by Polycomb Ezh2 Complex and Histone Deacetylase in Prostate Cancer. *Journal of Biological Chemistry.* 2005;280(23):22437-44.

112. Beke L, Nuytten M, Van Eynde A, Beullens M, and Bollen M. The gene encoding the prostatic tumor suppressor PSP94 is a target for repression by the Polycomb group protein EZH2. *Oncogene.* 2007;26(4590.

113. Fujii S, Ito K, Ito Y, and Ochiai A. Enhancer of Zeste Homologue 2 (EZH2) Down-regulates RUNX3 by Increasing Histone H3 Methylation. *Journal of Biological Chemistry.* 2008;283(25):17324-32.

114. Kim KH, and Roberts CWM. Targeting EZH2 in cancer. *Nat Med.* 2016;22(2):128-34.

115. Hussain M, Rao M, Humphries AE, Hong JA, Liu F, Yang M, Caragacianu D, and Schrump DS. Tobacco Smoke Induces Polycomb-Mediated Repression of Dickkopf-1 in Lung Cancer Cells. *Cancer Research.* 2009;69(8):3570-8.

116. McCabe MT, Ott HM, Ganji G, Korenchuk S, Thompson C, Van Aller GS, Liu Y, Graves AP, Iii ADP, Diaz E, et al. EZH2 inhibition as a therapeutic strategy for lymphoma with EZH2-activating mutations. *Nature.* 2012;492(108.

117. Morin RD, Johnson NA, Severson TM, Mungall AJ, An J, Goya R, Paul JE, Boyle M, Woolcock BW, Kuchenbauer F, et al. Somatic mutations altering EZH2 (Tyr641) in

follicular and diffuse large B-cell lymphomas of germinal-center origin. *Nat Genet.* 2010;42(2):181-5.

118. Morin RD, Mendez-Lago M, Mungall AJ, Goya R, Mungall KL, Corbett RD, Johnson NA, Severson TM, Chiu R, Field M, et al. Frequent mutation of histone-modifying genes in non-Hodgkin lymphoma. *Nature.* 2011;476(298.

119. McCabe MT, Graves AP, Ganji G, Diaz E, Halsey WS, Jiang Y, Smitheman KN, Ott HM, Pappalardi MB, Allen KE, et al. Mutation of A677 in histone methyltransferase EZH2 in human B-cell lymphoma promotes hypertrimethylation of histone H3 on lysine 27 (H3K27). *Proceedings of the National Academy of Sciences.* 2012;109(8):2989-94.

120. Ryan RJH, Nitta M, Borger D, Zukerberg LR, Ferry JA, Harris NL, Iafrate AJ, Bernstein BE, Sohani AR, and Le LP. EZH2 Codon 641 Mutations are Common in BCL2-Rearranged Germinal Center B Cell Lymphomas. *PLOS ONE.* 2011;6(12):e28585.

121. Gulati N, Béguelin W, and Giulino-Roth L. Enhancer of zeste homolog 2 (EZH2) inhibitors. *Leukemia & Lymphoma.* 2018:1-12.

122. Bödör C, Grossmann V, Popov N, Okosun J, O'Riain C, Tan K, Marzec J, Araf S, Wang J, Lee AM, et al. EZH2 mutations are frequent and represent an early event in follicular lymphoma. *Blood.* 2013;122(18):3165-8.

123. Souroullas GP, Jeck WR, Parker JS, Simon JM, Liu J-Y, Paulk J, Xiong J, Clark KS, Fedoriw Y, Qi J, et al. An oncogenic Ezh2 mutation induces tumors through global redistribution of histone 3 lysine 27 trimethylation. *Nature Medicine.* 2016;22(632.

124. Knutson SK, Warholic NM, Wigle TJ, Klaus CR, Allain CJ, Raimondi A, Porter Scott M, Chesworth R, Moyer MP, Copeland RA, et al. Durable tumor regression in genetically altered malignant rhabdoid tumors by inhibition of methyltransferase EZH2. *Proceedings of the National Academy of Sciences.* 2013;110(19):7922-7.

125. Januario T, Ye X, Bainer R, Alicke B, Smith T, Haley B, Modrusan Z, Gould S, and Yauch RL. PRC2-mediated repression of SMARCA2 predicts EZH2 inhibitor activity in SWI/SNF mutant tumors. *Proceedings of the National Academy of Sciences.* 2017;114(46):12249-54.

126. Wilson BG, Wang X, Shen X, McKenna ES, Lemieux ME, Cho Y-J, Koellhoffer EC, Pomeroy SL, Orkin SH, and Roberts CWM. Epigenetic Antagonism between Polycomb and SWI/SNF Complexes during Oncogenic Transformation. *Cancer Cell.* 2010;18(4):316-28.

127. Kim W, Bird GH, Neff T, Guo G, Kerenyi MA, Walensky LD, and Orkin SH. Targeted disruption of the EZH2–EED complex inhibits EZH2-dependent cancer. *Nature Chemical Biology.* 2013;9(643.

128. Simon C, Chagraoui J, Krosl J, Gendron P, Wilhelm B, Lemieux S, Boucher G, Chagnon P, Drouin S, Lambert R, et al. A key role for EZH2 and associated genes in mouse and human adult T-cell acute leukemia. *Genes & Development.* 2012;26(7):651-6.

129. Wang Y, Hou N, Cheng X, Zhang J, Tan X, Zhang C, Tang Y, Teng Y, and Yang X. Ezh2 Acts as a Tumor Suppressor in Kras-driven Lung Adenocarcinoma. *International Journal of Biological Sciences.* 2017;13(5):652-9.

130. de Vries Nienke A, Hulsman D, Akhtar W, de Jong J, Miles Denise C, Blom M, van Tellingen O, Jonkers J, and van Lohuizen M. Prolonged Ezh2 Depletion in Glioblastoma Causes a Robust Switch in Cell Fate Resulting in Tumor Progression. *Cell Reports.* 2015;10(3):383-97.

131. Hussein YR, Sood AK, Bandyopadhyay S, Albashiti B, Semaan A, Nahleh Z, Roh J, Han HD, Lopez-Berestein G, and Ali-Fehmi R. CLINICAL AND BIOLOGICAL RELEVANCE OF EZH2 IN TRIPLE NEGATIVE BREAST CANCER. *Human pathology.* 2012;43(10):1638-44.

132. Wang X, Hu B, Shen H, Zhou H, Xue X, Chen Y, Chen S, Han Y, Yuan B, Zhao H, et al. Clinical and prognostic relevance of EZH2 in breast cancer: A meta-analysis. *Biomedicine & Pharmacotherapy.* 2015;75(218-25.

133. Holm K, Grabau D, Lövgren K, Aradottir S, Gruvberger-Saal S, Howlin J, Saal LH, Ethier SP, Bendahl P-O, Stål O, et al. Global H3K27 trimethylation and EZH2 abundance in breast tumor subtypes. *Molecular Oncology.* 2012;6(5):494-506.

134. Wu Y, Zhang Z, Cenciarini ME, Proietti CJ, Amasino M, Hong T, Yang M, Liao Y, Chiang H-C, Kaklamani VG, et al. Tamoxifen Resistance in Breast Cancer Is Regulated by the EZH2–ERα–GREB1 Transcriptional Axis. *Cancer Research.* 2018;78(3):671-84.

135. Beca F, Kensler K, Glass B, Schnitt SJ, Tamimi RM, and Beck AH. EZH2 protein expression in normal breast epithelium and risk of breast cancer: results from the Nurses' Health Studies. *Breast Cancer Research.* 2017;19(1):21.

136. Gonzalez ME, Li X, Toy K, DuPrie M, Ventura AC, Banerjee M, Ljungman M, Merajver SD, and Kleer CG. Downregulation of EZH2 decreases growth of estrogen receptor-negative invasive breast carcinoma and requires BRCA1. *Oncogene.* 2008;28(843.

137. Yamaguchi H, Du Y, Nakai K, Ding M, Chang SS, Hsu JL, Yao J, Wei Y, Nie L, Jiao S, et al. EZH2 contributes to the response to PARP inhibitors through its PARP-mediated poly-ADP ribosylation in breast cancer. *Oncogene.* 2017;37(208.

138. Ding L, Erdmann C, Chinnaiyan AM, Merajver SD, and Kleer CG. Identification of EZH2 as a Molecular Marker for a Precancerous State in Morphologically Normal Breast Tissues. *Cancer Research.* 2006;66(8):4095-9.

139. Li X, Gonzalez ME, Toy K, Filzen T, Merajver SD, and Kleer CG. Targeted Overexpression of EZH2 in the Mammary Gland Disrupts Ductal Morphogenesis and Causes Epithelial Hyperplasia. *The American Journal of Pathology.* 2009;175(3):1246-54.

140. Yang X, Karuturi RKM, Sun F, Aau M, Yu K, Shao R, Miller LD, Tan PBO, and Yu Q. CDKN1C (p57KIP2) Is a Direct Target of EZH2 and Suppressed by Multiple Epigenetic Mechanisms in Breast Cancer Cells. *PLOS ONE.* 2009;4(4):e5011.

141. Zeidler M, Varambally S, Cao Q, Chinnaiyan AM, Ferguson DO, Merajver SD, and Kleer CG. The Polycomb Group Protein EZH2 Impairs DNA Repair in Breast Epithelial Cells. *Neoplasia.* 2005;7(11):1011-9.

142. Ren G, Baritaki S, Marathe H, Feng J, Park S, Beach S, Bazeley PS, Beshir AB, Fenteany G, Mehra R, et al. Polycomb Protein EZH2 Regulates Tumor Invasion via the Transcriptional Repression of the Metastasis Suppressor RKIP in Breast and Prostate Cancer. *Cancer Research.* 2012;72(12):3091-104.

143. Du J, Li L, Ou Z, Kong C, Zhang Y, Dong Z, Zhu S, Jiang H, Shao Z, Huang B, et al. FOXC1, a target of polycomb, inhibits metastasis of breast cancer cells. *Breast Cancer Research and Treatment.* 2012;131(1):65-73.

144. Bae WK, Yoo KH, Lee JS, Kim Y, Chung I-J, Park MH, Yoon JH, Furth PA, and Hennighausen L. The methyltransferase EZH2 is not required for mammary cancer development, although high EZH2 and low H3K27me3 correlate with poor prognosis of ER-positive breast cancers. *Molecular Carcinogenesis.* 2015;54(10):1172-80.

145. Koh CM, Iwata T, Zheng Q, Bethel C, Yegnasubramanian S, and De Marzo AM. Myc Enforces Overexpression of EZH2 in Early Prostatic Neoplasia via Transcriptional and Post-transcriptional Mechanisms. *Oncotarget.* 2011;2(9):669-83.

146. Chen L, Alexe G, Dharia NV, Ross L, Iniguez AB, Conway AS, Wang EJ, Veschi V, Lam N, Qi J, et al. CRISPR-Cas9 screen reveals a MYCN-amplified neuroblastoma dependency on EZH2. *The Journal of Clinical Investigation.* 2018;128(1):446-62.

147. Wu X, Liu D, Tao D, Xiang W, Xiao X, Wang M, Wang L, Luo G, Li Y, Zeng F, et al. BRD4 Regulates EZH2 Transcription through Upregulation of C-MYC and Represents a Novel Therapeutic Target in Bladder Cancer. *Molecular Cancer Therapeutics.* 2016;15(5):1029-42.

148. Bracken AP, Pasini D, Capra M, Prosperini E, Colli E, and Helin K. EZH2 is downstream of the pRB-E2F pathway, essential for proliferation and amplified in cancer. *The EMBO Journal.* 2003;22(20):5323-35.

149. Santos M, Martínez-Fernández M, Dueñas M, García-Escudero R, Alfaya B, Villacampa F, Saiz-Ladera C, Costa C, Oteo M, Duarte J, et al. In Vivo Disruption of an Rb–E2F–Ezh2 Signaling Loop Causes Bladder Cancer. *Cancer Research.* 2014;74(22):6565-77.

150. Richter GHS, Plehm S, Fasan A, Rössler S, Unland R, Bennani-Baiti IM, Hotfilder M, Löwel D, von Luettichau I, Mossbrugger I, et al. EZH2 is a mediator of EWS/FLI1 driven tumor growth and metastasis blocking endothelial and neuro-ectodermal differentiation. *Proceedings of the National Academy of Sciences.* 2009;106(13):5324-9.

151. Chen Y, Pan K, Wang P, Cao Z, Wang W, Wang S, Hu N, Xue J, Li H, Jiang W, et al. HBP1-mediated regulation of p21 through Mdm2/p53 and TCF4/EZH2 pathways and its impact on cell senescence and tumorigenesis. *Journal of Biological Chemistry.* 2016.

152. Yu J, Yu J, Mani R-S, Cao Q, Brenner CJ, Cao X, Wang X, Wu L, Li J, Hu M, et al. An Integrated Network of Androgen Receptor, Polycomb, and TMPRSS2-ERG Gene Fusions in Prostate Cancer Progression. *Cancer Cell.*17(5):443-54.

153. Alumkal JJ, and Herman JG. Distinct Epigenetic Mechanisms Distinguish TMPRSS2–ERG Fusion-Positive and -Negative Prostate Cancers. *Cancer discovery.* 2012;2(11):979-81.

154. Piper M, Barry G, Harvey TJ, McLeay R, Smith AG, Harris L, Mason S, Stringer BW, Day BW, Wray NR, et al. NFIB-Mediated Repression of the Epigenetic Factor Ezh2 Regulates Cortical Development. *The Journal of Neuroscience.* 2014;34(8):2921-30.

155. Sander S, Bullinger L, Klapproth K, Fiedler K, Kestler HA, Barth TFE, Möller P, Stilgenbauer S, Pollack JR, and Wirth T. MYC stimulates EZH2 expression by repression of its negative regulator miR-26a. *Blood.* 2008;112(10):4202-12.

156. Cao P, Deng Z, Wan M, Huang W, Cramer SD, Xu J, Lei M, and Sui G. MicroRNA-101 negatively regulates Ezh2 and its expression is modulated by androgen receptor and HIF-1α/HIF-1β. *Molecular Cancer.* 2010;9(108-.

157. Chiang C-W, Huang Y, Leong K-W, Chen L-C, Chen H-C, Chen S-J, and Chou C-K. PKCα mediated induction of miR-101 in human hepatoma HepG2 cells. *Journal of Biomedical Science.* 2010;17(1):35-.

158. Varambally S, Cao Q, Mani R-S, Shankar S, Wang X, Ateeq B, Laxman B, Cao X, Jing X, Ramnarayanan K, et al. Genomic Loss of microRNA-101 Leads to Overexpression of Histone Methyltransferase EZH2 in Cancer. *Science.* 2008;322(5908):1695-9.

159. Friedman JM, Liang G, Liu C-C, Wolff EM, Tsai YC, Ye W, Zhou X, and Jones PA. The Putative Tumor Suppressor microRNA-101 Modulates the Cancer Epigenome by Repressing the Polycomb Group Protein EZH2. *Cancer Research.* 2009;69(6):2623-9.

160. Juan AH, Kumar RM, Marx JG, Young RA, and Sartorelli V. Mir-214-Dependent Regulation of the Polycomb Protein Ezh2 in Skeletal Muscle and Embryonic Stem Cells. *Molecular Cell.*36(1):61-74.

161. Cha T-L, Zhou BP, Xia W, Wu Y, Yang C-C, Chen C-T, Ping B, Otte AP, and Hung M-C. Akt-Mediated Phosphorylation of EZH2 Suppresses Methylation of Lysine 27 in Histone H3. *Science.* 2005;310(5746):306-10.

162. Kikuchi J, Koyama D, Wada T, Izumi T, Hofgaard PO, Bogen B, and Furukawa Y. Phosphorylation-mediated EZH2 inactivation promotes drug resistance in multiple myeloma. *The Journal of Clinical Investigation.* 2015;125(12):4375-90.

163. Kim E, Kim M, Woo D-H, Shin Y, Shin J, Chang N, Oh Young T, Kim H, Rheey J, Nakano I, et al. Phosphorylation of EZH2 Activates STAT3 Signaling via STAT3 Methylation and Promotes Tumorigenicity of Glioblastoma Stem-like Cells. *Cancer Cell.*23(6):839-52.

164. Palacios D, Mozzetta C, Consalvi S, Caretti G, Saccone V, Proserpio V, Marquez VE, Valente S, Mai A, Forcales SV, et al. TNF/p38 alpha/Polycomb signalling to Pax7 locus in satellite cells links inflammation to the epigenetic control of muscle regeneration. *Cell stem cell.* 2010;7(4):455-69.

165. Consalvi S, Brancaccio A, Dall'Agnese A, Puri PL, and Palacios D. Praja1 E3 ubiquitin ligase promotes skeletal myogenesis through degradation of EZH2 upon p38α activation. *Nature Communications.* 2017;8(13956.

166. Mertins P, Qiao JW, Patel J, Udeshi ND, Clauser KR, Mani DR, Burgess MW, Gillette MA, Jaffe JD, and Carr SA. Integrated proteomic analysis of post-translational modifications by serial enrichment. *Nature Methods.* 2013;10(634.

167. Sharma K, D'Souza Rochelle CJ, Tyanova S, Schaab C, Wiśniewski Jacek R, Cox J, and Mann M. Ultradeep Human Phosphoproteome Reveals a Distinct Regulatory Nature of Tyr and Ser/Thr-Based Signaling. *Cell Reports.*8(5):1583-94.

168. Stuart SA, Houel S, Lee T, Wang N, Old WM, and Ahn NG. A Phosphoproteomic Comparison of B-RAFV600E and MKK1/2 Inhibitors in Melanoma Cells. *Molecular & Cellular Proteomics.* 2015;14(6):1599-615.

169. Lee Shuet T, Li Z, Wu Z, Aau M, Guan P, Karuturi RKM, Liou Yih C, and Yu Q. Context-Specific Regulation of NF-κB Target Gene Expression by EZH2 in Breast Cancers. *Molecular Cell.* 2011;43(5):798-810.

170. Lawrence CL, and Baldwin AS. Non-Canonical EZH2 Transcriptionally Activates RelB in Triple Negative Breast Cancer. *PLOS ONE.* 2016;11(10):e0165005.

171. Shi B, Liang J, Yang X, Wang Y, Zhao Y, Wu H, Sun L, Zhang Y, Chen Y, Li R, et al. Integration of Estrogen and Wnt Signaling Circuits by the Polycomb Group Protein EZH2 in Breast Cancer Cells. *Molecular and Cellular Biology.* 2007;27(14):5105-19.

172. Li J, Xi Y, Li W, McCarthy RL, Stratton SA, Zou W, Li W, Dent SY, Jain AK, and Barton MC. TRIM28 interacts with EZH2 and SWI/SNF to activate genes that promote mammosphere formation. *Oncogene.* 2017;36(21):2991-3001.

173. Gonzalez ME, Moore HM, Li X, Toy KA, Huang W, Sabel MS, Kidwell KM, and Kleer CG. EZH2 expands breast stem cells through activation of NOTCH1 signaling. *Proceedings of the National Academy of Sciences.* 2014;111(8):3098-103.

174. Jung H-Y, Jun S, Lee M, Kim H-C, Wang X, Ji H, McCrea Pierre D, and Park J-I. PAF and EZH2 Induce Wnt/β-Catenin Signaling Hyperactivation. *Molecular Cell.* 2013;52(2):193-205.

175. Biggar KK, and Li SSC. Non-histone protein methylation as a regulator of cellular signalling and function. *Nature Reviews Molecular Cell Biology.* 2014;16(5.

176. He A, Shen X, Ma Q, Cao J, von Gise A, Zhou P, Wang G, Marquez VE, Orkin SH, and Pu WT. PRC2 directly methylates GATA4 and represses its transcriptional activity. *Genes & Development.* 2012;26(1):37-42.

177. Kogure M, Takawa M, Saloura V, Sone K, Piao L, Ueda K, Ibrahim R, Tsunoda T, Sugiyama M, Atomi Y, et al. The Oncogenic Polycomb Histone Methyltransferase EZH2 Methylates Lysine 120 on Histone H2B and Competes Ubiquitination. *Neoplasia (New York, NY).* 2013;15(11):1251-61.

178. Wurm S, Zhang J, Guinea-Viniegra J, García F, Muñoz J, Bakiri L, Ezhkova E, and Wagner EF. Terminal epidermal differentiation is regulated by the interaction of Fra-2/AP-1 with Ezh2 and ERK1/2. *Genes & Development.* 2015;29(2):144-56.

179. Lee Ji M, Lee Jason S, Kim H, Kim K, Park H, Kim J-Y, Lee Seung H, Kim Ik S, Kim J, Lee M, et al. EZH2 Generates a Methyl Degron that Is Recognized by the DCAF1/DDB1/CUL4 E3 Ubiquitin Ligase Complex. *Molecular Cell.* 2012;48(4):572-86.

180. Gunawan M, Venkatesan N, Loh JT, Wong JF, Berger H, Neo WH, Li LYJ, La Win MK, Yau YH, Guo T, et al. The methyltransferase Ezh2 controls cell adhesion and migration through direct methylation of the extranuclear regulatory protein talin. *Nat Immunol.* 2015;16(5):505-16.

181. Dasgupta M, Dermawan JKT, Willard B, and Stark GR. STAT3-driven transcription depends upon the dimethylation of K49 by EZH2. *Proceedings of the National Academy of Sciences of the United States of America.* 2015;112(13):3985-90.

182. Vasanthakumar A, Xu D, Lun AT, Kueh AJ, van Gisbergen KP, Iannarella N, Li X, Yu L, Wang D, Williams BR, et al. A non-canonical function of Ezh2 preserves immune homeostasis. *EMBO reports.* 2017.

183. Hoffmeyer K, Junghans D, Kanzler B, and Kemler R. Trimethylation and Acetylation of β-Catenin at Lysine 49 Represent Key Elements in ESC Pluripotency. *Cell Reports.* 2017;18(12):2815-24.

184. Ardehali MB, Anselmo A, Cochrane JC, Kundu S, Sadreyev RI, and Kingston RE. Polycomb Repressive Complex 2 Methylates Elongin A to Regulate Transcription. *Molecular Cell.* 2017;68(5):872-84.e6.

185. Burstein HJ, Polyak K, Wong JS, Lester SC, and Kaelin CM. Ductal Carcinoma in Situ of the Breast. *New England Journal of Medicine.* 2004;350(14):1430-41.

186. Steeg PS. Metastasis suppressors alter the signal transduction of cancer cells. *Nature Reviews Cancer.* 2003;3(55.

187. Yan J, Li B, Lin B, Lee PT, Chung T-H, Tan J, Bi C, Lee XT, Selvarajan V, Ng S-B, et al. EZH2 phosphorylation by JAK3 mediates a switch to noncanonical function in natural killer/T-cell lymphoma. *Blood.* 2016;128(7):948-58.

188. Jin X, Yang C, Fan P, Xiao J, Zhang W, Zhan S, Liu T, Wang D, and Wu H. CDK5/FBW7-dependent ubiquitination and degradation of EZH2 inhibits pancreatic cancer cell migration and invasion. *Journal of Biological Chemistry.* 2017;292(15):6269-80.

189. Wan L, Xu K, Wei Y, Zhang J, Han T, Fry C, Zhang Z, Wang YV, Huang L, Yuan M, et al. Phosphorylation of EZH2 by AMPK Suppresses PRC2 Methyltransferase Activity and Oncogenic Function. *Molecular Cell.*69(2):279-91.e5.

190. Wu SC, and Zhang Y. CDK1-mediated phosphorylation of Ezh2 regulates its stability. *Journal of Biological Chemistry.* 2011.

191. Chen S, Bohrer LR, Rai AN, Pan Y, Gan L, Zhou X, Bagchi A, Simon JA, and Huang H. Cyclin-dependent kinases regulate epigenetic gene silencing through phosphorylation of EZH2. *Nature Cell Biology.* 2010;12(1108.

192. Ko H-W, Lee H-H, Huo L, Xia W, Yang C-C, Hsu JL, Li L-Y, Lai C-C, Chan L-C, Cheng C-C, et al. GSK3β inactivation promotes the oncogenic functions of EZH2 and enhances methylation of H3K27 in human breast cancers. *Oncotarget.* 2016;7(35).

193. Yang C-C, LaBaff A, Wei Y, Nie L, Xia W, Huo L, Yamaguchi H, Hsu Y-H, Hsu JL, Liu D, et al. Phosphorylation of EZH2 at T416 by CDK2 contributes to the malignancy of triple negative breast cancers. *American Journal of Translational Research.* 2015;7(6):1009-20.

194. Minnebo N, Görnemann J, O'Connell N, Van Dessel N, Derua R, Vermunt MW, Page R, Beullens M, Peti W, Van Eynde A, et al. NIPP1 maintains EZH2 phosphorylation and promoter occupancy at proliferation-related target genes. *Nucleic Acids Research.* 2013;41(2):842-54.

195. Wei Y, Chen Y-H, Li L-Y, Lang J, Yeh S-P, Shi B, Yang C-C, Yang J-Y, Lin C-Y, Lai C-C, et al. CDK1-dependent phosphorylation of EZH2 suppresses methylation of H3K27 and promotes osteogenic differentiation of human mesenchymal stem cells. *Nature Cell Biology.* 2010;13(87.

196. Nakanishi Y, Reina-Campos M, Nakanishi N, Llado V, Elmen L, Peterson S, Campos A, De SK, Leitges M, Ikeuchi H, et al. Control of Paneth Cell Fate, Intestinal Inflammation, and Tumorigenesis by PKCλ/&#x3b9. *Cell Reports.*16(12):3297-310.

197. Sahasrabuddhe AA, Chen X, Chung F, Velusamy T, Lim MS, and Elenitoba-Johnson KSJ. Oncogenic Y641 mutations in EZH2 prevent Jak2/β-TrCP-mediated degradation. *Oncogene.* 2014;34(445.

198. Li J, Hart RP, Mallimo EM, Swerdel MR, Kusnecov AW, and Herrup K. EZH2-mediated H3K27 trimethylation mediates neurodegeneration in ataxia-telangiectasia. *Nature Neuroscience.* 2013;16(1745.

199. Chu C-S, Lo P-W, Yeh Y-H, Hsu P-H, Peng S-H, Teng Y-C, Kang M-L, Wong C-H, and Juan L-J. O-GlcNAcylation regulates EZH2 protein stability and function. *Proceedings of the National Academy of Sciences of the United States of America.* 2014;111(4):1355-60.

200. Wan J, Zhan J, Li S, Ma J, Xu W, Liu C, Xue X, Xie Y, Fang W, Chin YE, et al. PCAF-primed EZH2 acetylation regulates its stability and promotes lung adenocarcinoma progression. *Nucleic Acids Research.* 2015;43(7):3591-604.

201. Healey MA, Hu R, Beck AH, Collins LC, Schnitt SJ, Tamimi RM, and Hazra A. Association of H3K9me3 and H3K27me3 repressive histone marks with breast cancer subtypes in the Nurses' Health Study. *Breast Cancer Research and Treatment.* 2014;147(3):639-51.

202. Igea A, and Nebreda AR. The Stress Kinase p38α as a Target for Cancer Therapy. *Cancer Research.* 2015;75(19):3997-4002.

203. Chen L, Mayer JA, Krisko TI, Speers CW, Wang T, Hilsenbeck SG, and Brown PH. Inhibition of the p38 Kinase Suppresses the Proliferation of Human ER-Negative Breast Cancer Cells. *Cancer Research.* 2009;69(23):8853-61.

204. Pereira L, Igea A, Canovas B, Dolado I, and Nebreda AR. Inhibition of p38 MAPK sensitizes tumour cells to cisplatin-induced apoptosis mediated by reactive oxygen species and JNK. *EMBO Molecular Medicine.* 2013;5(11):1759-74.

205. Campbell RM, Anderson BD, Brooks NA, Brooks HB, Chan EM, De Dios A, Gilmour R, Graff JR, Jambrina E, Mader M, et al. Characterization of LY2228820 Dimesylate, a Potent and Selective Inhibitor of p38 MAPK with Antitumor Activity. *Molecular Cancer Therapeutics.* 2014;13(2):364-74.

206. Wu X, Zhang W, Font-Burgada J, Palmer T, Hamil AS, Biswas SK, Poidinger M, Borcherding N, Xie Q, Ellies LG, et al. Ubiquitin-conjugating enzyme Ubc13 controls breast cancer metastasis through a TAK1-p38 MAP kinase cascade. *Proceedings of the National Academy of Sciences.* 2014;111(38):13870-5.

207. Wagner EF, and Nebreda AR. Signal integration by JNK and p38 MAPK pathways in cancer development. *Nat Rev Cancer.* 2009;9(8):537-49.

208. Kleer CG, Cao Q, Varambally S, Shen R, Ota I, Tomlins SA, Ghosh D, Sewalt RG, Otte AP, Hayes DF, et al. EZH2 is a marker of aggressive breast cancer and promotes neoplastic transformation of breast epithelial cells. *Proc Natl Acad Sci U S A.* 2003;100(20):11606-11.

209. Gonzalez ME, Martin EE, Anwar T, Arellano-Garcia C, Medhora N, Lama A, Chen YC, Tanager KS, Yoon E, Kidwell KM, et al. Mesenchymal Stem Cell-Induced DDR2 Mediates Stromal-Breast Cancer Interactions and Metastasis Growth. *Cell Rep.* 2017;18(5):1215-28.

210. Gonzalez ME, Moore HM, Li X, Toy KA, Huang W, Sabel MS, Kidwell KM, and Kleer CG. EZH2 expands breast stem cells through activation of NOTCH1 signaling. *Proc Natl Acad Sci U S A.* 2014;111(8):3098-103.

211. Holm K, Grabau D, Lovgren K, Aradottir S, Gruvberger-Saal S, Howlin J, Saal LH, Ethier SP, Bendahl PO, Stal O, et al. Global H3K27 trimethylation and EZH2 abundance in breast tumor subtypes. *Mol Oncol.* 2012;6(5):494-506.

212. Zarubin T, and Han J. Activation and signaling of the p38 MAP kinase pathway. *Cell Res.* 2005;15(1):11-8.

213. Jensen Karin J, Garmaroudi Farshid S, Zhang J, Lin J, Boroomand S, Zhang M, Luo Z, Yang D, Luo H, McManus Bruce M, et al. An ERK-p38 Subnetwork Coordinates Host Cell Apoptosis and Necrosis during Coxsackievirus B3 Infection. *Cell Host & Microbe.* 2013;13(1):67-76.

214. Xu K, Wu ZJ, Groner AC, He HH, Cai C, Lis RT, Wu X, Stack EC, Loda M, Liu T, et al. EZH2 oncogenic activity in castration-resistant prostate cancer cells is Polycomb-independent. *Science.* 2012;338(6113):1465-9.

215. Kim E, Kim M, Woo DH, Shin Y, Shin J, Chang N, Oh YT, Kim H, Rheey J, Nakano I, et al. Phosphorylation of EZH2 activates STAT3 signaling via STAT3 methylation and promotes tumorigenicity of glioblastoma stem-like cells. *Cancer Cell.* 2013;23(6):839-52.

216. Su Ih, Dobenecker M-W, Dickinson E, Oser M, Basavaraj A, Marqueron R, Viale A, Reinberg D, Wülfing C, and Tarakhovsky A. Polycomb Group Protein Ezh2 Controls Actin Polymerization and Cell Signaling. *Cell.* 2005;121(3):425-36.

217. Bryant RJ, Winder SJ, Cross SS, Hamdy FC, and Cunliffe VT. The polycomb group protein EZH2 regulates actin polymerization in human prostate cancer cells. *The Prostate.* 2008;68(3):255-63.

218. Kleer CG, Zhang Y, Pan Q, and Merajver SD. WISP3 (CCN6) Is a Secreted Tumor-Suppressor Protein that Modulates IGF Signaling in Inflammatory Breast Cancer. *Neoplasia (New York, NY).* 2004;6(2):179-85.

219. Chen Y-C, Allen SG, Ingram PN, Buckanovich R, Merajver SD, and Yoon E. Single-cell Migration Chip for Chemotaxis-based Microfluidic Selection of Heterogeneous Cell Populations. *Scientific Reports.* 2015;5(9980.

220. Burgos-Ojeda D, Wu R, McLean K, Chen Y-C, Talpaz M, Yoon E, Cho KR, and Buckanovich RJ. CD24⁺ Ovarian Cancer Cells Are Enriched for Cancer-Initiating Cells and Dependent on JAK2 Signaling for Growth and Metastasis. *Molecular Cancer Therapeutics.* 2015;14(7):1717-27.

221. Cheng Y-H, Chen Y-C, Brien R, and Yoon E. Scaling and automation of a high-throughput single-cell-derived tumor sphere assay chip. *Lab on a Chip.* 2016;16(19):3708-17.

222. Mellacheruvu D, Wright Z, Couzens AL, Lambert J-P, St-Denis NA, Li T, Miteva YV, Hauri S, Sardiu ME, Low TY, et al. The CRAPome: a contaminant repository for affinity purification-mass spectrometry data. *Nat Meth.* 2013;10(8):730-6.

223. Li T, Guo H, Song Y, Zhao X, Shi Y, Lu Y, Hu S, Nie Y, Fan D, and Wu K. Loss of vinculin and membrane-bound β-catenin promotes metastasis and predicts poor prognosis in colorectal cancer. *Molecular Cancer.* 2014;13(1):263.

224. Goldmann WH, Auernheimer V, Thievessen I, and Fabry B. Vinculin, cell mechanics and tumour cell invasion. *Cell Biology International.* 2013;37(5):397-405.

225. Auernheimer V, Lautscham LA, Leidenberger M, Friedrich O, Kappes B, Fabry B, and Goldmann WH. Vinculin phosphorylation at residues Y100 and Y1065 is required for cellular force transmission. *Journal of Cell Science.* 2015;128(18):3435-43.

226. Zhang Z, Izaguirre G, Lin S-Y, Lee HY, Schaefer E, and Haimovich B. The Phosphorylation of Vinculin on Tyrosine Residues 100 and 1065, Mediated by Src Kinases, Affects Cell Spreading. *Molecular Biology of the Cell.* 2004;15(9):4234-47.

227. Rubashkin MG, Cassereau L, Bainer R, DuFort CC, Yui Y, Ou G, Paszek MJ, Davidson MW, Chen Y-Y, and Weaver VM. Force Engages Vinculin and Promotes Tumor Progression by Enhancing PI3K Activation of Phosphatidylinositol (3,4,5)-Triphosphate. *Cancer Research.* 2014;74(17):4597-611.

228. Linder S. Invadosomes at a glance. *Journal of Cell Science.* 2009;122(17):3009-13.

229. Rodriguez FJ, Geiger B, Salomon D, Sabanay I, Zoller M, and Ben-Ze'Ev A. Suppression of tumorigenicity in transformed cells after transfection with vinculin cDNA. *J Cell Biol.* 1992;119(

230. Lifschitz-Mercer B, Czernobilsky B, Feldberg E, and Geiger B. Expression of the adherens junction protein vinculin in human basal and squamous cell tumors: relationship to invasiveness and metastatic potential. *Hum Pathol.* 1997;28(

231. Subauste MC, Pertz O, Adamson ED, Turner CE, Junger S, and Hahn KM. Vinculin modulation of paxillin-FAK interactions regulates ERK to control survival and motility. *J Cell Biol.* 2004;165(

232. Mierke CT, Kollmannsberger P, Zitterbart DP, Diez G, Koch TM, Marg S, Ziegler WH, Goldmann WH, and Fabry B. Vinculin Facilitates Cell Invasion into Three-dimensional Collagen Matrices. *Journal of Biological Chemistry.* 2010;285(17):13121-30.

233. Golji J, Wendorff T, and Mofrad MRK. Phosphorylation Primes Vinculin for Activation. *Biophysical Journal.* 2012;102(9):2022-30.

234. Cui L, Nakano K, Obchoei S, Setoguchi K, Matsumoto M, Yamamoto T, Obika S, Shimada K, and Hiraoka N. Small Nucleolar Noncoding RNA SNORA23, Upregulated in Human Pancreatic Ductal Adenocarcinoma, Regulates Expression of SYNE2 to Promote Growth and Metastasis of Xenograft Tumors in Mice. *Gastroenterology.*

235. Yao J, Weremowicz S, Feng B, Gentleman RC, Marks JR, Gelman R, Brennan C, and Polyak K. Combined cDNA Array Comparative Genomic Hybridization and Serial Analysis of Gene Expression Analysis of Breast Tumor Progression. *Cancer Research.* 2006;66(8):4065-78.

236. Offenhäuser N, Borgonovo A, Disanza A, Romano P, Ponzanelli I, Iannolo G, Di Fiore PP, and Scita G. The eps8 Family of Proteins Links Growth Factor Stimulation to Actin Reorganization Generating Functional Redundancy in the Ras/Rac Pathway. *Molecular Biology of the Cell.* 2004;15(1):91-8.

237. Fish L, Pencheva N, Goodarzi H, Tran H, Yoshida M, and Tavazoie SF. Muscleblind-like 1 suppresses breast cancer metastatic colonization and stabilizes metastasis suppressor transcripts. *Genes & Development.* 2016;30(4):386-98.

238. Teo G, Liu G, Zhang J, Nesvizhskii AI, Gingras A-C, and Choi H. SAINTexpress: Improvements and additional features in Significance Analysis of INTeractome software. *Journal of Proteomics.* 2014;100(37-43.

239. Choi H, Larsen B, Lin Z-Y, Breitkreutz A, Mellacheruvu D, Fermin D, Qin ZS, Tyers M, Gingras A-C, and Nesvizhskii AI. SAINT: probabilistic scoring of affinity purification-mass spectrometry data. *Nat Meth.* 2011;8(1):70-3.

240. Horzum U, Ozdil B, and Pesen-Okvur D. Step-by-step quantitative analysis of focal adhesions. *MethodsX.* 2014;1(56-9.

241. Trost M, Sauvageau M, Hérault O, Deleris P, Pomiès C, Chagraoui J, Mayotte N, Meloche S, Sauvageau G, and Thibault P. Posttranslational regulation of self-renewal capacity: insights from proteome and phosphoproteome analyses of stem cell leukemia. *Blood.* 2012;120(8):e17-e27.

242. Dephoure N, Gould KL, Gygi SP, and Kellogg DR. Mapping and analysis of phosphorylation sites: a quick guide for cell biologists. *Molecular Biology of the Cell.* 2013;24(5):535-42.

243. Chen Z, and Cole PA. Synthetic approaches to protein phosphorylation. *Curr Opin Chem Biol.* 2015;28(115-22.

244. Durocher D, Henckel J, Fersht AR, and Jackson SP. The FHA Domain Is a Modular Phosphopeptide Recognition Motif. *Molecular Cell.*4(3):387-94.

245. Zisch AH, Pazzagli C, Freeman AL, Schneller M, Hadman M, Smith JW, Ruoslahti E, and Pasquale EB. Replacing two conserved tyrosines of the EphB2 receptor with glutamic acid prevents binding of SH2 domains without abrogating kinase activity and biological responses. *Oncogene.* 2000;19(177.

246. Skinner JJ, Wang S, Lee J, Ong C, Sommese R, Sivaramakrishnan S, Koelmel W, Hirschbeck M, Schindelin H, Kisker C, et al. Conserved salt-bridge competition triggered by phosphorylation regulates the protein interactome. *Proc Natl Acad Sci U S A.* 2017;114(51):13453-8.

247. Harrod A, Fulton J, Nguyen VTM, Periyasamy M, Ramos-Garcia L, Lai CF, Metodieva G, de Giorgio A, Williams RL, Santos DB, et al. Genomic modelling of the ESR1 Y537S mutation for evaluating function and new therapeutic approaches for metastatic breast cancer. *Oncogene.* 2016;36(2286.

248. Castrogiovanni C, Waterschoot B, De Backer O, and Dumont P. Serine 392 phosphorylation modulates p53 mitochondrial translocation and transcription-independent apoptosis. *Cell Death And Differentiation.* 2017;25(190.

249. Kuzmichev A, Nishioka K, Erdjument-Bromage H, Tempst P, and Reinberg D. Histone methyltransferase activity associated with a human multiprotein complex containing the Enhancer of Zeste protein. *Genes & Development.* 2002;16(22):2893-905.

250. Helin K, and Dhanak D. Chromatin proteins and modifications as drug targets. *Nature.* 2013;502(480.

251. Jayo A, Malboubi M, Antoku S, Chang W, Ortiz-Zapater E, Groen C, Pfisterer K, Tootle T, Charras G, Gundersen Gregg G, et al. Fascin Regulates Nuclear Movement and Deformation in Migrating Cells. *Developmental Cell.* 2016;38(4):371-83.

252. Revach O-Y, Weiner A, Rechav K, Sabanay I, Livne A, and Geiger B. Mechanical interplay between invadopodia and the nucleus in cultured cancer cells. *Scientific Reports.* 2015;5(9466.

253. Matsumoto A, Hieda M, Yokoyama Y, Nishioka Y, Yoshidome K, Tsujimoto M, and Matsuura N. Global loss of a nuclear lamina component, lamin A/C, and LINC complex components SUN1, SUN2, and nesprin-2 in breast cancer. *Cancer Medicine.* 2015;4(10):1547-57.

254. Mori K, Furusawa T, Okubo T, Inoue T, Ikawa S, Yanai N, John K, and Obinata M. Genome Structure and Differential Expression of Two Isoforms of a Novel PDZ-Containing Myosin (MysPDZ) (Myo18A). *The Journal of Biochemistry.* 2003;133(4):405-13.

255. Cao J-M, Cheng X-N, Li S-Q, Heller S, Xu Z-G, and Shi D-L. Identification of novel MYO18A interaction partners required for myoblast adhesion and muscle integrity. *Scientific Reports.* 2016;6(36768.

256. Buschman MD, and Field SJ. MYO18A: An unusual myosin. *Advances in Biological Regulation.* 2018;67(84-92.

257. Makowska Katarzyna A, Hughes Ruth E, White Kathryn J, Wells Claire M, and Peckham M. Specific Myosins Control Actin Organization, Cell Morphology, and Migration in Prostate Cancer Cells. *Cell Reports.* 2015;13(10):2118-25.

258. Maier VK, Feeney CM, Taylor JE, Creech AL, Qiao JW, Szanto A, Das PP, Chevrier N, Cifuentes-Rojas C, Orkin SH, et al. Functional Proteomic Analysis of Repressive Histone Methyltransferase Complexes Reveals ZNF518B as a G9A Regulator. *Molecular & Cellular Proteomics : MCP.* 2015;14(6):1435-46.

259. First PARP Inhibitor Approved for Breast Cancer. *Cancer Discovery.* 2018.

260. Konecny GE, and Kristeleit RS. PARP inhibitors for BRCA1/2-mutated and sporadic ovarian cancer: current practice and future directions. *British Journal Of Cancer.* 2016;115(1157.

261. Schuller JM, Falk S, Fromm L, Hurt E, and Conti E. Structure of the nuclear exosome captured on a maturing preribosome. *Science.* 2018.

262. Kaneko S, Son J, Shen SS, Reinberg D, and Bonasio R. PRC2 binds active promoters and contacts nascent RNAs in embryonic stem cells. *Nature Structural &Amp; Molecular Biology.* 2013;20(1258.

263. Davidovich C, Zheng L, Goodrich KJ, and Cech TR. Promiscuous RNA binding by Polycomb repressive complex 2. *Nature Structural &Amp; Molecular Biology.* 2013;20(1250.

264. van Kruijsbergen I, Hontelez S, and Veenstra GJC. Recruiting polycomb to chromatin. *The International Journal of Biochemistry & Cell Biology.* 2015;67(177-87.

265. Wang X, Goodrich KJ, Gooding AR, Naeem H, Archer S, Paucek RD, Youmans DT, Cech TR, and Davidovich C. Targeting of Polycomb Repressive Complex 2 to RNA by Short Repeats of Consecutive Guanines. *Molecular Cell.*65(6):1056-67.e5.

266. van Haaften G, Dalgliesh GL, Davies H, Chen L, Bignell G, Greenman C, Edkins S, Hardy C, O'Meara S, Teague J, et al. Somatic mutations of the histone H3K27 demethylase gene UTX in human cancer. *Nature Genetics.* 2009;41(521.

267. Waddell N, Pajic M, Patch A-M, Chang DK, Kassahn KS, Bailey P, Johns AL, Miller D, Nones K, Quek K, et al. Whole genomes redefine the mutational landscape of pancreatic cancer. *Nature.* 2015;518(7540):495-501.

268. Kim KH, Kim W, Howard TP, Vazquez F, Tsherniak A, Wu JN, Wang W, Haswell JR, Walensky LD, Hahn WC, et al. SWI/SNF-mutant cancers depend on catalytic and non-catalytic activity of EZH2. *Nature Medicine.* 2015;21(1491.

269. Kadoch C, Hargreaves DC, Hodges C, Elias L, Ho L, Ranish J, and Crabtree GR. Proteomic and bioinformatic analysis of mammalian SWI/SNF complexes identifies extensive roles in human malignancy. *Nature Genetics.* 2013;45(592.

270. Mahara S, Lee PL, Feng M, Tergaonkar V, Chng WJ, and Yu Q. HIFI-α activation underlies a functional switch in the paradoxical role of Ezh2/PRC2 in breast cancer. *Proceedings of the National Academy of Sciences.* 2016;113(26):E3735-E44.

271. Verma SK, Tian X, LaFrance LV, Duquenne C, Suarez DP, Newlander KA, Romeril SP, Burgess JL, Grant SW, Brackley JA, et al. Identification of Potent, Selective, Cell-Active Inhibitors of the Histone Lysine Methyltransferase EZH2. *ACS Medicinal Chemistry Letters.* 2012;3(12):1091-6.

272. Scott MT, Korfi K, Saffrey P, Hopcroft LEM, Kinstrie R, Pellicano F, Guenther C, Gallipoli P, Cruz M, Dunn K, et al. Epigenetic Reprogramming Sensitizes CML Stem Cells to Combined EZH2 and Tyrosine Kinase Inhibition. *Cancer Discovery.* 2016.

273. Xing L. Clinical candidates of small molecule p38 MAPK inhibitors for inflammatory diseases. *2016.* 2016;4(1).

274. Han S, Witt RM, Santos TM, Polizzano C, Sabatini BL, and Ramesh V. Pam (Protein associated with Myc) functions as an E3 Ubiquitin ligase and regulates TSC/mTOR signaling. *Cellular Signalling.* 2008;20(6):1084-91.

275. Park E, and Maquat LE. Staufen-mediated mRNA decay. *Wiley interdisciplinary reviews RNA.* 2013;4(4):423-35.

276. Lam I, and Keeney S. Mechanism and regulation of meiotic recombination initiation. *Cold Spring Harbor perspectives in biology.* 2015;7(1):a016634-a.

277. Su L, Hershberger RJ, and Weissman IL. LYAR, a novel nucleolar protein with zinc finger DNA-binding motifs, is involved in cell growth regulation. *Genes & Development.* 1993;7(5):735-48.

278. Lee T, and Pelletier J. The biology of DHX9 and its potential as a therapeutic target. *Oncotarget.* 2016;7(27):42716-39.

279. Takeyama K, Aguiar RCT, Gu L, He C, Freeman GJ, Kutok JL, Aster JC, and Shipp MA. The BAL-binding Protein BBAP and Related Deltex Family Members Exhibit Ubiquitin-Protein Isopeptide Ligase Activity. *Journal of Biological Chemistry.* 2003;278(24):21930-7.

280. Krishnakumar R, and Kraus WL. The PARP Side of the Nucleus: Molecular Actions, Physiological Outcomes, and Clinical Targets. *Molecular Cell.*39(1):8-24.

281. Schellenberg MJ, Tumbale PP, and Williams RS. Molecular Underpinnings of Aprataxin RNA/DNA Deadenylase Function and Dysfunction in Neurological Disease. *Progress in biophysics and molecular biology.* 2015;117(0):157-65.

282. Sanidas I, Polytarchou C, Hatziapostolou M, Ezell Scott A, Kottakis F, Hu L, Guo A, Xie J, Comb Michael J, Iliopoulos D, et al. Phosphoproteomics Screen Reveals Akt Isoform-Specific Signals Linking RNA Processing to Lung Cancer. *Molecular Cell.*53(4):577-90.

283. Larsen NB, and Hickson ID. In: Spies M ed. *DNA Helicases and DNA Motor Proteins*. New York, NY: Springer New York; 2013:161-84.

284. Morton DJ, Kuiper EG, Jones SK, Leung SW, Corbett AH, and Fasken MB. The RNA exosome and RNA exosome-linked disease. *RNA.* 2018;24(2):127-42.

285. Gupta S, Fanzo JC, Hu C, Cox D, Jang SY, Lee AE, Greenberg S, and Pernis AB. T Cell Receptor Engagement Leads to the Recruitment of IBP, a Novel Guanine Nucleotide Exchange Factor, to the Immunological Synapse. *Journal of Biological Chemistry.* 2003;278(44):43541-9.

Appendix

A number of people contributed to the data presented in chapters 2 to 4 of this dissertation. Their contributions are listed below.

Talha Anwar designed and performed experiments, and analyzed data. Caroline Arellano-Garcia assisted with experimental execution of immunoprecipitations. James Ropa performed analysis of LC MS/MS data. Yu-Chih Chen developed, performed, and analyzed high throughput single cell migration assays. Eusik Yoon. contributed with microfluidics migration assays. Sierrah Grigsby performed bio-layer interferometry assays. Venkatesha Basrur and Alexey Nesvizhskii performed and assisted with LC MS/MS data interpretation. Zaneta Nikolovska-Coleska contributed with BLI data. Maria Gonzalez and Hong Suny Kim assisted with experimental strategies and data analysis. Celina Kleer contributed to project conception and experimental design.